ISLAMIC UNIVERSITY OF TECHNOLOGY (IUT)

3D CFD BASED OPTIMIZED MUFFLER DESIGN, CONSTRUCTION AND PROTOTYPE VALIDATION OF MOTORCYCLE

M.Sc. Engineering (Mechanical) THESIS

BY

AHMAD SYED ANWAR
Department of Mechanical and Chemical Engineering
Islamic University of Technology (IUT), Gazipur-1704, Bangladesh.
STUDENT NO: 121602

SUPERVISED BY

DR. MOHAMMAD AHSAN HABIB

JANUARY 2016

3D CFD BASED OPTIMIZED MUFFLER DESIGN, CONSTRUCTION AND PROTOTYPE VALIDATION OF MOTORCYCLE

BY

AHMAD SYED ANWAR
STUDENT NO: 121602

A THESIS PRESENTED TO THE DEPARTMENT OF MECHANICAL AND CHEMICAL ENGINEERING, ISLAMIC UNIVERSITY OF TECHNOLOGY DHAKA IN PARTIAL FULFILMENT OF THE REQUIREMENT FOR THE AWARD OF DEGREE FOR

MASTER OF SCIENCE (M. Sc.) IN MECHANICAL ENGINEERING

JANUARY 2016

Candidate's Declaration

It is hereby declared that this thesis or any part of it has not been submitted elsewhere for the award of any degree or diploma.

Signature of the Candidate

_____

Ahmad Syed Anwar
Student No.: 121602
Session 2012-2013
Department of Mechanical and Chemical Engineering (MCE)
Islamic University of Technology (IUT), OIC
Board Bazar, Gazipur
Dhaka, Bangladesh.

Signature of the Supervisor

_____

Dr. Mohammad Ahsan Habib
Assistant Professor
Department of Mechanical & Chemical Engineering (MCE)
Islamic University of Technology (IUT), OIC
Board Bazar, Gazipur
Dhaka, Bangladesh.

Certificate of Approval

The thesis titled "3D CFD based optimized muffler design, construction and prototype validation of motorcycle" submitted by Ahmad Syed Anwar bearing Student No. 121602 of Academic Year 2012-2013 has been found as satisfactory and accepted as partial fulfillment of the requirement for the degree of Master of Science in Mechanical Engineering on 12 January, 2016.

BOARD OF EXAMINERS

---

1. **Dr. Mohammad Ahsan Habib**
   Assistant Professor
   Department of Mechanical and Chemical Engineering
   Islamic University of Technology (IUT)
   Board Bazar, Gazipur
   Dhaka, Bangladesh.

---

2. **Dr. Md. A.K.M Sadrul Islam**
   Professor and Head
   Department of Mechanical and Chemical Engineering
   Islamic University of Technology (IUT)
   Board Bazar, Gazipur
   Dhaka, Bangladesh.

---

3. **Dr. Md. Anayet Ullah Patwari**
   Professor
   Department of Mechanical and Chemical Engineering
   Islamic University of Technology (IUT)
   Board Bazar, Gazipur
   Dhaka, Bangladesh.

---

4. **Dr. Mohammed Kamruzzaman**
   Head, IPE Department
   Dhaka University of Engineering and Technology (DUET)
   Board Bazar, Gazipur
   Dhaka, Bangladesh.

Acknowledgements

I would like to begin by saying Alhamdullilah and grateful to Almighty Allah who made it possible for me to finish this project successfully on time. Equally say a big thank to my supervisor Dr. Mohammad Ahsan Habib, Assistant Professor, Department of Mechanical and Chemical Engineering, IUT for all his support, ideas about experiments, discussions, time and for explaining so patiently the hard topics and checking this thesis and papers above all his care and concern. These will ever remain in my memory. Thanks to my examiners for their constructive ideas, suggestions and double checking my work.

Special thanks to all faculties for their support and encouragement throughout the period of my studies. Special thanks also to Roadmaster Motrs Ltd for their useful workshop support and cooperation which made it easier for me to carry out the experiments.

I will like to say a big thank you to the Head of Department Professor Dr. A.K.M. Sadrul Islam for his continues encouragement and support during the period of my studies. Finally, I will like to express my lasting gratitude to my family members for their patience, support, encouragement, enthusiasm and prayers.

Table of Contents

List of Figures

List of Tables

Abstract

In order to minimize the sound transmission due to exhaust gases, the most common and important part of the engine system is muffler. A backpressure on engine is always produce due to the use of the exhaust muffler. This back pressure represents the extra static pressure exerted by the muffler on the engine through the restriction in flow of exhaust gases. The back pressure mainly depends on the internal shape and overall design of the exhaust muffler. Design of muffler is a complex function that affects noise characteristics, emission and fuel efficiency of engine. In this study, a combine model of response surface methodology (RSM), Artificial Bee Colony and Grey analysis is used for optimizing the back pressure and other internal plates pressure of a motorcycle reactive muffler, in order to improve the performance of the muffler. For this optimization process, the design variable parameters are diameter of perforation, number of perforation and chamber size. To measure the back pressure 3D CFD based CAE software has been used. Prediction of acoustics transmission loss is an important analysis required for the development of muffler at an initial design stage. For this reason, acoustics transmission loss analysis is conducted. It is found that after optimizing the design of the muffler, the back pressure and other internal plate pressures are decreased and the acoustics transmission loss is increased that can ensure the improvement of the muffler efficiency. It has been also found that for a constant exit diameter of an exhaust muffler the back pressure varies with the change of the engine speed. Due to this variation of the back pressure, the fuel consumption per unit distance is also varies. An attempt has been made in this study to stabilize the back pressure to a suitable value by using an automated mechanical IRIS. The function of the mechanical IRIS is to provide a variable exit diameter to the exhaust muffler. An automated mechanical system will be integrated with the IRIS, so that the exit diameter will vary automatically depending on the engine speed. It has been found through 3D based CFD simulation that the back pressure remains constant for a wide range of speed of the engine. This will ensure maximum the fuel consumption per unit distance throughout the wide range of speed variation.

Chatper 1 Introduction

The sole purpose of an automotive muffler is to reduce engine noise emission. If you have ever heard a car running without a muffler you will have an appreciation for the significant difference in noise level a muffler can make. If vehicles did not have a muffler there would be an unbearable amount of engine exhaust noise in our environment. Noise is defined as unwanted sound.

Sound is a pressure wave formed from pulses of alternating high and low pressure air. In an automotive engine, pressure waves are generated when the exhaust valve repeatedly opens and lets high-pressure gas into the exhaust system. These pressure pulses are the sound we hear. As the engine rpm increases so do the pressure fluctuations and therefore the sound emitted is of a higher frequency.

All noise emitted by an automobile does not come from the exhaust system. Other contributors to vehicle noise emission include intake noise, mechanical noise and vibration induced noise from the engine body and transmission.

The automotive muffler has to be able to allow the passage of exhaust gasses whilst restricting the transmission of sound.

1.1 Muffler Design

There are numerous variations of the two main types of muffler designs commonly used, namely absorptive and reactive. Generally automotive mufflers will have both reactive and absorptive properties.

The reactive or reflective mufflers use the phenomenon of destructive interference to reduce noise. This means that they are designed so that the sound waves produced by an engine partially cancel themselves out in the muffler. For complete destructive interference to occur a reflected pressure wave of equal amplitude and 180 degrees out of phase needs to collide with the transmitted pressure wave. Reflections occur where there is a change in geometry or an area discontinuity.

A reactive muffler, as shown in Figure 1.1, generally consists of a series of resonating and expansion chambers that are designed to reduce the sound pressure level at certain frequencies. The inlet and outlet tubes are generally offset and have perforations that allow sound pulses to scatter out in numerous directions inside a chamber resulting in destructive interference.

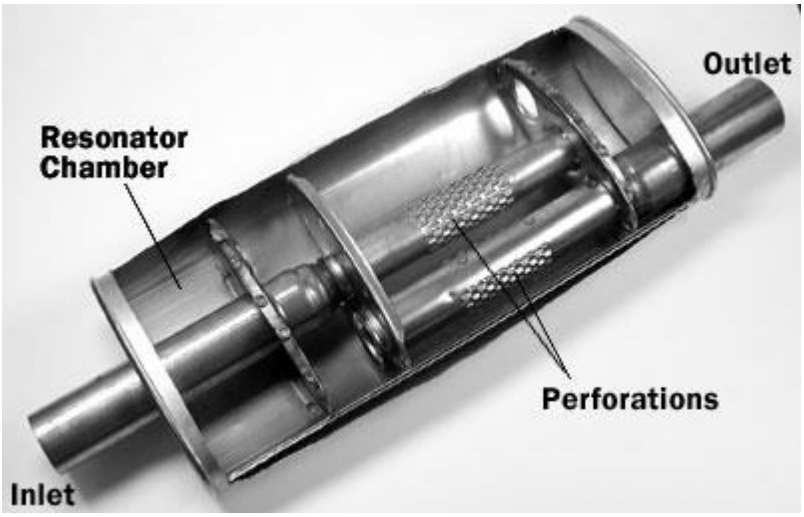

Figure 1.1: Typical reactive automotive muffler

Reactive mufflers are used widely in car exhaust systems where the exhaust gas flow and hence noise emission varies with time. They have the ability to reduce noise at various frequencies due to the numerous chambers and changes in geometry that the exhaust gasses are forced to pass through.

The down side to reactive mufflers is that larger backpressures are created, however for passenger cars where noise emission and passenger comfort are highly valued reactive mufflers are ideal and can be seen on most passenger vehicles on our roads today.

An absorptive or dissipative muffler, as shown in Figure 1.2, uses absorption to reduce sound energy. Sound waves are reduced as their energy is converted into heat in the absorptive material. A typical absorptive muffler consists of a straight, circular and perforated pipe that is encased in a larger steel housing. Between the perforated pipe and the casing is a layer of sound absorptive material that absorbs some of the pressure pulses. Absorptive mufflers create less backpressure then reactive mufflers, however they do not reduce noise as well.

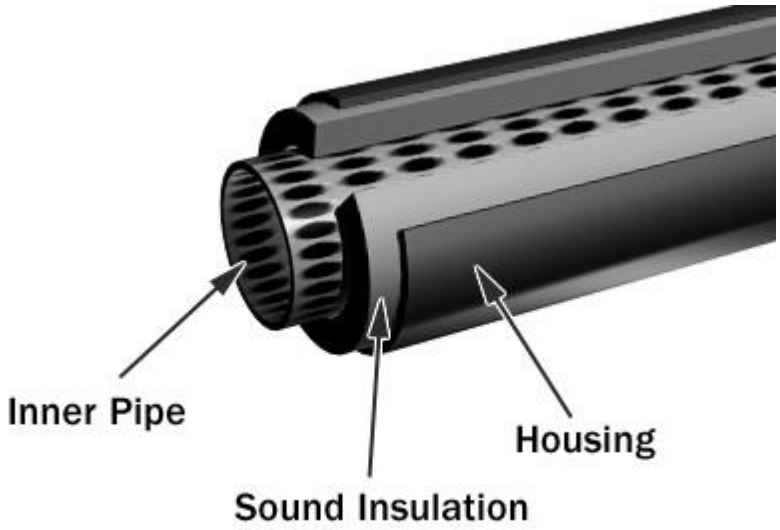

Figure 1.2: Typical absorptive automotive muffler

Generally reactive mufflers use resonating chambers that target specific frequencies to control noise whereas an absorptive silencer reduces noise considerably over the entire spectrum and more so at higher frequencies. It is good practice to design a muffler to work best in the frequency range where the engine has the highest sound energy. In practice the sound spectrum of an engine exhaust is continually changing, as it is dependent on the engine speed that is continually varying when the car is being driven. It is impossible to design a muffler that achieves complete destructive interference, however some will always occur.

Noise spectrum variation makes muffler design quite difficult and testing is the only sure way to determine whether the muffler performs well at all engine speeds. However, as a general rule of thumb, exhaust noise is generally limited to the fundamental frequency and the first few harmonics, which can be calculated, therefore these frequencies should be used as a starting point for preliminary muffler design.

A practical way of determining the frequency range to be controlled is to measure the unmuffled engine noise. This measured spectrum can then be used to identify the frequencies, at which the higher noise levels occur. The high noise level frequencies should be treated with appropriate noise control to achieve an overall noise reduction. There is always more than one way to design a muffler for a specific application,

however if the designed muffler is practical and achieves the required noise reduction and meets all functional requirements then the designer has succeeded.

1.2 Functional Requirements of an Engine Exhaust Muffler

There are numerous functional requirements that should be considered when designing a muffler for a specific application. Such functional requirements may include adequate insertion loss, backpressure, size, durability, desired sound, cost, shape and style. These functional requirements are detailed below focusing on an automotive mufflers functional requirements.

1.2.1 Adequate Insertion Loss

The main function of a muffler is to “muffle” or attenuate sound. An effective muffler will reduce the sound pressure of the noise source to the required level. In the case of an automotive muffler the noise in the exhaust system, generated by the engine, is to be reduced.

A mufflers performance or attenuating capability is generally defined in terms of insertion loss or transmission loss. Insertion loss is defined as the difference between the acoustic power radiated without and with a muffler fitted. The transmission loss is defined as the difference (in decibels) between the sound power incident at the entry to the muffler to that transmitted by the muffler. The muffler designer must determine the required insertion loss so that a suitable style of muffler can be designed for the specific purpose.

As a general principle when designing an automotive muffler, a reactive muffler with many area discontinuities will achieve a greater attenuation than one with fewer area discontinuities. The addition of sound absorptive material will always increase the attenuation capacity of a muffler, but should be located in an appropriate place.

1.2.2 Backpressure

Backpressure represents the extra static pressure exerted by the muffler on the engine through the restriction in flow of exhaust gasses. Generally, the better a muffler is at

attenuating sound the more backpressure is generated. In a reactive muffler where good attenuation is achieved the exhaust gasses are forced to pass through numerous geometry changes and a fair amount of backpressure may be generated, which reduces the power output of the engine. Backpressure should be kept to a minimum to avoid power losses especially for performance vehicles where performance is paramount.

Every time the exhaust gasses are forced to change direction additional backpressure is created. Therefore, to limit backpressure geometric changes are to be kept to a minimum, a typical example of this is a "straight through" absorption silencer. Exhaust gasses are allowed to pass virtually unimpeded through the straight perforated pipe.

1.2.3 Size

The available space has a great influence on the size and therefore type of muffler that may be used. A muffler may have its geometry designed for optimum attenuation however if it does not meet the space constraints, it is useless.

Generally the larger a muffler is, the more it weighs and the more it costs to manufacture. For a performance vehicle every gram saved is crucial to its performance/acceleration, especially when dealing with light open wheeled race vehicles. Therefore a small lightweight muffler is desirable.

Effectively supporting a muffler is always a design issue and the larger a muffler is the more difficult it is to support. A muffler's mounting system not only needs to support the mufflers weight but it also needs to provide vibration isolation so that the vibration of the exhaust system is not transferred to the chassis and then to the passenger cabin. This vibration isolation is usually achieved with the use of hard rubber inserts and brackets that isolate or dampen vibration from the muffler to the chassis.

1.2.4 Durability

The life expectancy of a muffler is another important functional requirement especially when dealing with hot exhaust gasses and absorptive silencers that are found in performance vehicles.

Overtime, hot exhaust gasses tend to clog the absorptive material with unburnt carbon particles or burn the absorptive material in the muffler. This causes the insertion loss to deteriorate. There are however, good products such as mineral wool, fiberglass, sintered metal composites and white wool that resist such unwanted effects.

Reactive type mufflers with no absorptive material are very durable and their performance does not diminish with time. Generally, mufflers are made from corrosion resistive materials such as stainless steel or aluminum. Mild steel or aluminized steel is generally used for temperatures up to 500°C, type 409 stainless steel up to 700°C and type 321 stainless steel for even higher temperatures. Automotive exhaust gas temperatures are usually around 750°C.

1.2.5 Desired Sound

Generally, a muffler is used to reduce the sound of a combustion engine to a desired level that provides comfort for the driver and passengers of the vehicle as well as minimizing sound pollution to the environment. Muffler designs generally aim to reduce any annoying characteristics of the untreated exhaust noise such as low frequency rumble.

There has however been a growing trend in Australia in recent years for young drivers wanting to "hot up" their vehicles and this includes muffler modification. Muffler modification of a stock vehicle is generally done for two reasons being performance and sound. Vehicles leave the factory floor with mufflers generally designed for noise control not optimal performance. The standard reactive muffler is generally replaced with a straight through absorption silencer for aesthetics and to minimize backpressure and therefore improve vehicle performance.

Having exchanged the stock muffler for an absorptive type performance muffler generally means that exhaust noise is increased, leaving a noticeable deep rumble in the exhaust system. In most cases this sound is what the owner of the vehicle desires so that the public is aware of their presence. However in the main mufflers should be designed so that exhaust noise emission is only barely audible within the passenger cabin and the appropriate government regulations are adhered to. Breakout noise from the muffler

shell may be a problem and should be minimized together with flow-generated noise, especially when designing a muffler for a high insertion loss.

1.2.6 Cost

A major factor in any component is the cost to the consumer. Silencers not only have to be effective in performing their task they need to be affordable otherwise the product will fail in the marketplace. Aftermarket car exhaust mufflers vary in price from $90 to $700. The cost is dependent on the materials used in the construction of the muffler, design integrity, durability and labor costs.

1.2.7 Shape and Style

Automotive mufflers come in all different shapes, styles and sizes depending on the desired application. Generally automotive mufflers consist of an inlet and outlet tube separated by a larger chamber that is oval or round in geometry. The inside detail of this larger chamber may be one of numerous constructions. The end user of the muffler usually does not care what is inside this chamber so long as the muffler produces the desired sound and is aesthetically pleasing. It is therefore the task of the muffler designer to ensure that the muffler is functional as well as marketable.

1.3 Background and present state of the problem:

Since the invention of the internal combustion engine in the latter part of the nineteenth century, the noise created by it has been a constant source of trouble to the environment. Significantly, the exhaust noise in terms of pressure is about 10 times all the other noises combined. Therefore, the problems of reducing engine noise consist, mainly in attenuating exhaust noise. Noise legislation for automotive vehicles has led to the development of properly designed exhaust muffler. Well-designed engine exhaust systems collect exhaust gases from engine cylinders and discharge them as quickly and silently as possible. The parametric and shape optimization techniques presented by Key Fonseca de Lima and others produces good designed and optimized reactive mufflers. Reactive mufflers rarefy the sound mainly by increasing and decreasing the cross section of the fluid flow path when the fluid is travelling from one chamber to another. Every change in cross-section results in a reflection of part of the wave with a 180°- phase

shift. This difference in phase results in cancellation of part of the incoming wave. Muffler's performance is mainly dependent on the values of backpressure. Pressure drop of exhaust system includes losses due to piping, muffler, and termination. High backpressure can cause a decrease in engine efficiency or increase in fuel consumption, overheating, and may result in a complete shutdown of the engine potentially causing significant damage.

In Bangladesh, motorcycle industry make muffler just modifying of the old model to new one by trial and error method. Therefore, industry often fails to reach optimum solution. To some extent, they failed to reach closer to optimum solution. Therefore, there is plenty of opportunity to conduct research to find the optimum design criteria for better muffler. Figure 1.3 shows a muffler of a motorcycle named Deviser from Road Mater Motors Ltd. The specification of the motorcycle engine is given in Table 1.1.

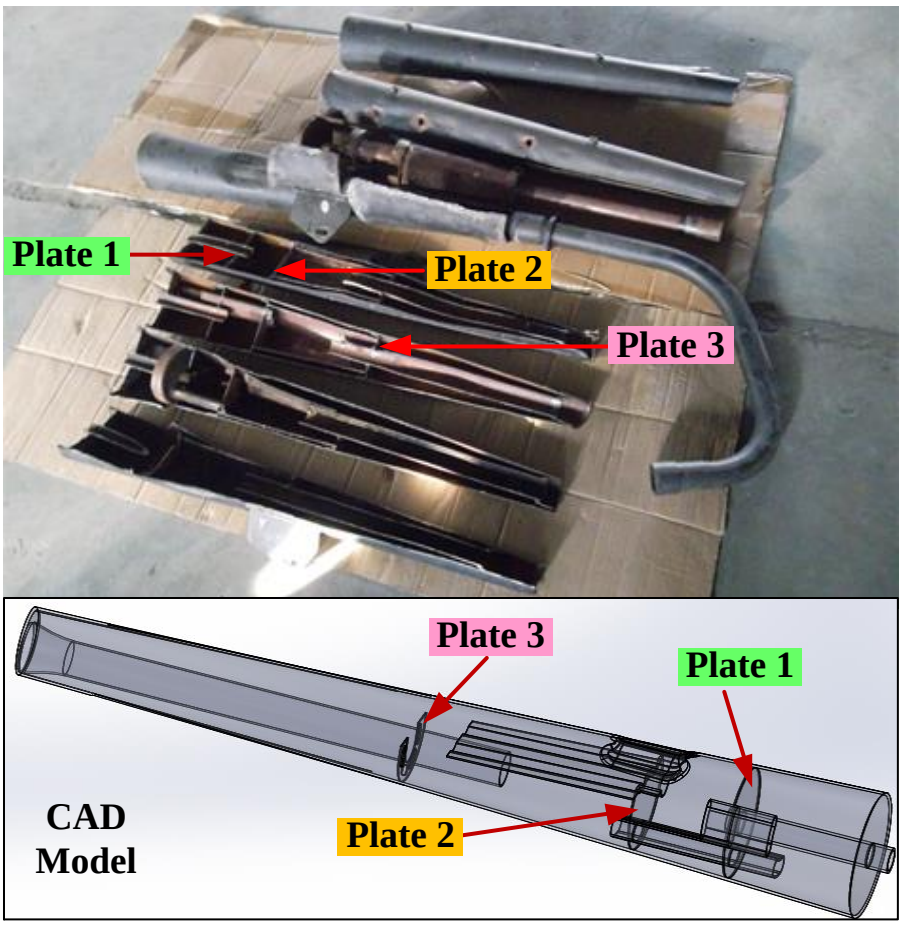

Figure 1.3: Muffler used for Motorcycle Deviser, Roadmaster Motors Ltd.

Table 1.1: Engine Specification

Engine Mode	Single Cylinder, 4-Stroke, Air-cooled
Displacement (ml)	120
Related Power Revolution (Kw/rpm)	6.9/7500
Maximum Torque (N.m/rpm)	7.6/8500
Transmission	5 Speed
Ignition	CDI
Starting Mode	Electric / Kick

Roadmaster Motors Ltd. gives motor parts sales warranty of this model up to 10,000Km run. However, last three years record states that most of the motorcycle owner of this particular model comes to the service center for troubleshooting of the engine muffler after 4,000 to 5,000 Km running. For this reason, the company feels to troubleshoot the problem and redesign the muffler accordingly.

In this context, the muffle has cut and investigated (Appendix C). It has found that, there are some crack and brakeage in the welded joint of plate 1, 2 and 3. Then the muffler is designed in the CAD software and pressure and acoustic transmission loss analysis is conducted for this design. It has also found that the average acoustic transmission loss is not above 30dB (recommended limit for engine muffler) (Nazirkar, et al. 2014) .

For this, the muffler is redesigned and the design is optimized using a novel multi objective optimization technique of Artificial Bee Colony (ABC) and Grey Analysis. Basically, there are five different design criterion of mufflers design. These are - Acoustical Criterion, Aero-dynamical Criterion, Mechanical Criterion, Geometrical Criterion and Economical Criterion. Among these criterions, the research work has been conducted on based on Aero-dynamical Criterion, and also the Geometrical, Economical Criterion with the engine performance viz. backpressure. The new trend in the muffler design process is to use as much as possible the Computer Aided Design (CAD) tools to simulate its behavior for several attributes in order to reduce both time and cost involved in the development process. The experimental tests also have been conducted to find the design performance.

1.4 Objective with specific aims:

Present work aims to design an optimum muffler by CAD design for better performance of the automotive vehicle, moderate acoustic level of the exhaust, possible geometrical shape construct and also economical as per fuel economical and production concept. An experimental setup will also be performed, which will be able to measure performance of the muffler in terms of backpressure, sound level and fuel economical criterions.

The research work has following objectives:

1. To find the problem of existing muffler design by visual investigation and CFD analysis.
2. To study the effect of plate position and perforation effect on current muffler by CFD analysis and design optimization using a hybrid algorithm of Artifical Bee Colony (ABC) and Grey Analysis.
3. To analysis acoustic transmission loss of original design and optimized design.
4. To observe the real effects by making prototype and to validate the design.
5. To introduce a novel idea of Mechanical IRIS in order to improve muffler performance.

1.5 Organization of this thesis

This thesis comprises of seven chapters. Chapter 1 gives a brief overview of the background and concept of this study. Finally, significance of the research and the objectives of this study are summarized. This chapter also outlines the organization of this dissertation.

A comprehensive literature review is given in the Chapter 2, which categorized into three sections. First section describes different research work on muffler analysis. In the second section, different multi objective optimization processes will be discussed. Finally, extensive literature review on Artificial Bee Colony (ABC) with Grey Analysis will be discussed.

Chapter 3 describes the methodology and design of experiment of the study. In addition, it describes the flow chart of optimization algorithm and details description of the algorithm.

Chapter 4 describes the details muffler design process. Moreover, the fabrication process of the muffler and acoustics transmission loss analysis are presented in this chapter.

Chapter 5 presents a novel idea of implementing a mechanical IRIS in the muffler. It also describes the working principle and CFD analysis of the muffler with IRIS.

The conclusions and summary of the contributions are presented in chapter 6. In addition, some directions for future work related to this study are also presented.

Chatper 2 Literature Review

Since the invention of the internal combustion engine in the latter part of the nineteenth century, the noise has become a constant source of trouble to the environment. Significantly, the exhaust noise in terms of pressure is about 10 times all the other noises (structural noise) combined. Therefore, the problems of reducing engine noise consist, mainly in attenuating exhaust noise.

The design of mufflers has been a topic of great interest for many years and hence a great deal of understanding has been gained. Most of the advances in the theory of acoustic filters and exhaust mufflers have come about in the last four decades. Hence, good design of the muffler should give the best noise reduction and offer optimum backpressure for the engine. Moreover, for a given internal configuration mufflers have to work for a broad range of engine speed. Usually when mufflers are designed by well-established numerical techniques like boundary element method or finite element method, the numerical model generation is time consuming often limiting the user to try various other possible design alternates. The process might be lengthy and laborious as it involves a more iteration with different prototypes.

2.1 Muffler Analysis

Limaa et al. (2011) showed the application of shape and parametric optimization techniques in the study of reactive silencers with extended inlet and outlet ducts. Parametric optimization was employed to evaluate the appropriate size of the inlet and outlet ducts. Shape optimization was employed to establish the proper profile of these ducts in order to improve the acoustic features of these mufflers in a specific frequency range. The objective function used in the optimization processes were defined through the average transmission loss (TL) for the desired frequency range. This type of objective function is strongly non-linear and the genetic algorithm, GA, was chosen as a mathematical method for determining the maximum of this function. The Finite

Element Method with an axisymmetric formulation along with the modified four-parameter method were used to calculate the TL.

Blanco et al. (2001) described methodologies developed to reduce the noise radiated from silencers while keeping or improving engine performance; i.e. whilst minimizing the pressure loss through the silencer. That work was successfully developed to help motorcycle designers to meet the current legal noise limitations with minimum detriment to engine performance. Innovative designs for reactive silencers have resulted, with improved acoustic and engine performance levels, compared with traditional systems. The methodology was developed using the boundary element method (BEM). That method was able to calculate the acoustic variables in the interior and exterior fluid of the silencer.

The transfer matrix method is known to be well suited for a complete analysis of a lumped as well as distributed element, one-dimensional, linear dynamical system with a marked chain topology. However, general subroutines of the type available for classical matrix methods are not available in the current literature on transfer matrix methods. **Munjal et al. (1973)** presented a general expression for various aspects of analysis-viz., natural frequency equation, modal vectors, forced response and filter performance—have been evaluated in terms of a single parameter, referred to as velocity ratio. Subprograms have been developed for use with the transfer matrix method for the evaluation of velocity ratio and related parameters. It was observed that the transfer matrix method with the velocity ratio approach has certain advantages over the existing general matrix methods in the analysis of one-dimensional systems.

Munjal et al. (1975) developed a method for the evaluation of exhaust muffers with mean flow. A new set of variables, convective pressure and convective mass velocity, have been defined to replace the acoustic variables. An expression for attenuation (insertion loss) of a muffler has been proposed in terms of convective terminal impedances and a velocity ratio, on the lines of the one existing for acoustic filters. In order to evaluate the velocity ratio in terms of convective variables, transfer matrices for various muffler elements have been derived from the basic relations of energy, mass and momentum.

A conventional muffler of internal combustion engine is mostly constructed as a mixture or combination of perforated ducts, baffle or perforated baffle, expansion chamber, etc., and the noise reduction is limited and backpressure is high hence the fuel efficiency is low. In order to solve the problems of traditional exhaust silencers with poor characteristics of noise reduction in low-frequency range and high exhaust resistance, a new theory of exhaust silencer of diesel engine based on counter-phase counteract and split-gas rushing has been proposed. Taking the single-cylinder diesel engine CG25 as the experimental engine, the author measured the exhaust noise and its spectra. (**Shao, 2011).**

Young et al. (1975) showed a numerical technique based on the finite−element method has been developed for analyzing the performance of systems of acoustic elements including expansion chambers in mufflers. The theories developed are, firstly, the variational formulation of the acoustic field existing in the system and, secondly, the finite−element approximate solutions of the variational problems. The predictions of transmission loss were then made by forming the equivalent acoustic four−terminal transmission network in which the acoustic four−pole constants were calculated from the finite−element method.

Commercial automotive mufflers are often too complex to be broken into a cascade of one-dimensional elements with predetermined transfer matrices. **Panigrahi et al. (2007)** attempted to exploit the speed of the one-dimensional analysis with the flexibility, generality and user-friendliness of three-dimensional analysis using geometric modeling. A code based on the developed algorithm has been employed to demonstrate the generality of the proposed method in analyzing commercial mufflers by considering three very diverse classes of mufflers with different kinds of combinations of reactive, perforated and absorptive elements.

Middelberg et al. (2004) have modeled different configurations of simple expansion chamber mufflers, including extended inlet/outlet pipes and baffles, numerically using Computational Fluid Dynamics (CFD) in order to determine their acoustic response. The CFD results were compared with published experimental results. The CFD model consisted of an axisymmetric grid with a single period sinusoid of suitable amplitude

and duration imposed at the inlet boundary. The time history of the acoustic pressure and particle velocity was recorded at two points, one point in the inlet pipe and one point in the outlet pipe. These time histories are Fourier Transformed and the transmission loss of the muffler was calculated.

A three-dimensional finite element method has been implemented to predict the transmission loss of a packed muffler and a parallel baffle silencer for a given frequency range by **Mehdizadeh et al. (2005).** Iso-parametric quadratic tetrahedral elements have been chosen due to their flexibility and accuracy in modeling geometries with curved surfaces. For accurate physical representation, perforated plates were modeled with complex acoustic impedance while absorption linings were modeled as a bulk media with a complex speed of sound and mean density. Domain decomposition and parallel processing techniques were applied to address the high computational and memory requirements.

Bruyneel (2006) presented a general and effective procedure based on a mathematical programming approach for composite structures optimal design, under weight, stiffness and strength criteria. Effective means that the developed approach was able to find a local optimum in few iterations, even with a large number of design variables. In addition, as the formulation may include strength constraints, it was shown that not only plies thickness but also fiber orientations should be considered as design variables. Besides this, it was explained how these angular variables can improve the structural performance.

2.2 Multi objective optimization

Multiobjective optimization of a symmetrically laminated composite plate was presented by Kumar et al. Designs were obtained to realize maximum in-plane compressive load, maximum in-plane shear load, maximum bending strength, and maximum stiffness, two criteria being considered at a time. Design variables were fiber orientations and thicknesses of different layers. It was observed that nonconvex sets appear in the problem and consequently the weighting min-max method, rather than the pure weighting method, was used to reduce the vector maximum problem to a scalar one **(Kumar and Tauchert 2008).**

Pelletier et al. presented a methodology for the multi-objective optimization of laminated composite materials that was based on an integer-coded genetic algorithm. The fiber orientations and fiber volume fractions of the laminate were chosen as the primary optimization variables. Simplified micromechanics equations were used to estimate the stiffnesses and strength of each lamina using the fiber volume fraction and material properties of the matrix and fibers **(Pelletier and Vel 2006).**

Venkataraman et al provided an overview of modeling, analysis and optimization complexities encountered in the design of composite panels. Restrictions or limitations on available computer resources have limited research to problems with complexity in one of the areas. Venkataraman provided an overview of the research on optimization of composite panels and identifies new areas where more research and development was needed **(Venkataraman and Haftka 1999).**

Omkar et al. presented a generic method/model for multi-objective design optimization of laminated composite components, based on vector evaluated particle swarm optimization (VEPSO) algorithm. VEPSO was a novel, co-evolutionary multi-objective variant of the popular particle swarm optimization algorithm (PSO). In his work a modified version of VEPSO algorithm for discrete variables has been developed and implemented successfully for the, multi-objective design optimization of composites **(Omkar, Mudigere, et al. 2008).**

Parsopoulos et al. studied a parallel version of the Vector Eval uated Particle Swarm Optimization (VEPSO) method for multiobjective problems. Experiments on well known and widely used test problems are performed, aiming at inves tigating both the efficiency of VEPSO as well as the advan tages of the parallel implementation **(Parsopoulos, Tasoulis and Vrahatis 2004).**

Omkara et al. presented a new, generic method/model for multi-objective design optimization of laminated composite components using a novel multi-objective optimization algorithm developed on the basis of the artificial immune system (AIS) paradigm. A co-variant of the popular clonal selection principle called as the Objective Switching Clonal Selection Algorithm (OSCSA) has been developed and implemented

successfully for the multi-objective design optimization of composites **(Omkara, et al. 2008).**

A multi-objective optimization of the drilling process of a laminate composite material was proposed by Sardiñasa et al. Two mutually conflicting objectives were optimized: material removal rate, which represents the productivity; and delamination factor, which characterizes the superficial quality. A micro-genetic algorithm was implemented to carry out the optimization process. An a posteriori approach was used to obtain a set of optimal solutions **(Sardiñasa, Reisb and Davim 2006).**

An application of a genetic algorithm to a material- and sizing-optimization problem of a plate is described by Costa et al. This approach has obvious advantages: it does not require any derivative information and it does not impose any restriction, in terms of convexity, on the solution space. The plate optimization problem was firstly formulated as a constrained mixed-integer programming problem with a single objective function **(Costa, et al. 2004).**

A methodology for using genetic algorithms with the finite element method to minimise a weighted sum of the mass and deflection of fibre reinforced structures with several design variables was described by Walker et al. The design constraint implemented was based on the Tsai–Wu failure criterion. Symmetrically laminated composite rectangular plates with eight layers were used to demonstrate the technique. Thus, the four fibre orientations and laminate thicknesses were to be determined optimally by defining a design index comprising a weighted average of the objective functions and determining the minimum **(Walker and Smith 2003).**

The task of optimizing a complex system presents at least two levels of problems for the system designer by Grefenstette. First, a class of optimization algorithms must be chosen that is suitable for application to the system. Second, various parameters of the optimization algorithm need to be tuned for efficiency. A class of adaptive search procedures called genetic algorithms (GA) has been used to optimize a wide variety of complex systems **(Grefenstette 1986).**

Shuffled Frog Leaping Algorithm (SFLA) is a meta-heuristic for solving discrete optimization problems. Here it was applied to determine optimal discrete pipe sizes for new pipe networks and for network expansions. SFLA was a population based, cooperative search metaphor inspired by natural memetics. The algorithm used memetic evolution in the form of infection of ideas from one individual to another in a local search **(Eusuff and Lansey 2003).**

After outlining analytical methods for layout optimization and illustrating them with examples, the COC algorithm was applied to the simultaneous optimization of the topology and geometry of trusses with many thousand potential members. The numerical results obtained were shown to be in close agreement (up to twelve significant digits) with analytical results **(Zhou and Rozvany 1991).**

Sequential quadratic programming (SQP) methods have proved highly effective for solving constrained optimization problems with smooth nonlinear functions in the objective and constraints. There they considered problems with general inequality constraints (linear and nonlinear) **(Gill, Murray and Saunders 2006).**

Selection of the optimal values of different process parameters, such as pulse duration, pulse frequency, duty factor, peak current, dielectric flow rate, wire speed, wire tension, effective wire offset of wire electrical discharge machining (WEDM) process is of utmost importance for enhanced process performance. The major performance measures of WEDM process generally include material removal rate, cutting width (kerf), surface roughness and dimensional shift **(Mukherjee, Chakraborty and Samanta 2012).**

A survey of current continuous nonlinear multi-objective optimization (MOO) concepts and methods was presented. It consolidates and relates seemingly different terminology and methods. The methods were divided into three major categories: methods with a priori articulation of preferences, methods with a posteriori articulation of preferences, and methods with no articulation of preferences **(Marler and Arora 2004).**

Coello et al. provided a general overview of the field now known as "evolutionary multi-objective optimization," which refered to the use of evolutionary algorithms to solve problems with two or more (often conflicting) objective functions. Using as a framework

the history of this discipline, they discussed some of the most representative algorithms that have been developed so far, as well as some of their applications **(Coello and A, Evolutionary multi-objective optimization: a historical view of the field 2006).**

The genetic algorithm (GA), however, was readily modified to deal with multiple objectives by incorporating the concept of Pareto domination in its selection operator, and applying a niching pressure to spread its population out along the Pareto optimal tradeoff surface **(Horn and Nafpliotis 1994).**

Ehrgott provided a survey of the research in and an annotated bibliography of multiple objective combinatorial optimization, MOCO. He presented a general formulation of MOCO problems, described the main characteristics of MOCO problems, and review the main properties and theoretical results for these problems **(Ehrgott and Gandibleux 2000).**

Jaszkiewicz presented a new genetic local search (GLS) algorithm for multi-objective combinatorial optimization (MOCO). The goal of the algorithm was to generate in a short time a set of approximately efficient solutions that will allow the decision maker to choose a good compromise solution **(Jaszkiewicz 2002).**

The multi-objective optimization of industrial operations using genetic algorithm and its variants, often requires inordinately large amounts of computational (CPU) time. Any adaptation to speed up the solution procedure was, thus, desirable. An adaptation was developed in this study that is inspired from natural genetics. It was based on the concept of jumping genes (JG; transposons) **(B, et al. 2003).**

Coello et al. presented a critical review of the most important evolutionary-based multiobjective optimization techniques developed over the years, emphasizing the importance of analyzing their Operations Research roots as a way to motivate the development of new approaches that exploit the search capabilities of evolutionary algorithms **(Coello and A, A Comprehensive Survey of Evolutionary-Based Multiobjective Optimization Techniques 1999).**

Coello et al. introduced a proposal to extend the heuristic called "particle swarm optimization" (PSO) to deal with multiobjective optimization problems. Their approach

uses the concept of Pareto dominance to determine the flight direction of a particle and it maintains previously found nondominated vectors in a global repository that is later used by other particles to guide their own flight **(Coello and A, MOPSO: a proposal for multiple objective particle swarm optimization 2002).**

Many real world design problems involve multiple, usually conflicting optimization criteria. Often, it is very difficult to weight the criteria exactly before alternatives are known. Multi-Objective Evolutionary Algorithms based on the principle of Pareto optimality were designed to explore the complete set of non-dominated solutions, which then allows the user to choose among many alternatives **(Branke, Kaußler and Schmeck 2001).**

Coello et al. provided a short review of some of the main topics in which the current research in evolutionary multi-objective optimization was being focused. The topics discussed include new algorithms, efficiency, relaxed forms of dominance, scalability, and alternative metaheuristics **(Coello and A, Evolutionary multi-objective optimization: some current research trends and topics that remain to be explored 2009).**

Tripathi et al. described a novel Particle Swarm Optimization (PSO) approach to multi-objective optimization (MOO), called Time Variant Multi-Objective Particle Swarm Optimization (TV-MOPSO). TV-MOPSO was made adaptive in nature by allowing its vital parameters (viz., inertia weight and acceleration coefficients) to change with iterations **(Tripathi, Bandyopadhyay and Pal 2007).**

Parsopoulos et al. constituted a first study of the Particle Swarm Optimization (PSO) method in Multiobjective Optimization (MO) problems. The ability of PSO to detect Pareto Optimal points and capture the shape of the Pareto Front was studied through experiments on well-known non-trivial test functions. The Weighted Aggregation technique with fixed or adaptive weights was considered (Parsopoulos and Vrahatis 2002). The multi-objective generation dispatch in electric power systems treats economic and emission impact as competing objectives, which requires some reasonable tradeoff among objectives to reach an optimal solution. In their study, a fuzzified multi-objective particle swarm optimization (FMOPSO) algorithm was proposed and

implemented to dispatch the electric power considering both economic and environmental issues **(Wang and Singh 2007).**

Evolutionary techniques for multi-objective (MO) optimization are currently gaining significant attention from researchers in various fields due to their effectiveness and robustness in searching for a set of trade-off solutions **(Tan, Lee and Khor 2002).**

Multi response parameter design problems have become increasingly important and have received considerable attention from both researchers and practitioners since there were usually several quality characteristics that must be optimized simultaneously in most modern products/processes **(Hsu 2014).**

Pholdee proposed a hybrid meta-heuristic based on integrating a local search simplex downhill (SDH) method into the search procedure of real-code ant colony optimization (ACOR). This hybridisation leads to five hybrid algorithms where a Monte Carlo technique, a Latin hypercube sampling technique (LHS) and a translational propagation Latin hypercube design (TPLHD) algorithm were used to generate an initial population **(Pholdee and Bureerat 2016).**

Grinding processes aim to produce work pieces with high technological characteristics, such as: fine surface finish, great geometrical accuracy and specific material properties, and specific economic objectives. Despite these technological and economic objectives, it is more and more important to consider the environmental impact of grinding processes **(Winter, et al. 2014).**

Ultrasonic machining (USM) is a mechanical material removal process used to erode holes and cavities in hard or brittle workpieces by using shaped tools, high-frequency mechanical motion and an abrasive slurry. Unlike other non-traditional machining processes, such as laser beam and electrical discharge machining, USM process does not thermally damage the workpiece or introduce significant levels of residual stress, which is important for survival of materials in service **(Goswami and Chakraborty 2015).**

Chen focused on an approach to determine such a range for the Multi-mode Resource Constrained Project Scheduling Problem (MRCPSP), a widely researched, NP-complete

problem, but without adding any subjective considerations to its estimation. They did this by using a concept well known in the domain of thermodynamics, entropy and a three-stage approach. First they used Artificial Bee Colony (ABC)—an effective and powerful meta-heuristic—to determine a schedule with minimized makespan which serves as a lower bound. **(Chen, Liang and Jose 2014)**

2.3 Artificial Bee Colony (ABC) Algorithm

Phama et al. described the first application of the Bees Algorithm to multi-objective optimisation problems. The Bees Algorithm is a search procedure inspired by the way honey bees forage for food. A standard mechanical design problem, the design of a welded beam structure, was used to benchmark the Bees Algorithm. The results obtained show the robust performance of the Bees Algorithm **(Phama and Ghanbarzadeh 2008).**

Omkar et al. presented a generic method/model for multi-objective design optimization of laminated composite components, based on Vector Evaluated Artificial Bee Colony (VEABC) algorithm. VEABC is a parallel vector evaluated type, swarm intelligence multi-objective variant of the Artificial Bee Colony algorithm (ABC). In that work a modified version of VEABC algorithm for discrete variables has been developed and implemented successfully for the multi-objective design optimization of composites. The problem was formulated with multiple objectives of minimizing weight and the total cost of the composite component to achieve a specified strength. Finally the performance was evaluated in comparison with other nature inspired techniques which includes Particle Swarm Optimization (PSO), Artificial Immune System (AIS) and Genetic Algorithm (GA). The performance of ABC was at par with that of PSO, AIS and GA for all the loading configurations **(Omkar, Senthilnath, et al. 2011).**

Akbaria et al. presented a multi-objective optimization method based on the artificial bee colony, called the MOABC, for optimizing problems with multiple objectives. The employed bees adjust their trajectories based on the non-dominated solutions maintained in the external archive. On the other hand, the onlooker bees select the food sources advertised by the employed bees to update their positions. The qualities of these food sources are computed based on the Pareto dominance notion. The scout bees were used

by the MOABC to get rid of food sources with poor qualities. The proposed algorithm was evaluated on a set of standard test problems in comparison with other state-of-the-art algorithms **(Akbaria, et al. 2012).**

Hedayatzadeh et al. proposed a multi-objective artificial bee colony (MOABC) for optimizing problems with multiple objectives. They have adapted the original Artificial Bee Colony (ABC) algorithm to multi objective problems with a grid-based approach for maintaining and adaptively assessing the Pareto front. The Pareto set was used to control the flying behaviours of the individuals and structuring the bee colony. The proposed algorithm was evaluated upon numerical benchmark problems **(Hedayatzadeh, et al. 2010).**

Khorsandia et. al presented a fuzzy based modified artificial bee colony (MABC) algorithm to solve discrete optimal power flow (OPF) problem that has both discrete and continuous variables considering valve point effects. The OPF problem was formulated as a multi-objective mixed-integer nonlinear problem, where optimal settings of the OPF control variables for simultaneous minimization of total fuel cost of thermal units, total emission, total real power losses, and voltage deviation were obtained **(Khorsandia, Hosseiniana and Ghazanfarib 2013).**

2.4 Summary

From the above discussion of the literature study following it can be said that there are many algorithm used to optimized multi objective. Whereas no work of multi objective optimization is done by Artificial Bee Colony (ABC). Moreover, Grey analysis never used with Artificial Bee Colony (ABC). Even Multi objective optimization algorithm not yet conducted in muffler design. Therefore, using this type of hybrid technique of muffler design optimization not done before. In addition, until now no researcher used mechanical IRIS for improving the performance of engine muffler.

Chatper 3 Methodology and Design of Experiment

3.1 Introduction

Engine muffler is one of the important part of an automobile system. Figure 1.1 shows cross section of some typically manufactured motorcycle mufflers used in this study. It has been found that these kind of locally manufactured mufflers are not able to provide better fuel consumption per unit distant for a wide range of engine speed.

In order to optimize the design of the muffler the study flow chart is given in Figure 3.1. Here the existing design is modified by CAD software. In order to modify the design the design of experiment is done using central composite design (CCD). After that, backpressure and other plate pressure were calculated using CFD analysis. Then, fitness functions were created for separate conditions and their adequacy were check. Next, Optimization is done using hybrid algorithm of Artificial Bee Colony (ABC) and Grey Analysis. Finally, transmission loss analysis is conducted and compared with the original design.

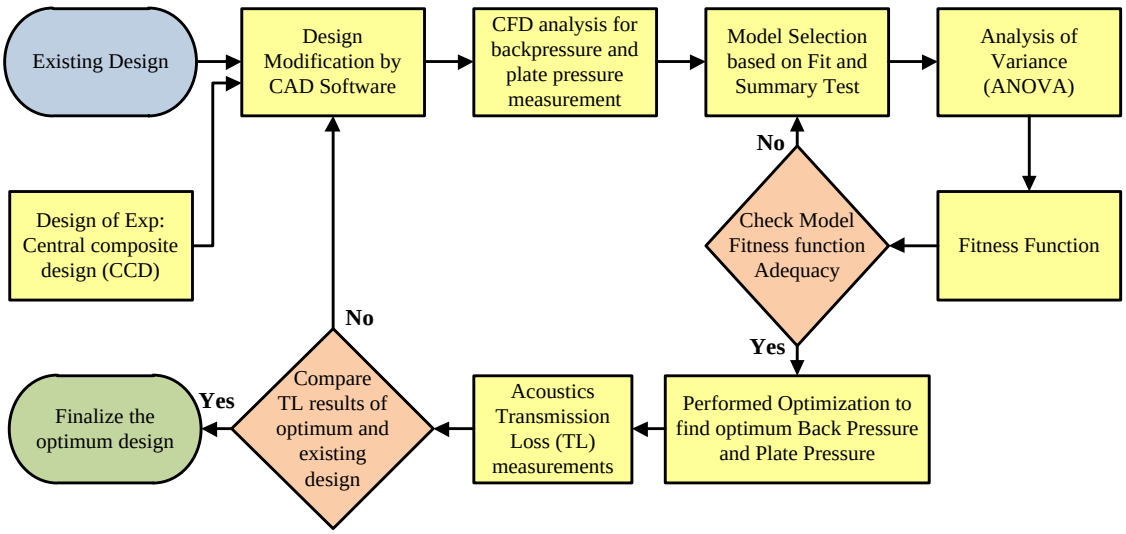

Figure 3.1: Study flow diagram for finalizing the optimum design

3.2 Design of Experiment for Design Modification

3.2.1 Experimental plan

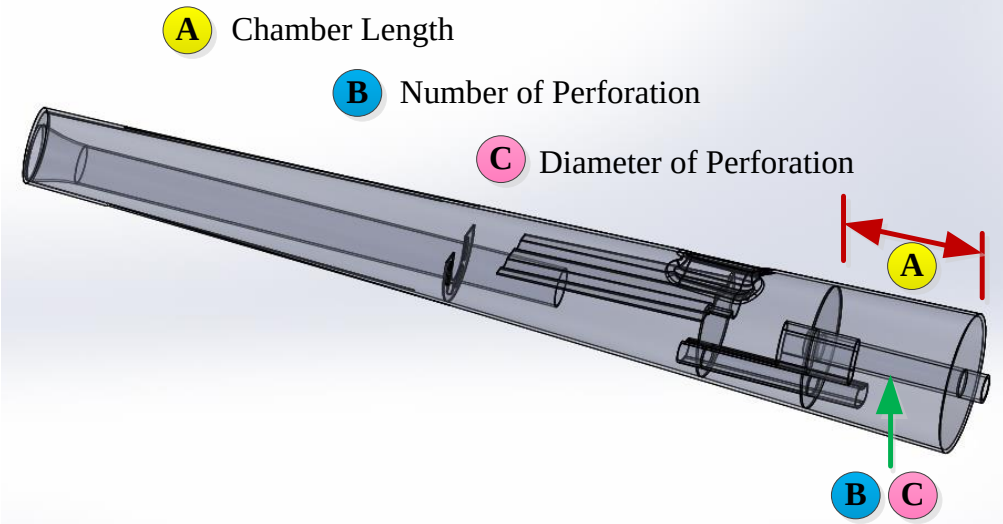

Figure 3.2: Design showing variable parameters of optimization process

Experimental design is widely used for controlling the effects of parameters in many processes. Its usage decreases number of experiments, using time and material resources. Furthermore, the analysis performed on the results is easily realized and experimental errors are minimized. Statistical method measures the effects of change in operating variables and their mutual interactions on process through experimental design way. The three steps used in experimental design included statistical design experiments, estimation of coefficient through a mathematical model and analysis of the model's applicability.

In order to the get the optimize design the internal shape of the muffler is changed depending on the available technology. For this optimization process, the design variable parameters are diameter of perforation, number of perforation and chamber size (Figure 3.2). Table 3.1 shows the limits of the each parameters. The limits are set depending on the manufacturing capability. Table 3.2 shows using central composite design (CCD), total twenty model are designed, where, 14 of them are non-center points and 6 of them are center points. The details of central composite design (CCD) is discussed in the next section.

The output measured variables are back pressure, plate 1 pressure, plate 2 pressure ad plate 3 pressure.

Table 3.1: Parameter values with ranges

Parameters	Symbols	Levels				
		$-\sqrt{2}$	−1	0	+1	$+\sqrt{2}$
Chamber Size [mm]	**A**	75.04	83.10	102.55	122.00	130.06
No of Perforation	**B**	4	5	6	7	8
Diameter of Perforation [mm]	**C**	5.07	5.50	6.55	7.60	8.03

3.2.2 Central Composite Design (CCD)

The experimental design techniques commonly used for process analysis and modeling are the full factorial, partial factorial and central composite rotatable designs. A full factorial design requires at least three levels per variable to estimate the coefficients of the quadratic terms in the response model. Thus for the four independent variables 81 experiments plus replications would have to be conducted. A partial factorial design requires fewer experiments than the full factorial. However, the former is particularly useful if certain variables are already known to show no interaction.

An effective alternative to the factorial design is the central composite design (CCD), originally developed by Box and Wilson and improved upon by Box and Hunter. The CCD gives almost as much information as a three-level factorial, requires much fewer tests than the full factorial and has been shown to be sufficient to describe the majority of steady-state process responses.

The number of tests required for the CCD includes the standard 2k factorial with its origin at the center, 2k points fixed axially at a distance, say b, from the center to generate the quadratic terms, and replicate tests at the center; where k is the number of

variables. The axial points are chosen such that they allow rotatability, which ensures that the variance of the model prediction is constant at all, points equidistant from the design center. Replicates of the test at the center are very important as they provide an independent estimate of the experimental error. For three variables, the recommended number of tests at the center is six. Hence the total number of tests required for the four independent variables is $2^3 + (2 * 3) + 6 = 20$. The experimental layout for the three independent variables using CCD is shown in Table 3.2

The experiments were performed according to the central composite design (CCD) matrix given in Table 3.2. This design is composed of 2^3 factorial design (runs 1-8; see Table 5.2), six-star points (9–14) and 6 replicates runs (14–20).

3.3 Optimization Algorithm: Hybrid ABC and Grey Analysis

3.3.1 Traditional ABC algorithm

ABC algorithm is inspired by the foraging behavior of real bee colony. The objective of a bee colony is to maximize the nectar amount stored in the hive. The mission is implemented by all the members of the colony, by efficient division of labor and role transforming. Each bee performs one of following three kinds of roles: employed bees (EB), onlooker bees (OB), and scout bees (SB). They could transform from one role to another in different phases of foraging. The flow of nectar collection is as follow:

1. In initial phase, there are only some SB and OB in the colony. SB are sent out to search for potential nectar source, and OB wait near the hive for being recruited. If any SB finds a nectar source, it will transform into EB.
2. EB collect some nectar and go back to the hive, and then dance with different forms to share information of the source with OB. Diverse forms of dance represent different quality of nectar source.
3. Each OB estimates quality of the nectar sources found by all EB, then follows one of EB to the corresponding source. All OB choose EB according to some probability. Better sources (more nectar) are more attractive (with larger probability to be selected) to OB.

4. Once any sources are exhausted, the corresponding EB will abandon them, transform into SB and search for new source.

Table 3.2 Central composite rotatable design layout for Experimental design

	Input Variables			Output Variables			
Model No	**A:** Chamber Size [mm]	B: No of Perforation	C: Size of Perforation [mm]	Back Pressure [Pa]	Plate 1 [Pa]	Plate 2 [Pa]	Plate 3 [Pa]
1	83.10	5	5.50				
2	122.00	5	5.50				
3	83.10	7	5.50				
4	122.00	7	5.50				
5	83.10	5	7.60				
6	122.00	5	7.60				
7	83.10	7	7.60				
8	122.00	7	7.60				
9	75.04	6	6.55				
10	130.06	6	6.55				
11	102.55	4	6.55				
12	102.55	8	6.55				
13	102.55	6	5.07				
14	102.55	6	8.03				
15	102.55	6	6.55				
16	102.55	6	6.55				
17	102.55	6	6.55				
18	102.55	6	6.55				
19	102.55	6	6.55				
20	102.55	6	6.55				

In this way, the bee colony assigns more members to collect the better source and few members to collect the ordinary ones. Thus, the nectar collection is more effective.

Analogously, in ABC algorithm, position of nectar source is presented by the coordinate in D-dimensional space. It is the solution vector $\vec{x}$ of some special problem, and the quality of nectar source is presented by the objective function $f(\vec{x})$ of this problem. Accordingly, optimization of this problem is implemented by simulating behaviors of the three kinds of bees. The flowchart of original ABC algorithm is shown in Figure 3.3. The main steps are as follow.

1. Parameters initialization of ABC algorithm.

Population number (PN) and scout bee triggering threshold (Limit) are the key parameters of ABC algorithm. Maximum cycle number (MCN) or ideal fitness threshold (IFT) could be set for terminating algorithm. All variables to be optimized form a D-dimensional vector $\vec{x}$. Restrict both upper bound (UB) and lower bound (LB) of each variable. In this study, the value of PN, MNC and Limits are 20, 50 and 6.

2. Bee colony initialization.

In ABC algorithm, since SB transform into EB, they are not reckoned in PN. Generally, the initial nectar sources are found by PN/2 SB, and then they all transform into EB. The other PN/2 bees are OB. The initial PN/2 solutions are generated by Equation 3.1 in principle. Specified initial value could be used only if needed. All further modifications are based on these PN/2 solutions, which is corresponding to the PN/2 EB.

$$x_i^{(j)} = LB^{(j)} + \phi^{(j)}\left(UB^{(j)} - LB^{(j)}\right)$$
$$\text{where}, i = 1, 2, ..., PN/2 \qquad j = 1, 2, ..., D \tag{3.1}$$

where $x_i^{(j)}$ is the j^{th} elements of the i^{th} solution. $\phi_i^{(j)}$ is uniformly distributed random real number in therange of [0, 1]. Objective function $f(\vec{x})$ is introduced to estimate the fitness of each solution $\vec{x}$. For parameter optimization of SVM classifier, $f(\vec{x})$ could be minimum classification error or maximum classification accuracy. Vector Failure is a counter, length PN/2, and is set to zero for counting optimizing failure of each EB.

3. Each cycle includes following phases:

1) Employed bee: Each EB randomly modifies single element $x_i^{(j)}$ of source *i* by Equation 3.2. Then fitness of the two solutions (before and after modification) is estimated. Greedy selection criterion is introduced to choose the one with better fitness, and the reserved one becomes new solution of this EB. If fitness of EB is not improved after modification, corresponding Failure counters will increase by 1.

$$\bar{x}_i^{(j)} = x_i^{(j)} + \lambda_i^{(j)} \left(x_i^{(j)} - x_k^{(j)} \right) \tag{3.2}$$

where $x_i^{(j)}$ is defined as in formula (2), and $\bar{x}_i^{(j)}$ is the corresponding new element of the solution after modification. $\lambda_i^{(j)}$ is uniformly distributed random real number in the range of [−1, 1], and $x_k^{(j)}$ is the j^{th} elements of $\overrightarrow{x_k}$. Note that $k \neq i$

2) Estimate recruiting probability.

By Equation 3.3, fitness and recruiting probability of each EB are calculated.

$$\begin{cases} \text{Fitness}(i) = \dfrac{1}{1 + f\left(\overrightarrow{x_i}\right)} \\ \text{prob}(i) = \dfrac{\text{Fitness}(i)}{\sum_{i=1}^{PN/2} \text{Fitness}(i)} \end{cases} \tag{3.3}$$

3) Onlooker bee: ‘roulette wheel’ selection mechanism is introduced. It forces each OB following one of EB according recruiting probability. Owing to better solutions corresponding to larger recruiting probability, they obtain more chance to be optimized. Then each solution will be modified again by its followers (OB), using same steps as employed bee phase, from steps 1 to 6.

4) Record best solution. All PN/2 solutions after modification are ranked according to their fitness, and best solution of current cycle is reserved. The termination conditions are then checked. When cycle counter reach the MCN or an ideal solution is found (reach IFT), the algorithm is over.

5) Scout bee. If Failure counters of any solutions exceed Limit, the corresponding solution is abandoned, and scout bee is triggered. For example, if the lth solution is abandoned, a new solution is generated to replace the original one using formula (2), where set $i = l$.

By above operations, ABC algorithm performs optimization. Nevertheless, in both EB and OB phases, the algorithm merely modify single element of the solution in each cycle. If the length of the solution vector D is large, it makes inefficiency improvement in each cycle. Modification Rate (MR) is a real number factor in [0, 1]. For $x_i^{(j)}$ of solution *i*, a uniformly distributed random real number ($0 \le R_i^{(j)} \le 1$) is produced. If $R_i^{(j)} \le MR$, element $x_i^{(j)}$ will be modified and others not. Moreover, if all $R_i^{(j)}$ are larger than MR, ensure at least one parameter being modified by original algorithm. Although this MR-ABC algorithm improves the convergence rate of basic algorithm to some extent, its robustness is not ideal according to testing by abundant experiments.

The flow cart of ABC with RSM is shown in Figure 3.3.

3.3.2 Grey Relational Analysis

The grey system theory initiated by Deng in 1982 has been proven to be useful for dealing with poor, incomplete, and uncertain information. The grey relational analysis based on the grey system theory can be used to solve the complicated interrelationships among the multiple performance characteristics effectively.

In grey relational analysis, black represents having no information system has a level of information between black and white. In other words, in a grey system, some information is known and some information is unknown. In a white system, the relationships among factors in the system are certain; in a grey system, the relationships among factors in the system are uncertain.

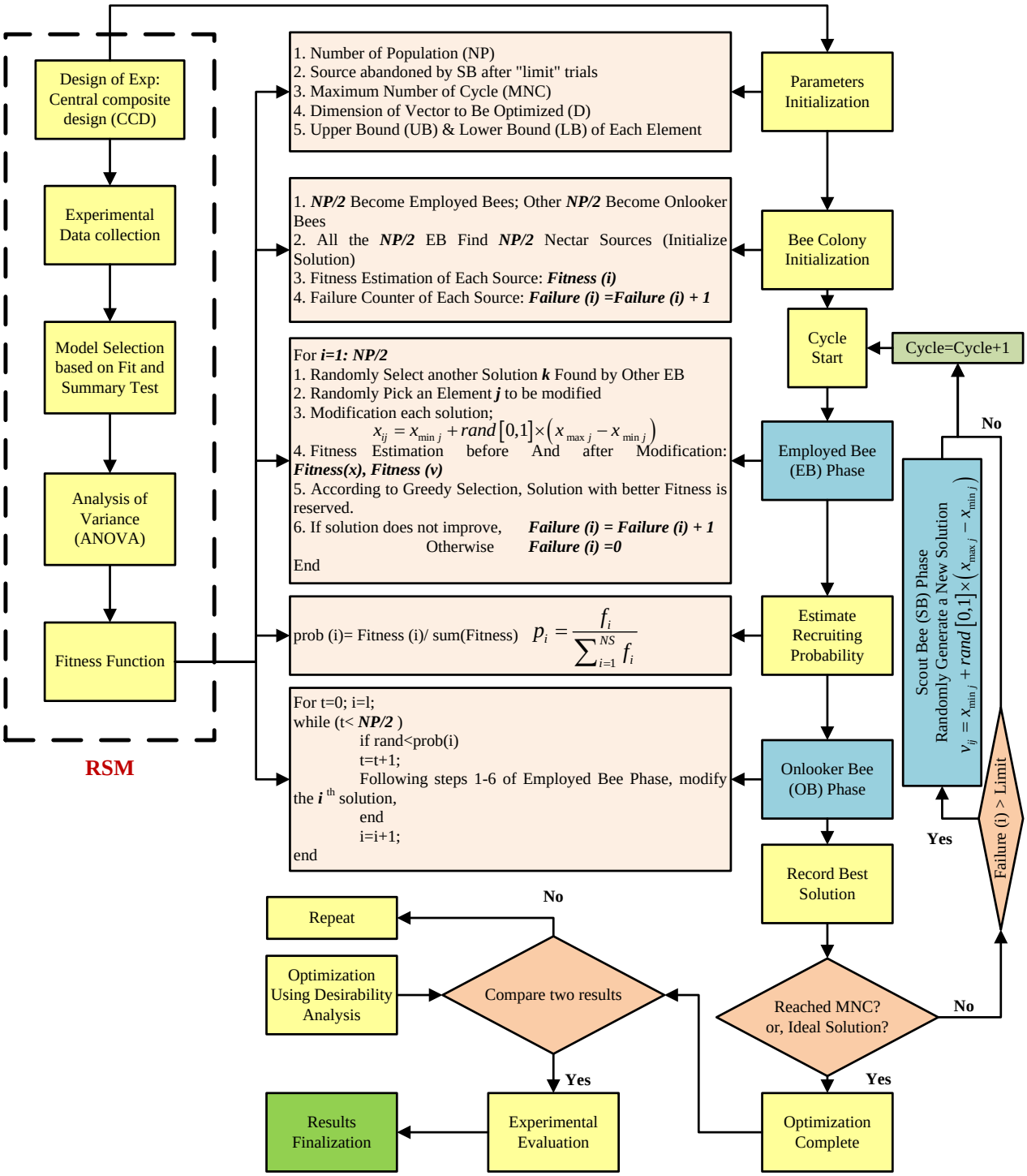

Figure 3.3 Flow chart of ABC with CCD (RSM)

3.3.2.1 Data pre-processing

Data pre-processing is normally required since the range and unit in one data sequence may differ from the others. Data preprocessing is also necessary when the sequence scatter range is too large, or when the directions of the target in the sequences are different. Data pre-processing is a means of transferring the original sequence to a comparable sequence. Depending on the characteristics of a data sequence, there are various methodologies of data pre-processing available for the grey relational analysis.

If the target value of original sequence is infinite, then it has a characteristic of the "higher is better". The original sequence can be normalized as follows:

$$x_i^*(k) = \frac{x_i^0(k) - \min x_i^0(k)}{\max x_i^0(k) - \min x_i^0(k)} \qquad 3.4$$

When the "lower is better" is a characteristic of the original sequence, then the original sequence should be normalized as follows:

$$x_i^*(k) = \frac{\max x_i^0(k) - x_i^0(k)}{\max x_i^0(k) - \min x_i^0(k)} \qquad 3.5$$

Where i =1 … … … m; k = 1 … … … n; m is the number of experimental data items and n is the number of parameters. $x_i^0(k)$ denotes the original sequence, $x_i^*(k)$ the sequence after the data pre-processing, $\max x_i^0(k)$ the largest value of $x_i^0(k)$, $\min x_i^0(k)$ the smallest value of $x_i^0(k)$ and $x_0^*(k)$ is the desired value, which is assumed 1.

3.3.2.2 Grey relational coefficient

In grey relational analysis, the measure of the relevancy between two systems or two sequences is defined as the grey relational grade. When only one sequence, $x_0^*(k)$, is available as the reference sequence, and all other sequences serve as comparison sequences, it is called a local grey relation measurement. After data pre-processing is carried out, the grey relation coefficient $\xi_i(k)$ for the k^{th} performance characteristics in the i^{th} experiment can be expressed as:

$$\xi_i(k) = \frac{\Delta_{\min} + \zeta\Delta_{\max}}{\Delta_{0i}(k) + \zeta\Delta_{\max}} \qquad 3.6$$

where, $\Delta_{0i}(k)$ is the deviation sequence of the reference sequence and the comparability sequence.

$$\begin{aligned} \Delta_{0i}(k) &= \left\| x_0^*(k) - x_i^*(k) \right\| \\ \Delta_{\min} &= \min_{\forall j \in i} \min_{\forall k} \left\| x_0^*(k) - x_j^*(k) \right\| \\ \Delta_{\max} &= \max_{\forall j \in i} \max_{\forall k} \left\| x_0^*(k) - x_j^*(k) \right\| \end{aligned} \qquad 3.7$$

$x_0^*(k)$ denotes the reference sequence and $x_i^*(k)$ denotes the comparability sequence. ζ is distinguishing or identification coefficient: $\zeta \in [0,1]$ (the value may be adjusted based on the actual system requirements). A value of ζ is the smaller and the distinguished ability is the larger. $\zeta = 0.5$ is generally used.

3.3.2.3 Grey relational grade

After the grey relational coefficient is derived, it is usual to take the average value of the grey relational coefficients as the grey relational grade. The grey relational grade is defined as follows:

$$\gamma_i = \frac{1}{n}\sum_{k=1}^{n} \xi_i(k) \qquad 3.8$$

However, in a real engineering system, the importance of various factors to the system varies. In the real condition of unequal weight being carried by the various factors, the grey relational grade in Equation 3.8 was extended and defined as:

$$\gamma_i = \frac{1}{n}\sum_{k=1}^{n} w_k \xi_i(k) \qquad \sum_{k=1}^{n} w_k = 1 \qquad 3.9$$

Figure 3.4 shows how the ABC and grey analysis is synchronized with one another to get the optimum result.

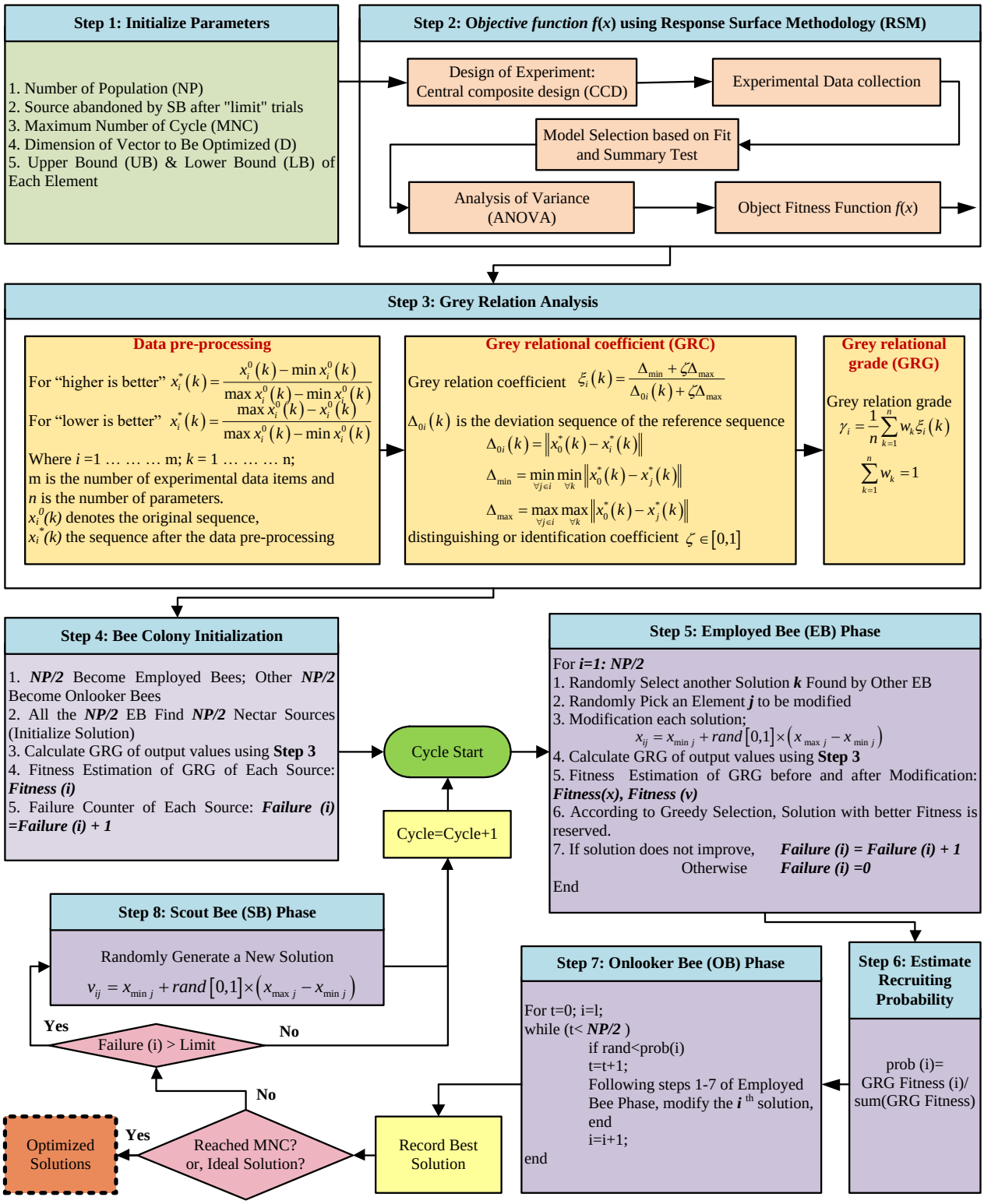

Figure 3.4: Hybrid Algorithm Flow Cart of ABC and Grey Analysis

3.4 Schemes used for CFD analysis

In this study, the speed of the engine is limited to 60 km/hr. The physical model of this test setup would be passing air at fixed mass flow rate through the muffler and measuring pressure drop across the muffler. The time conditions implemented are steady state. The Mass flow rate of the exhaust gas is set as a constant number 114 gm/sec, so the flow is subsonic flow.

The solver implemented was pressure based as it is used for incompressible flows to keep the pressure field from oscillating, which may arise due to difficulties in preserving incompressibility conditions or conservation of mass as the speed of sound become much higher than convection velocity components. Thus to preserve the incompressibility conditions, pressure correction algorithms have to be used, for pressure based solvers.

Pressure velocity coupling refers to numerical algorithm which uses a combination of continuity and momentum equations to derive the equation for pressure when using the pressure based solver. From the available algorithms Semi Implicit with splitting of operators (SIMPLE) is used as it provides solution without iterations, with large time steps and less computing efforts.

In fluent solver variable are stored at the center of grid cells. To solve the transport equations we need to know the values of quantities at the faces of control volume and gradient of these quantities in the cell. The quantities are namely momentum, turbulent kinetic energy, turbulent dissipation rate So, for interpolating the cell center data various interpolating schemes are available in fluent. This interpolation in ANSYS-FLUENT is called upwind schemes. Of the available schemes second order upwind method is used for interpolating the values of these quantities so as to reduce computation effort. Gradients are needed not only for constructing values of a scalar at the cell faces, but also for computing secondary diffusion terms and velocity derivatives. The gradient of a given variable is used to discretize the convection and diffusion terms in the flow conservation equations. Thus, to determine the gradient of these variables Green –Gauss node based method is implemented. This scheme reconstructs exact values of a linear

function at a node from surrounding cell-centered values on arbitrary unstructured meshes by solving a constrained minimization problem, preserving a second-order spatial accuracy. The node-based gradient is more accurate than other gradient schemes especially on (skewed and distorted) unstructured meshes, at a higher computing power cost.

For calculating the cell-face pressure, as pressure based solver is implemented, standard interpolation scheme is used. Most of the engineering flows are turbulent. Turbulence occurs when velocity gradients are high, resulting in disturbances in flow domain as a function of space and time. Turbulent flow arises in contact with walls or in between two neighboring layers of different velocities. With velocity gradient increasing, the flow becomes rotational, leading to vigorous stretching of vortex lines, which can only be supported in three dimensional. So, turbulent flows are always physically three dimensional. In turbulent flows large and small scales of continuous energy spectrum, which are proportional to the size of eddy motions, are mixed. Here, eddies are overlapping in spaces with large ones carrying the small ones. In this process the turbulent kinetic energy transfer from larger eddies to smaller ones, with the smallest eddies eventually dissipating into heat through molecular viscosity.

Therefore, it is necessary to model the turbulence model appropriately. The Standard K-Epsilon model (SKE) is the used as it is accurately represent engineering turbulence for industrial applications. Also, it is Robust and reasonably accurate for a wide range of applications. In addition, it accurately represents low speed incompressible flows in isotropic turbulence.

Standard K-Epsilon model is a Two-equation turbulence models and allows the determination of both, a turbulent length and time scale by solving two separate transport equations. It is based on model transport equations for the turbulence kinetic energy (K) and its dissipation rate (ε). The model transport equation for K is derived from the exact equation, while the model transport equation for ε is obtained using physical reasoning. In the derivation of the K-ε model, the assumption is that the flow is fully turbulent, and the effects of molecular viscosity are negligible. The standard K-ε model is therefore valid only for fully turbulent flows.

3.5 Simulation process

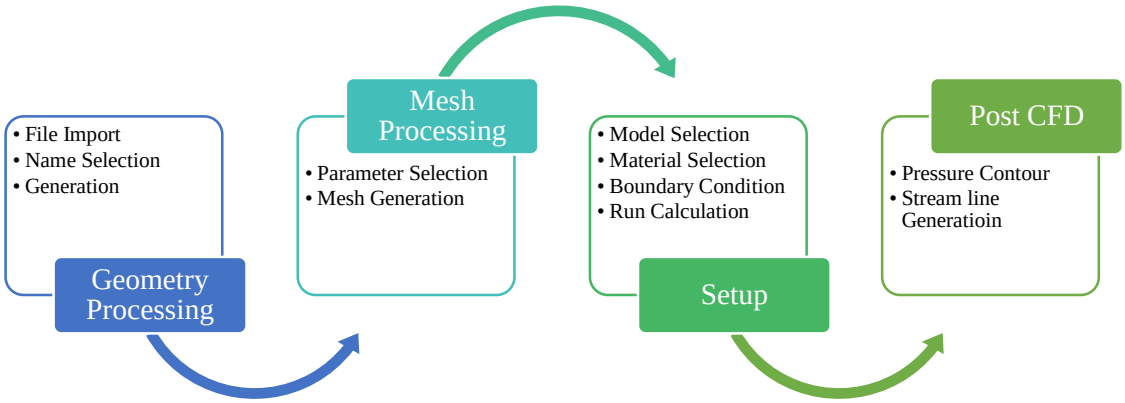

Figure 3.5: Simulation Flow Chart

3.5.1 Geometry processing

Step 1: 1st "Fluid Flow (fluent)" module dragged into Project Schematic. Then "Geometry" started. (Figure 3.6)

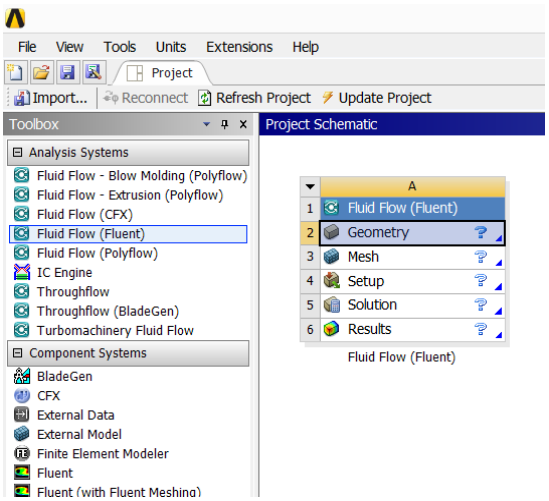

Figure 3.6: "Fluid Flow (fluent)" Start

Step 2: File >> "Import External Geometry Files" (Figure 3.7)

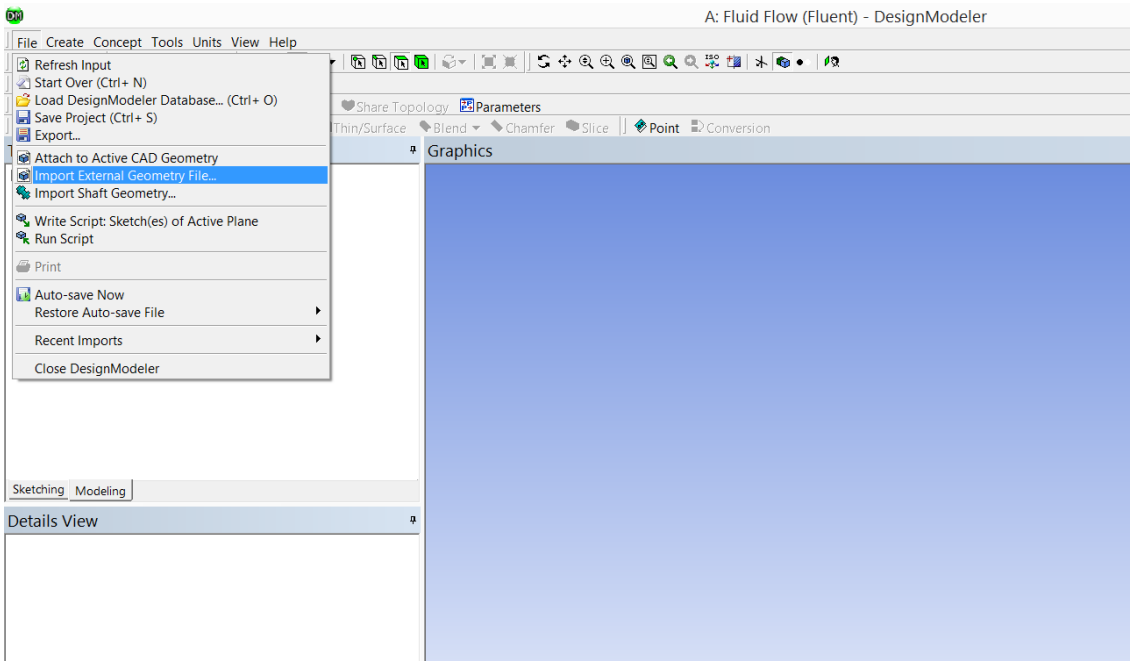

Figure 3.7: File import to Design Module

Step 3: Design file selected from destination folder (Figure 3.8)

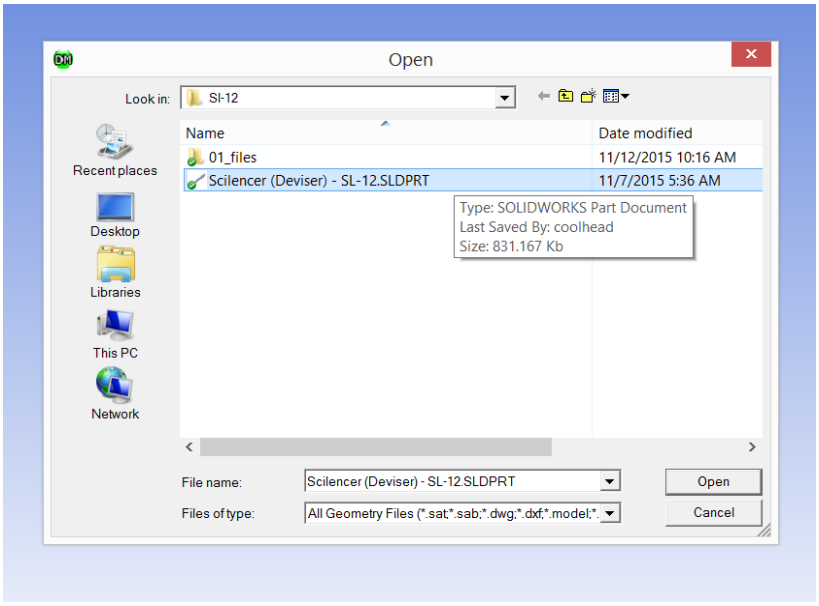

Figure 3.8: Design File selection

Step 4: Design generated from the imported design file (Figure 3.9). Hence it will be seen like Figure 3.10.

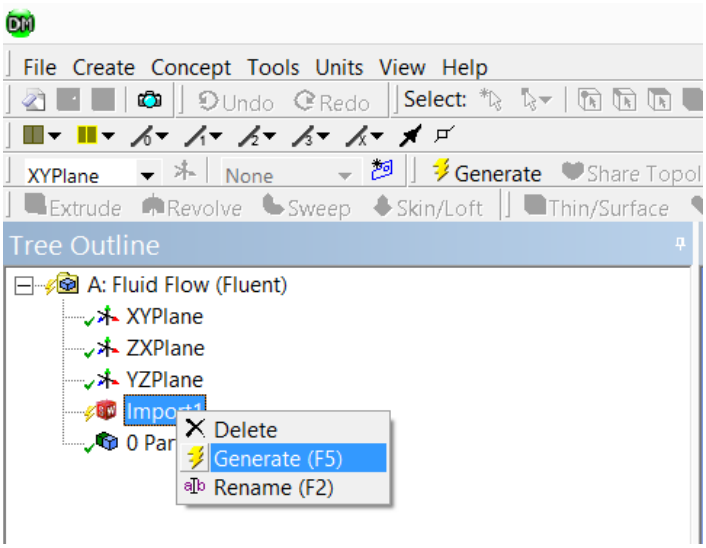

Figure 3.9: Design Generation from the external file import

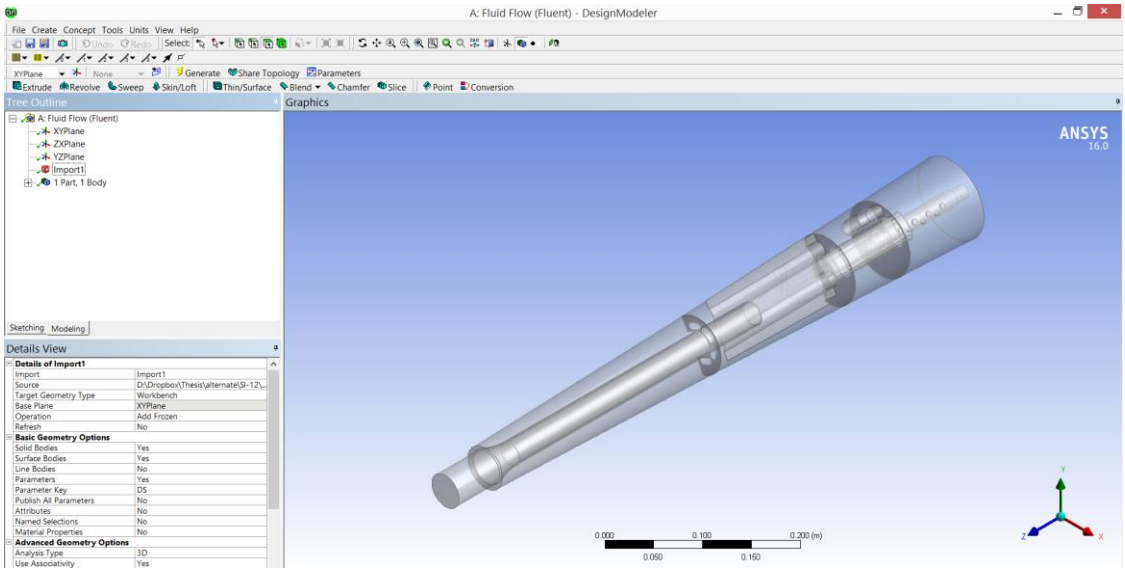

Figure 3.10: Design status after generation

Step 5: After doing right click in desired face “Named selection” to declare different surface (Figure 3.11). Proper name should be declare so that next process will be easier (Figure 3.12). Finally that named selection needs to generate (Figure 3.13).

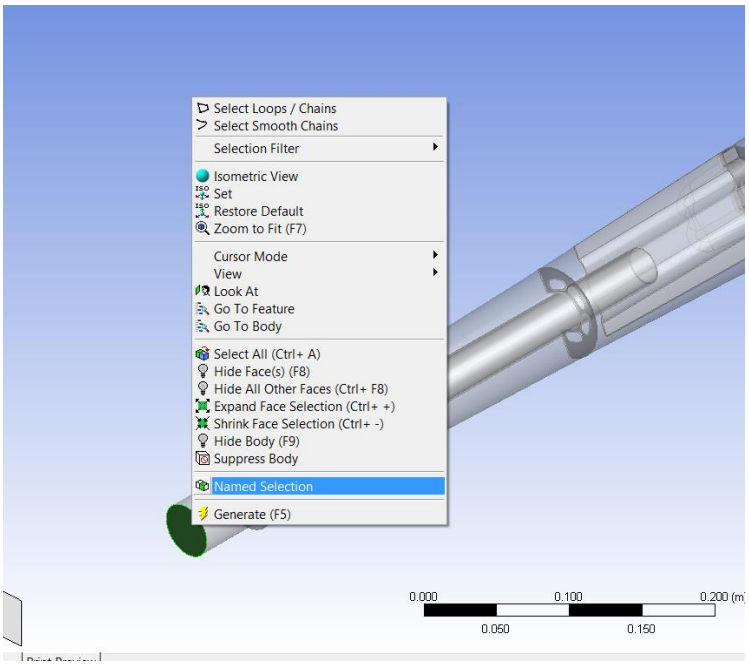

Figure 3.11: Named Selection creation in different position

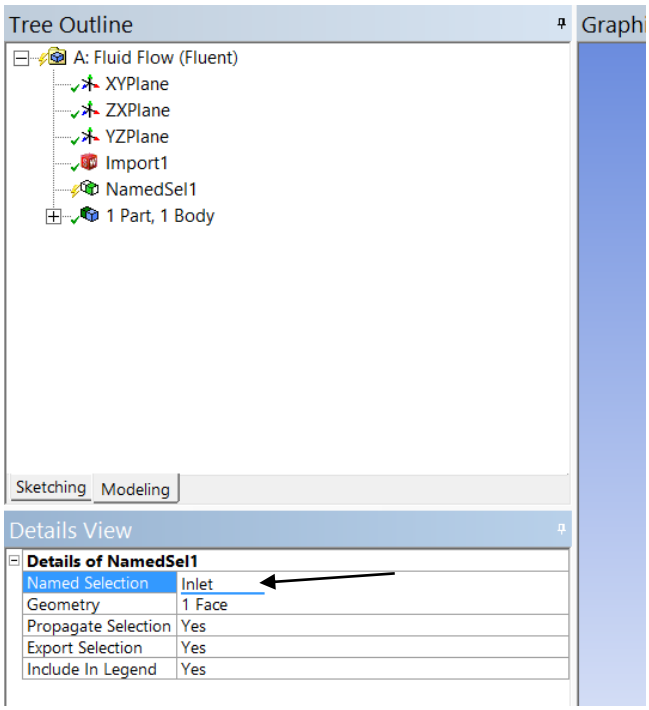

Figure 3.12: Naming of the “Named Selection”

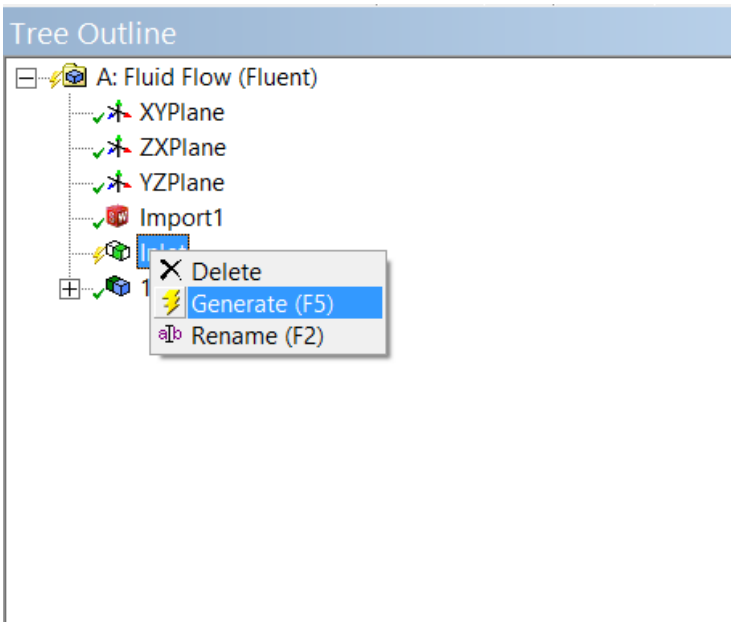

Figure 3.13: Generation of the Named selection

Step 6: Same procedure for other named selection such as “Plate 1” (Figure 3.15), “Plate 2” (Figure 3.16) & “Plate 3” (Figure 3.17). To select properly the exact selection there is an option in bottom corner of Figure 3.14. This avail to select selection beyond the overlapping face.

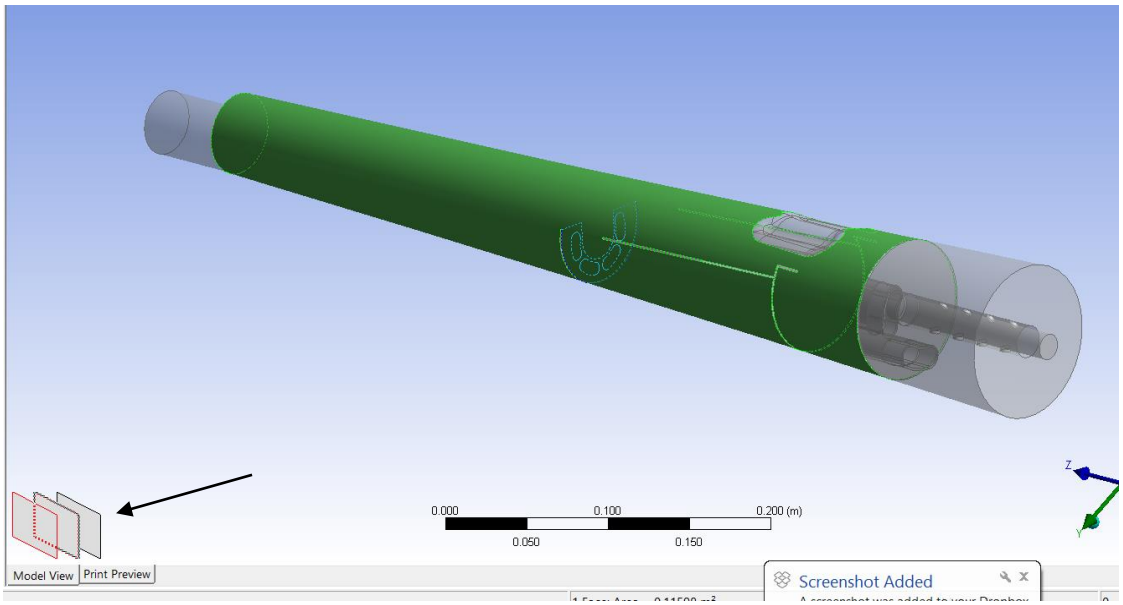

Figure 3.14: Selection process for overlapping face.

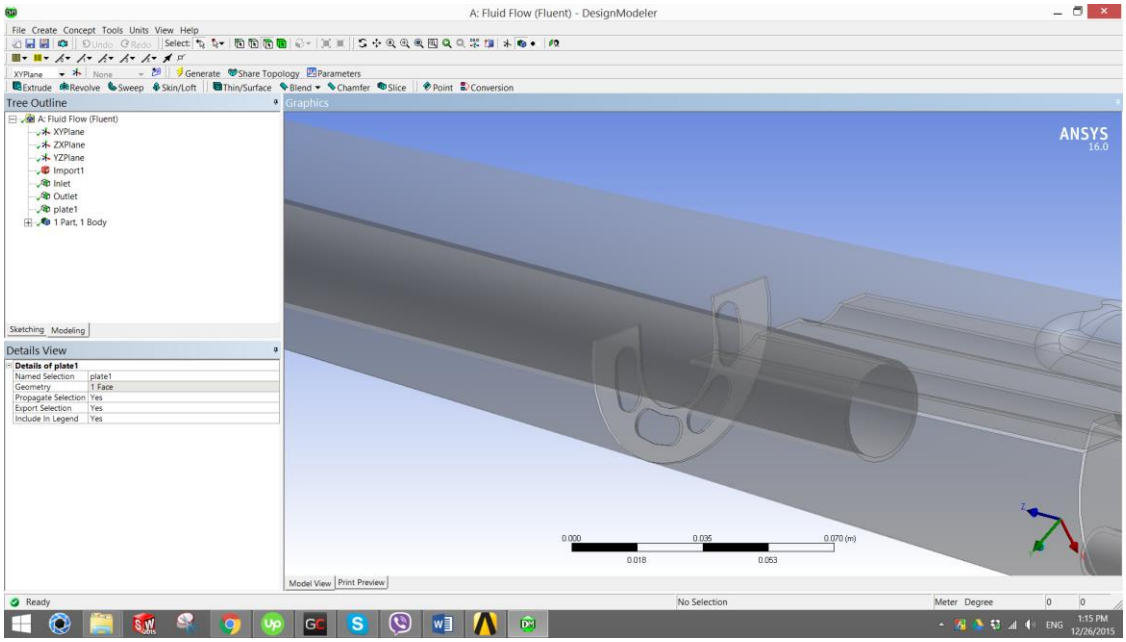

Figure 3.15: “Plate 1” selection

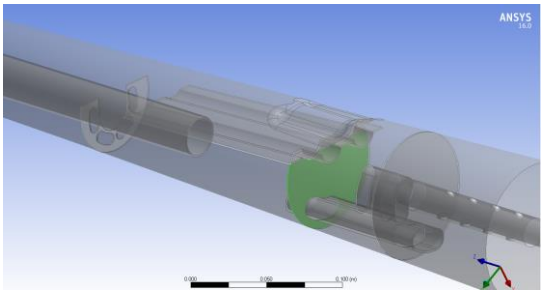

Figure 3.16: “Plate 2” selection

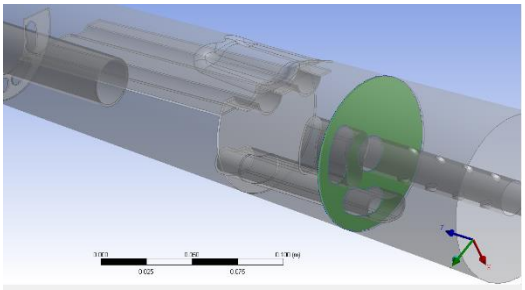

Figure 3.17: “Plate 3” selection

Step 7: Finally the exterior wall selection. To do this all surfaces needs to be selected by (Ctrl + A) and then specific surfaces needs to be deselected like Figure 3.18. Finally, it will be like Figure 3.19. Final status of geometry will be like Figure 3.20.

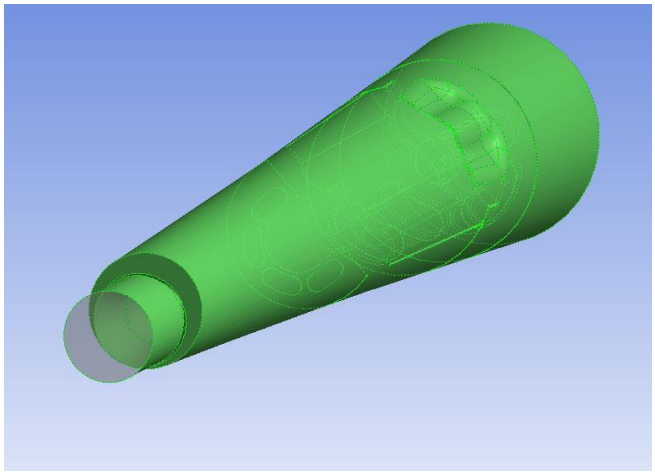

Figure 3.18: Deselecting the other selection from exterior selection.

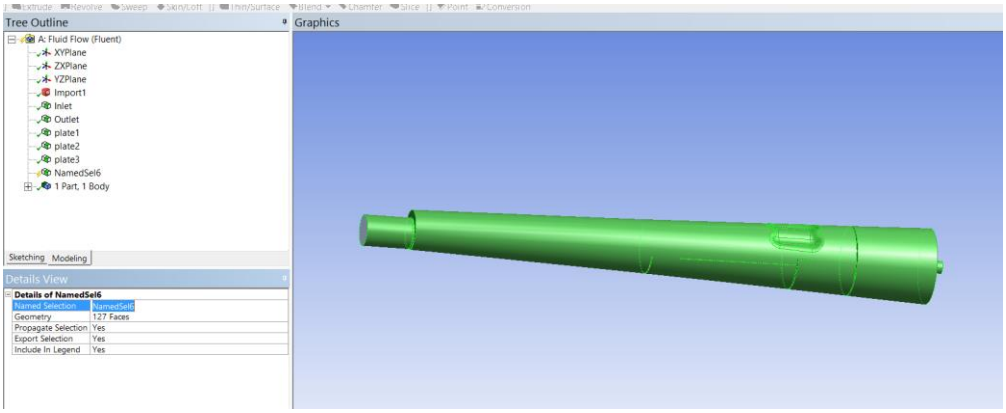

Figure 3.19: Exterior wall selection

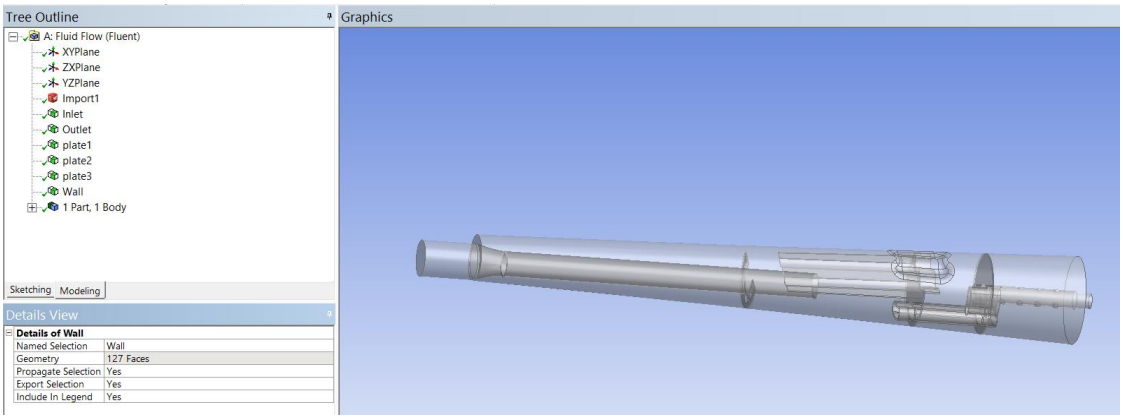

Figure 3.20: Final status of Named Selection

3.5.2 Mesh processing

Step 8: After finishing the geometry "Mesh" Module needs to open to make proper mesh of the design. It is shown in Figure 3.21. After opening the "Mesh Module" in "sizing" there is a option of "Max size". That is marked as "1" in Figure 3.22. This value should be 3mm or less for this type of simulation. For this case 2.4mm is been used. Then finally "Update" button needs to click to generate the mesh data and update into the project. After mesh generation complete Figure 3.23 shows the node number of this mesh.

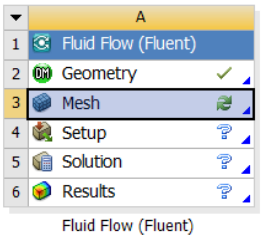

Figure 3.21: "Mesh" in project

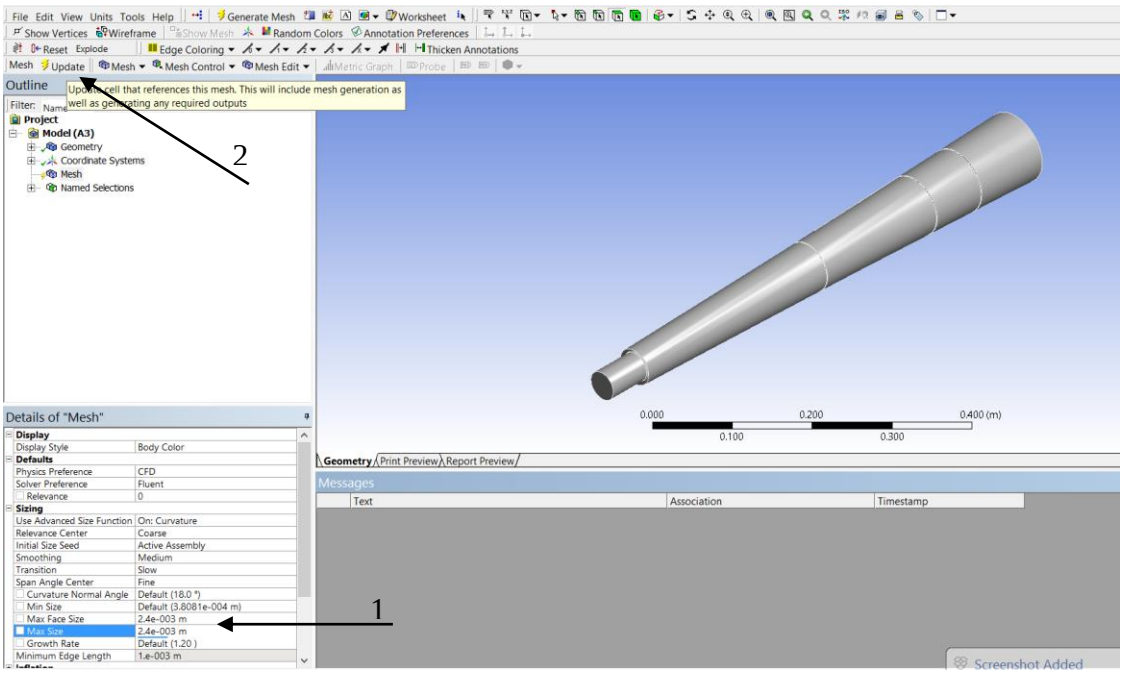

Figure 3.22: Meshing with proper Node size.

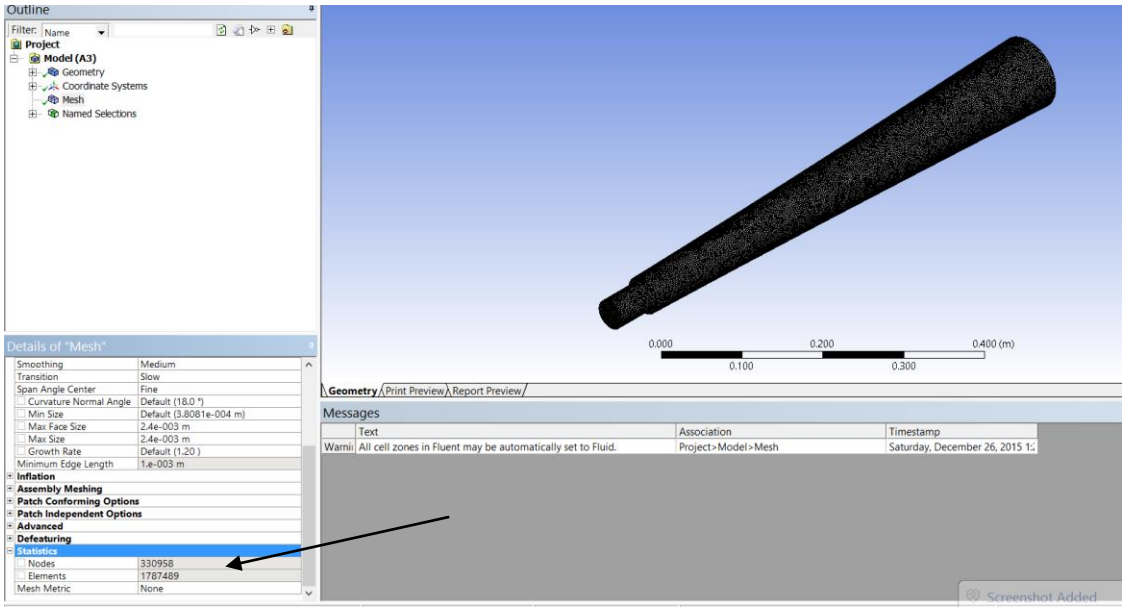

Figure 3.23: Nodes and element number in mesh.

3.5.3 Setup of simulation

Step 9: After "Mesh" done "Setup" module needs to be launched Figure 3.24. After double click in "Setup" Figure 3.25 will appear. There Parallel mode needs to be selected according to CPU core numbers. Also GPU selection option available for good graphics card. It helps to calculate more faster.

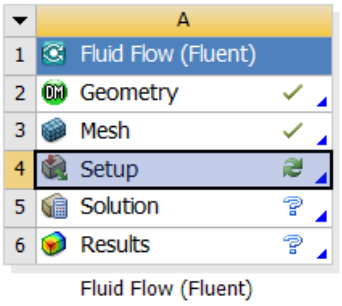

Figure 3.24: Setup module

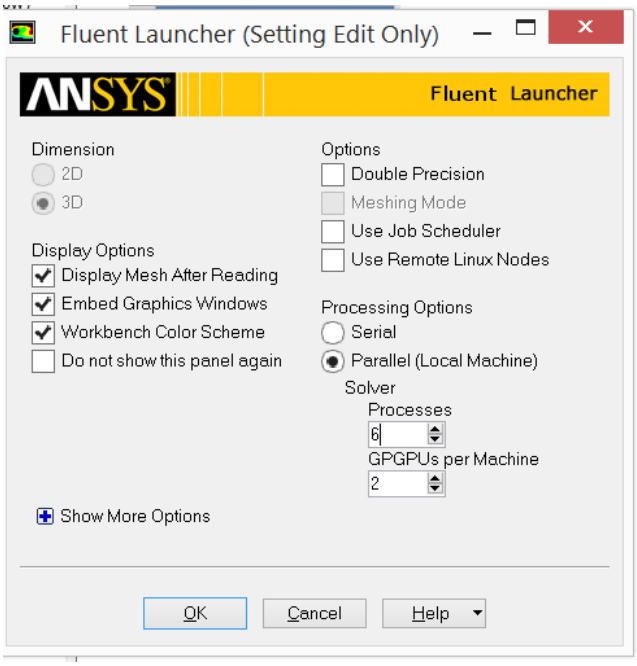

Figure 3.25: Configuration of "Setup Module"

Step 10: In "setup" 1st thing is to select "Pressure-Based" solver shown in Figure 3.26. Figure 3.27 shows the viscosity selection in "Model". Under "viscosity" "k-eplison" mode needs to be selected. Figure 3.28 shows the material customization. Under material double clicking on "Air" will open another window where the desity is given as 1.0675 as density is lower in higher tempereture[1]. Figure 3.29 shows the boundary condition. "Inlet" is been declared as "mass flow inlet". Then Figure 3.30 will appear. There "normal to bourdary" and like Figure 3.31 the value 0.011359kg/s should be set as inlet flow. We collected an experimental setup.

[1] https://en.wikipedia.org/wiki/Density_of_air

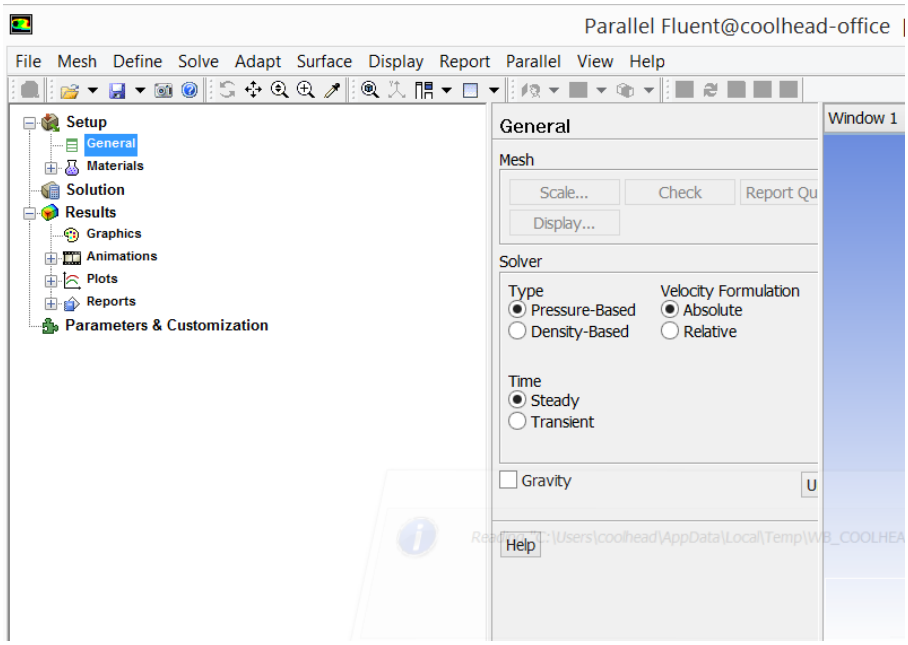

Figure 3.26: “Pressure Based” Solver selection.

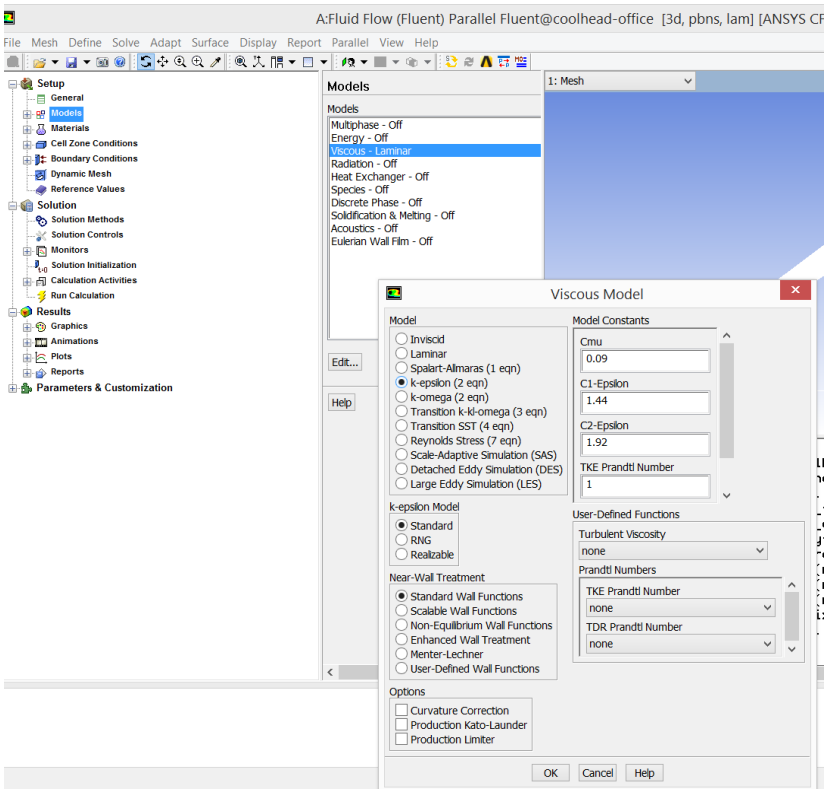

Figure 3.27: Viscosity selection in Model

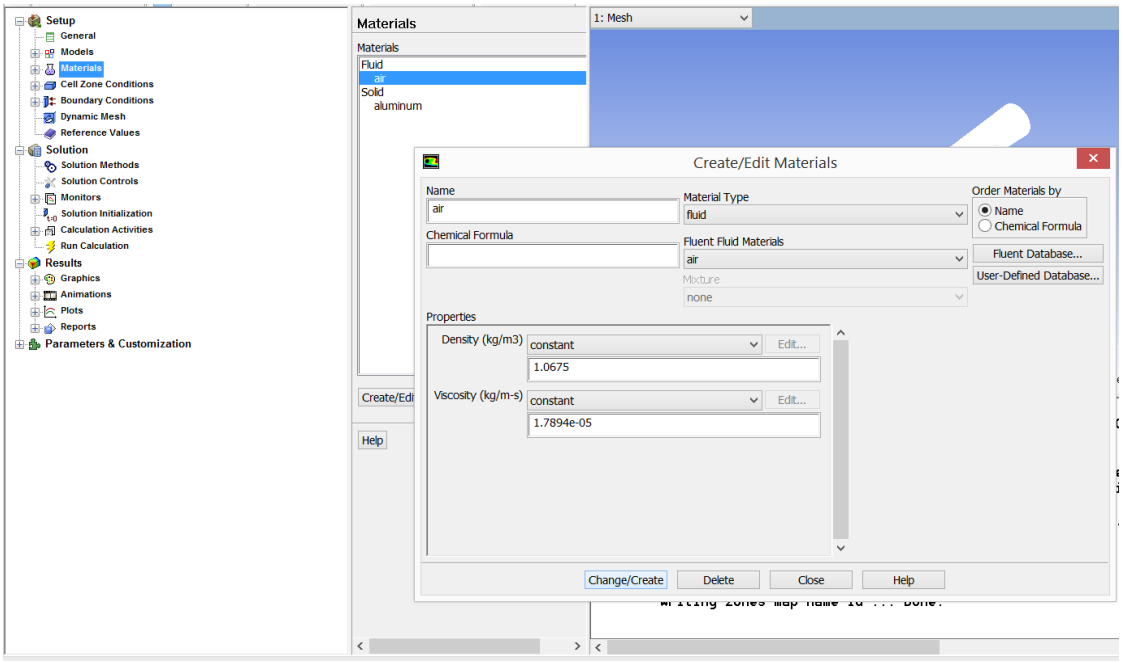

Figure 3.28: Material customization

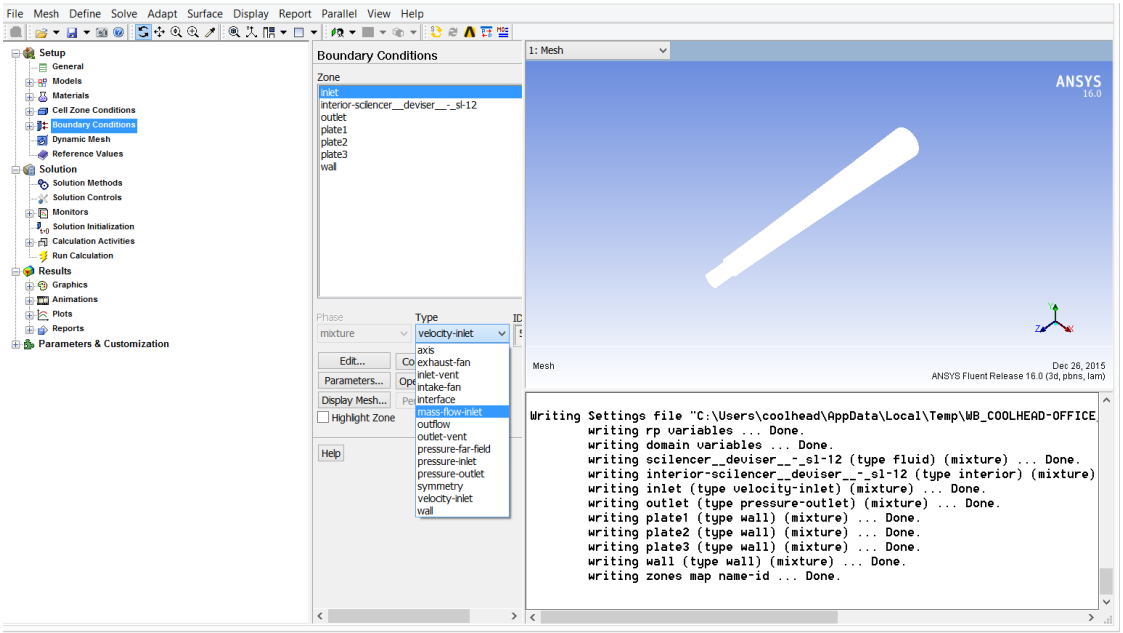

Figure 3.29: Boundary condition for inlet

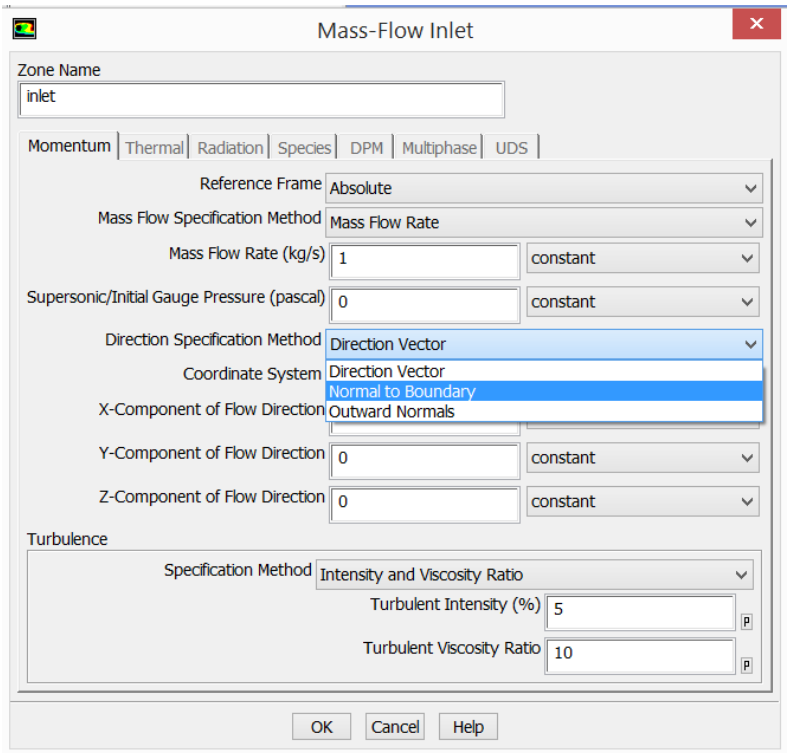

Figure 3.30: Direction of flow selection

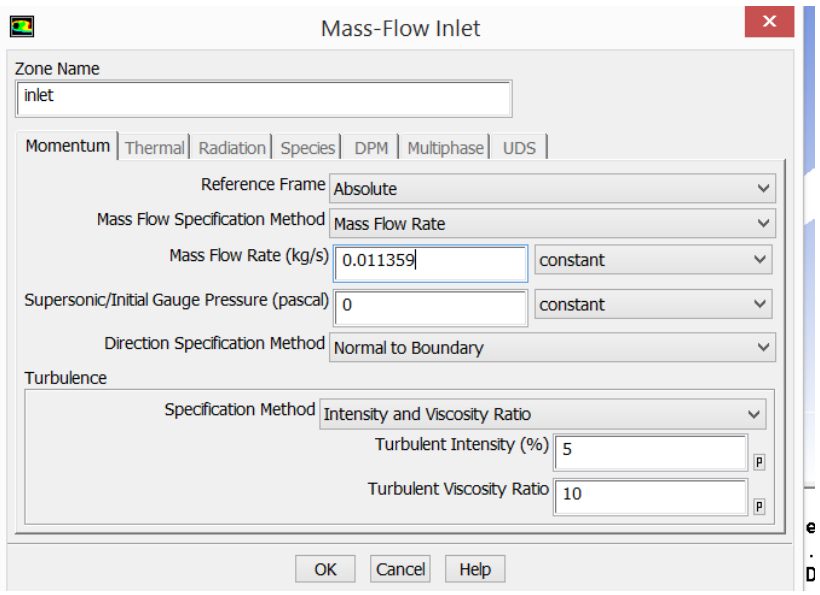

Figure 3.31: Inlet flow value

Step 11: Figure 3.32 shows the reference zone and value set as 0.001133mm square.

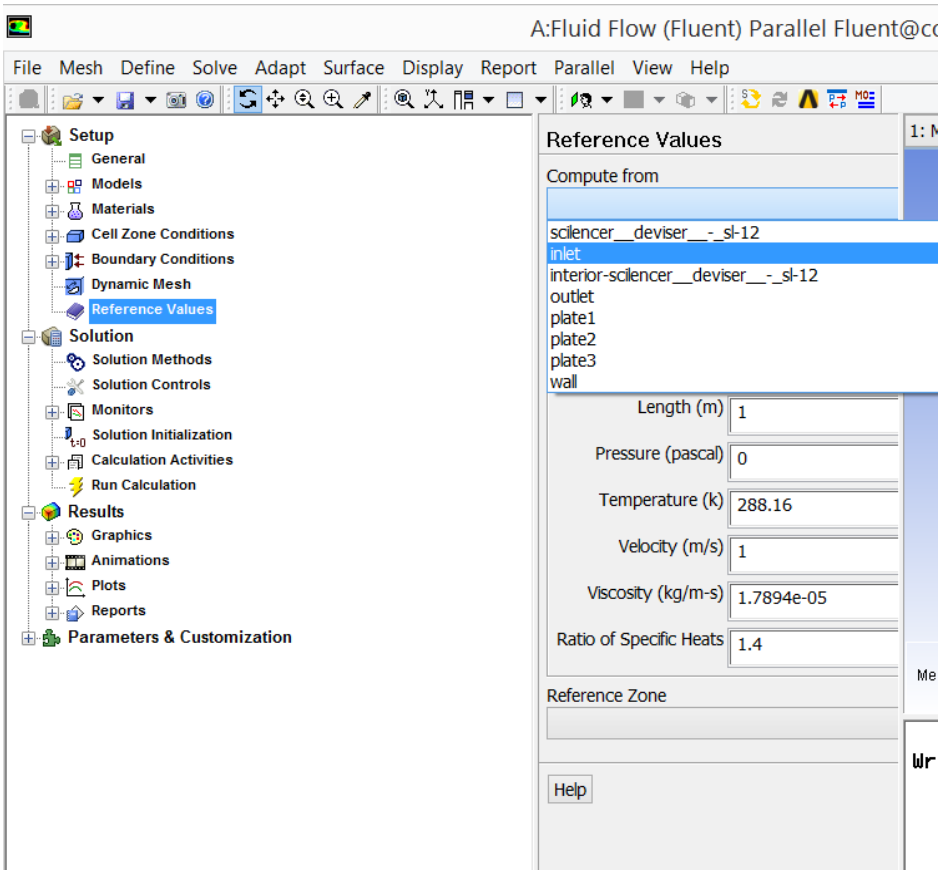

Figure 3.32: Reference zone declaration

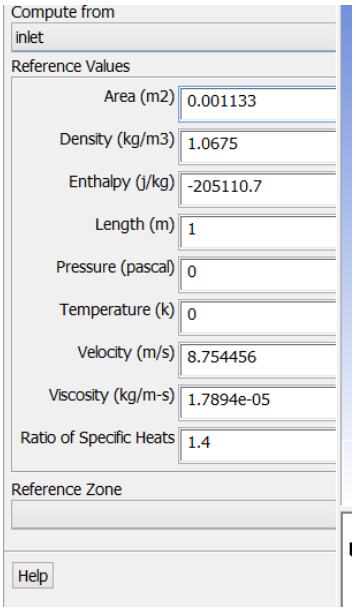

Figure 3.33: Inlet area declaration

Step 12: Figure 3.34 shows the "Solution Method" declaration. There the Gradient selected as "Green-Gauss Node Based". Then Figure 3.35 shows the "Solution Initialization" by selecting the "Inlet" and then clicking on "Initialize" button. Figure 3.36 shows the "Run calculation" segment. There for primary case 600 iteration selected. If necessary 1000 or even 2000 iteration can be selected. If the 600 iteration do not converse then more 1000 can be added later which will start iteration after 600. Therefore, no calculation will be wasted.

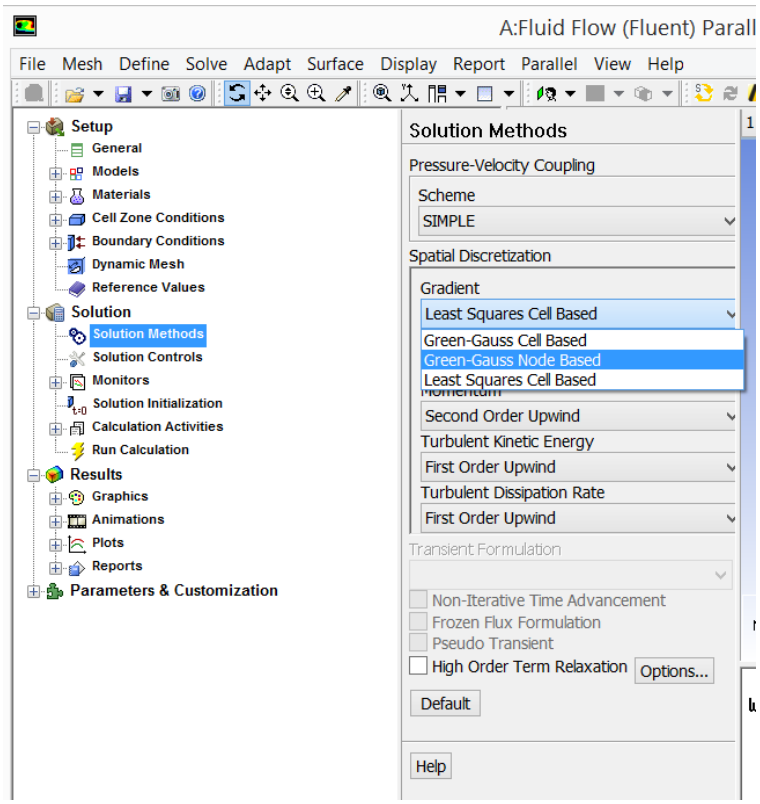

Figure 3.34: Solution method selection.

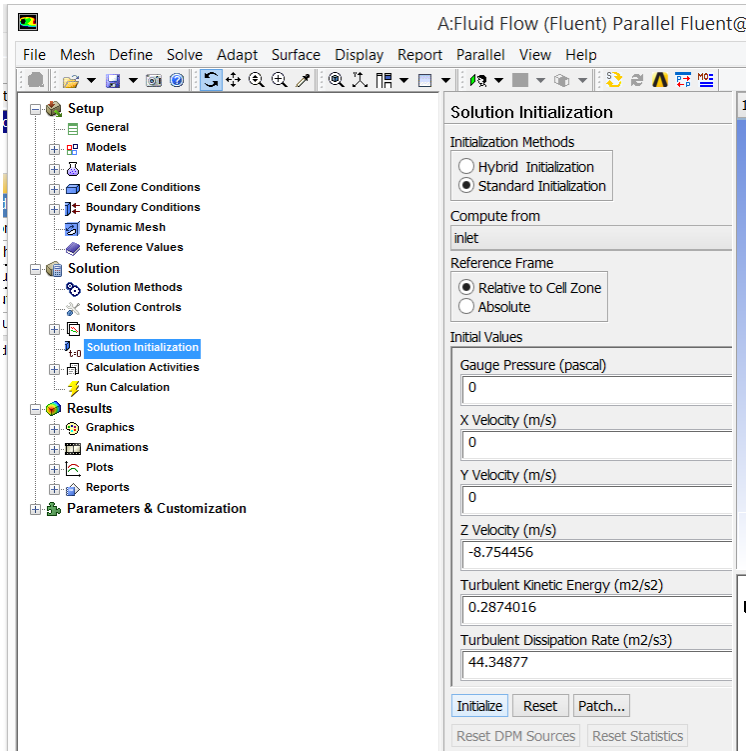

Figure 3.35: Solution Initialization

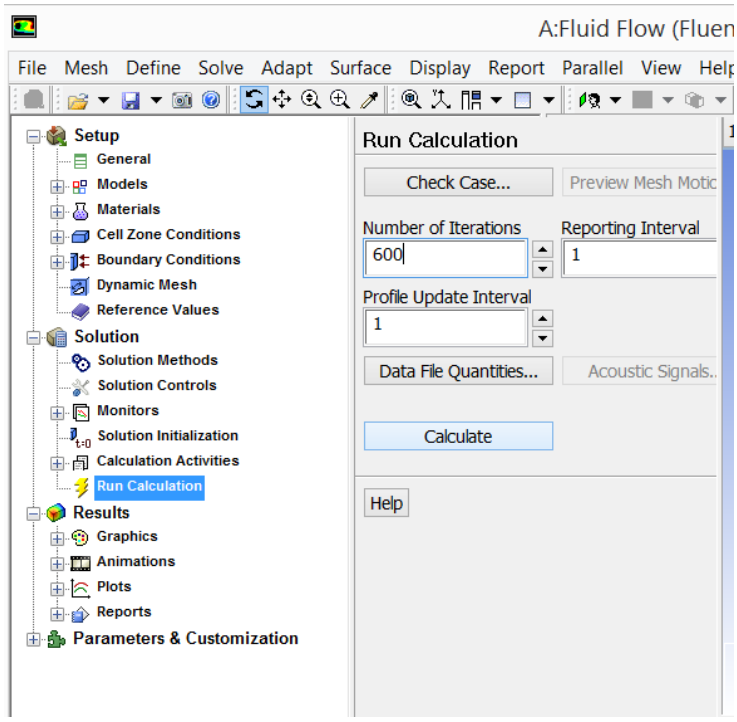

Figure 3.36: Running the Calculation

3.5.4 Solution of Simulation processing

Step 13: After the solution converse the "Solution" module needs to be started from the project menu (Figure 3.37). It will appear like the Figure 3.37. Then contour needs to be selected as Figure 3.39. Then "location" should be selected as "Inlet" like Figure 3.40. Then "variable" as Pressure and "range" as local shown in Figure 3.41. Then after applying the graphics in inlet area seen like marked "1" in that figure. Also the range in marked "2". Figure 3.42 shows another conture for "pressure plate 2".

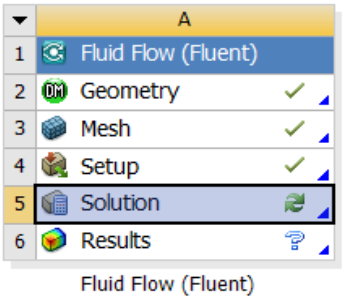

Figure 3.37: Solution module in project

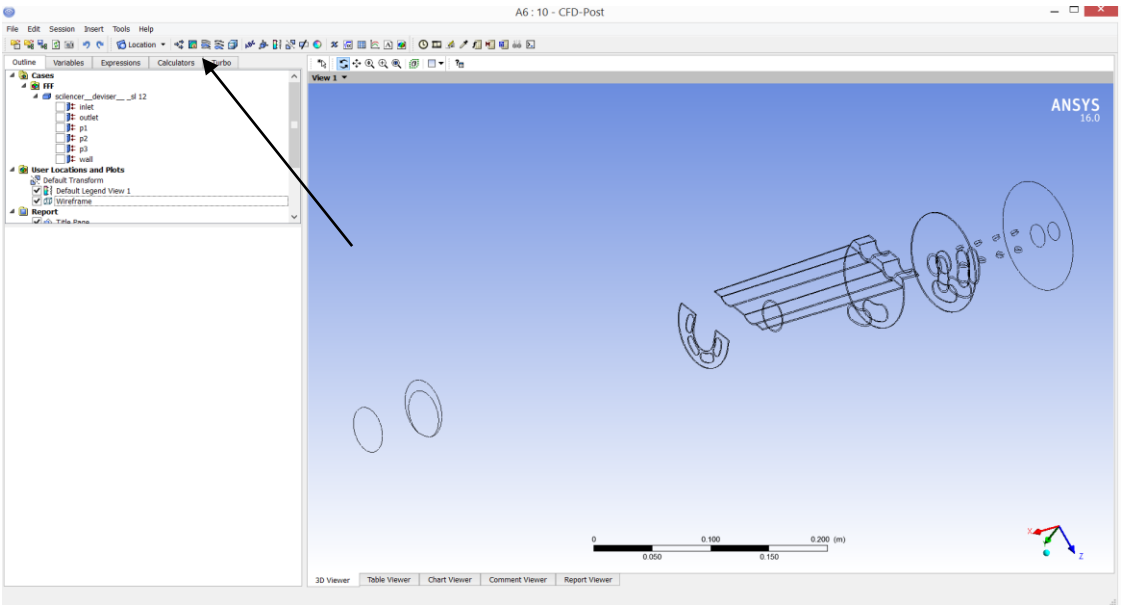

Figure 3.38: Solution module view in wire frame mode

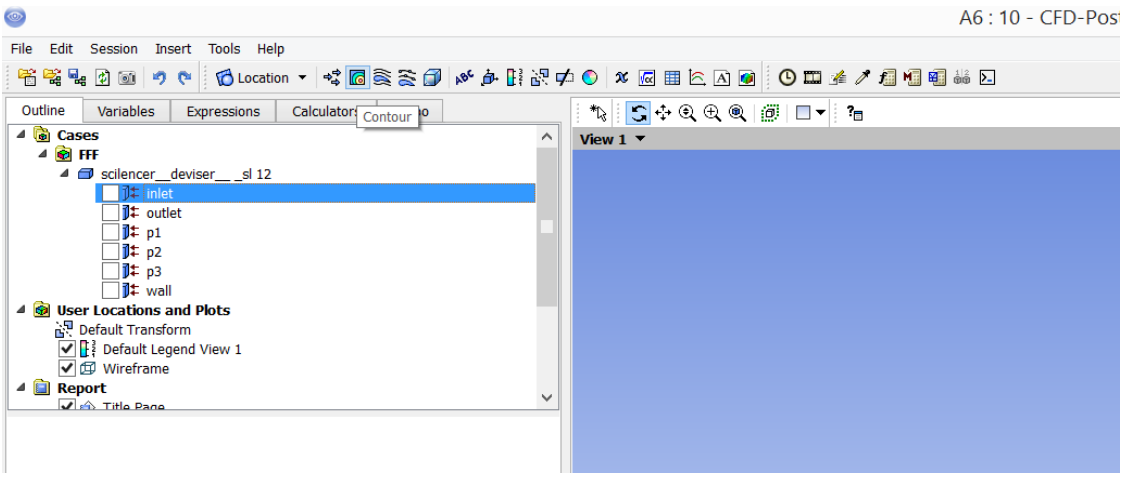

Figure 3.39: Couture selection

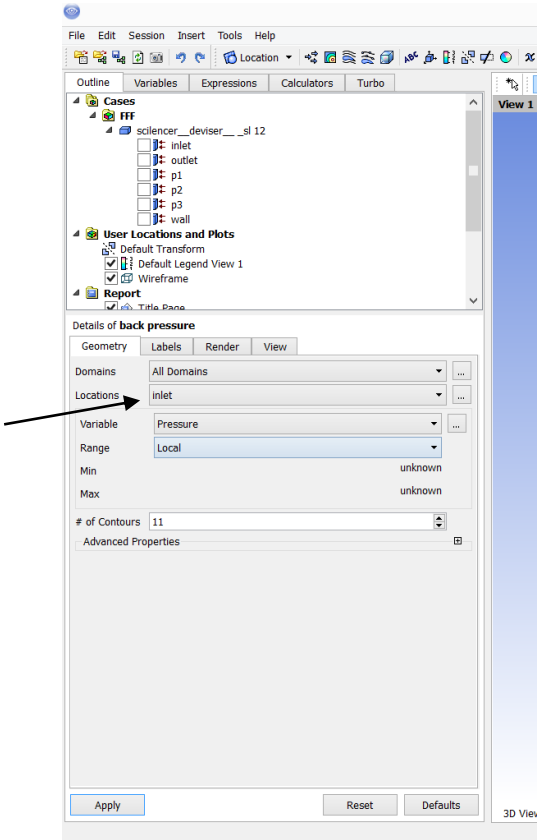

Figure 3.40: Location selection

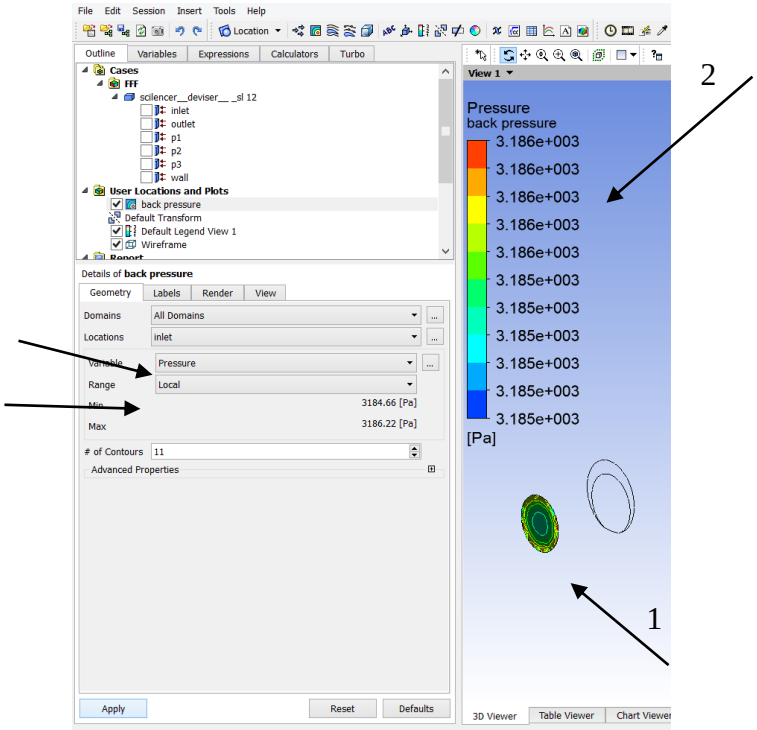

Figure 3.41: Variable and range selection

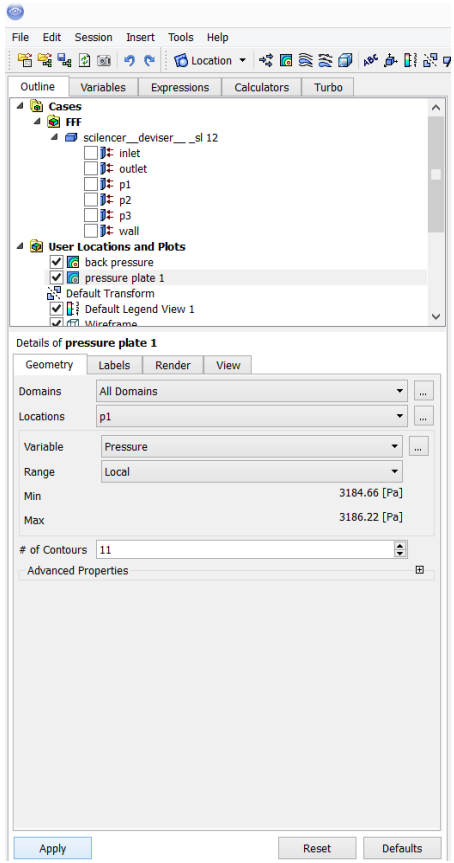

Figure 3.42: Pressure Plate 2 conture

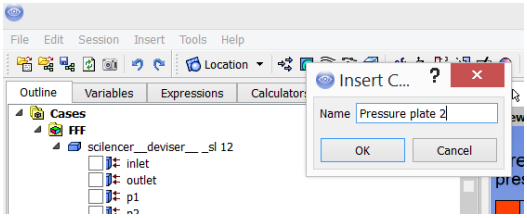

Figure 3.43: Naming of pressure plate 2

3.5.5 Final result processing

Step 14: And then the naming of pressure plate 2 shown in Figure 3.43. The properties of pressure plate 2 conture selected as Figure 3.44. Figure 3.45 shows the steamline button. Figure 3.46 shows the streamline properties. It should start from “inlet” and “# of points” should be at least 100. It also can be set as 150 / 200 for more dense streamline. Finally, Figure 3.47 shwos the streamline and couture altogether.

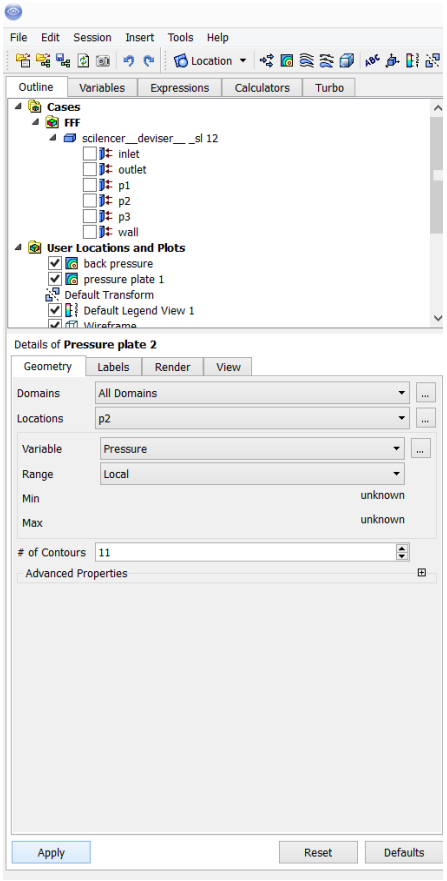

Figure 3.44: Pressure plate 2 properties

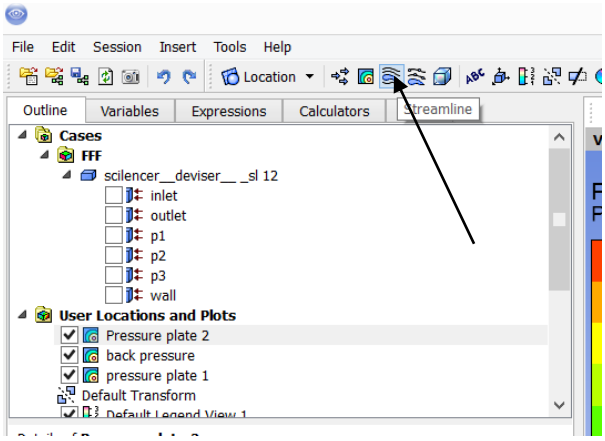

Figure 3.45: Streamline selection

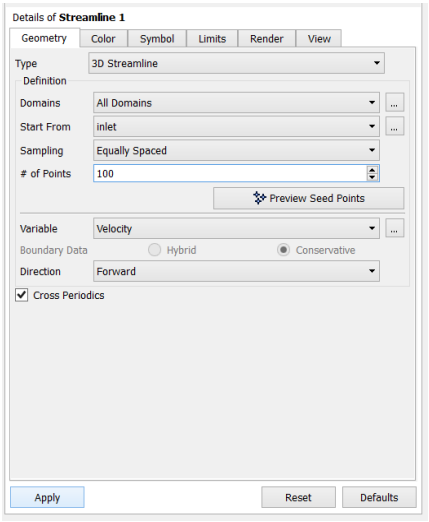

Figure 3.46: Streamline properties

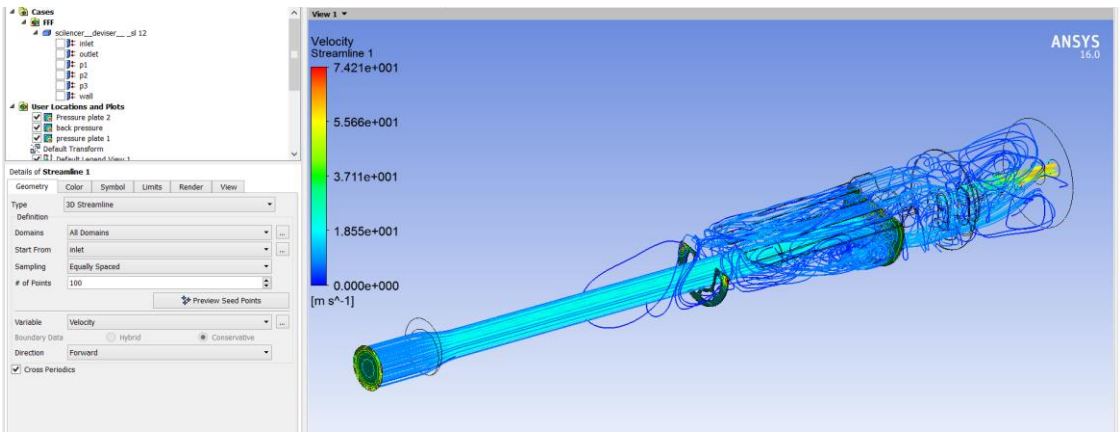

Figure 3.47: Final view of streamline and couture altogether.

This way all the simulation in different configuration is been done for this thesis.

3.6 Final fabrication and Acoustics transmission loss analysis

After the simulation process, the results will be analyzed and optimization process will be used to finalize the optimum results. Once the design is ready then it will be sent to the fabrication shop for muffler fabrication.

It is done in simple way. The major parts are collected from old muffler. Then the chamber size modified and the perforation added according to optimized design. Then a piece of sheet metal wrapped as cone shape of muffler. After that the new optimized setup sent into that cone shaped exterior shell Finally, welded from outside to keep the plate position steady. In this way the fabrication process done for this type of project.

Then acoustics transmission loss analysis will be conducted. This analysis is discussed in the next chapter.

Chatper 4 Design Modification and Optimization

4.1 Introduction

Mufflers are important part of engine system and commonly used in exhaust system to minimize sound transmissions caused by exhaust gases. Design of mufflers is a complex function that affects noise characteristics, emission and fuel efficiency of engine. Therefore muffler design becomes more and more important for noise reduction. Hence good design of the muffler should give the best noise reduction and offer optimum backpressure for the engine.

For this optimization process, the design variable parameters are size of perforation, number of perforation and chamber size. In this study, a combine model of response surface methodology (RSM), ABC and Grey analysis is used for optimizing the backpressure of a motorcycle reactive muffler, in order to improve the performance of the muffler. After that, virtual acoustics transmission loss analysis is conducted for both optimize and original design and compared. Finally, the optimized design is installed in the motorcycle for the real performance.

4.2 Simulation results

The simulation results for twenty different models are given in Table 4.1. In this process backpressure, plate 1 pressure, plate 2 pressure and plate 3 pressure are calculated using ANSYS CFD analysis. Figure 4.1 shows the backpressure and plate 1 pressure for model 1. Figure 4.2 shows the plate 2 pressure and plate 3 pressure for model 1. Figure 4.3 shows the backpressure and plate 7 pressure for model 1. Figure 4.4 shows the plate 2 pressure and plate 3 pressure for model 7. Other simulation results are shown in the appendix section.

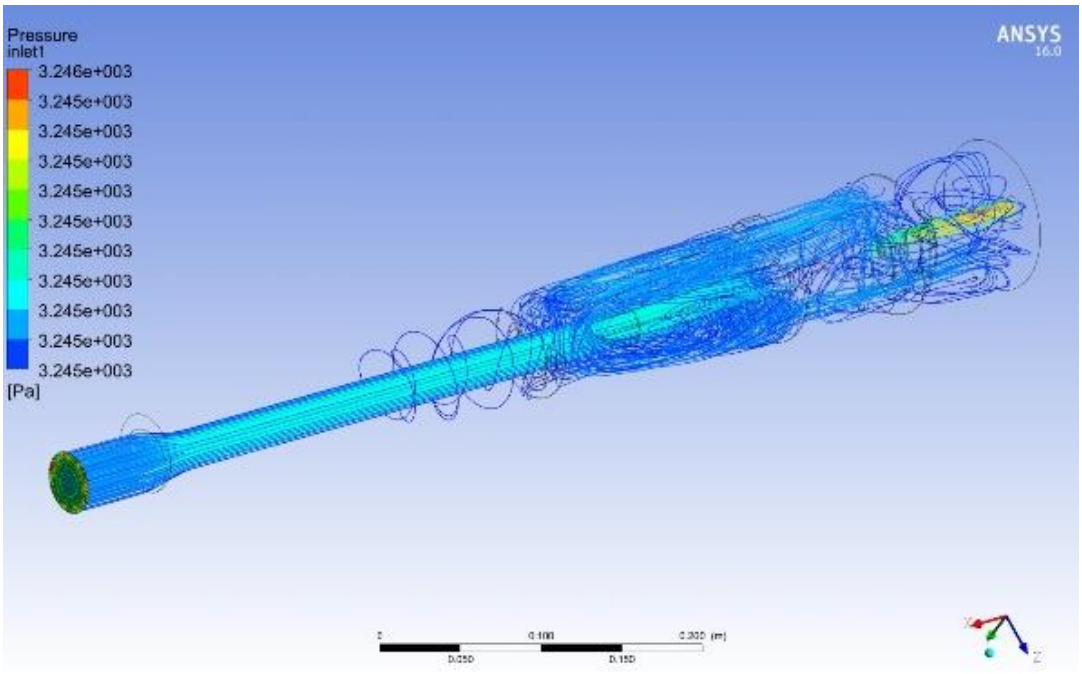

(a)

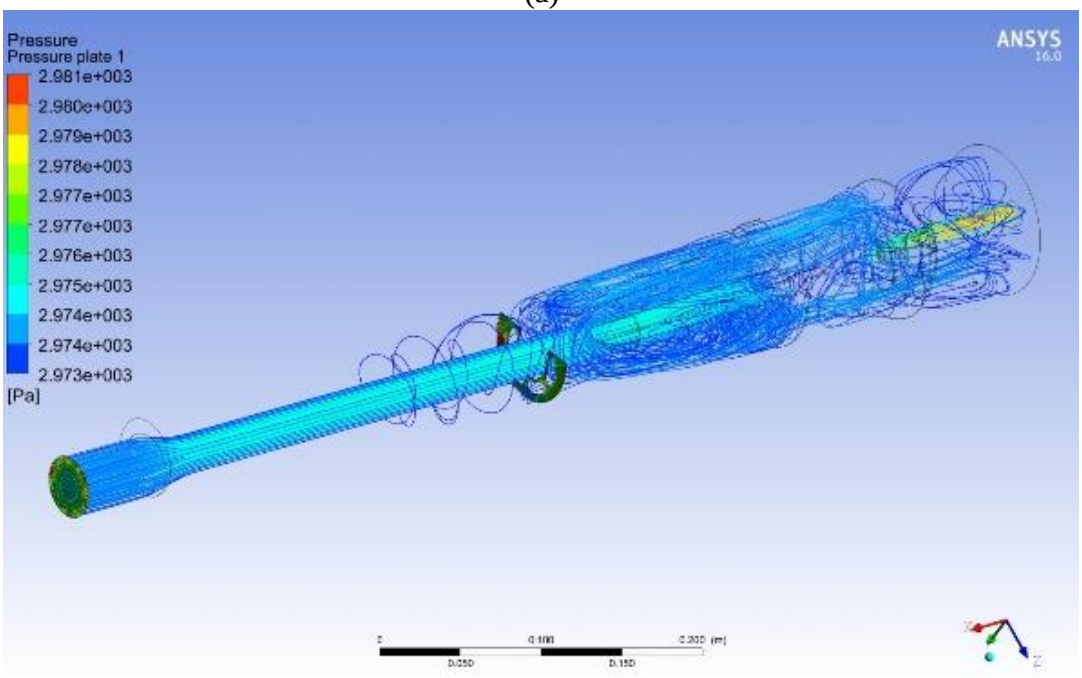

(b)

Figure 4.1: ANSYS simulation result for Model 1

Chamber size 83.1, No of perforation 5 and 5.50 mm dia each

(a) Back Pressure (b) Plate 1 Pressure

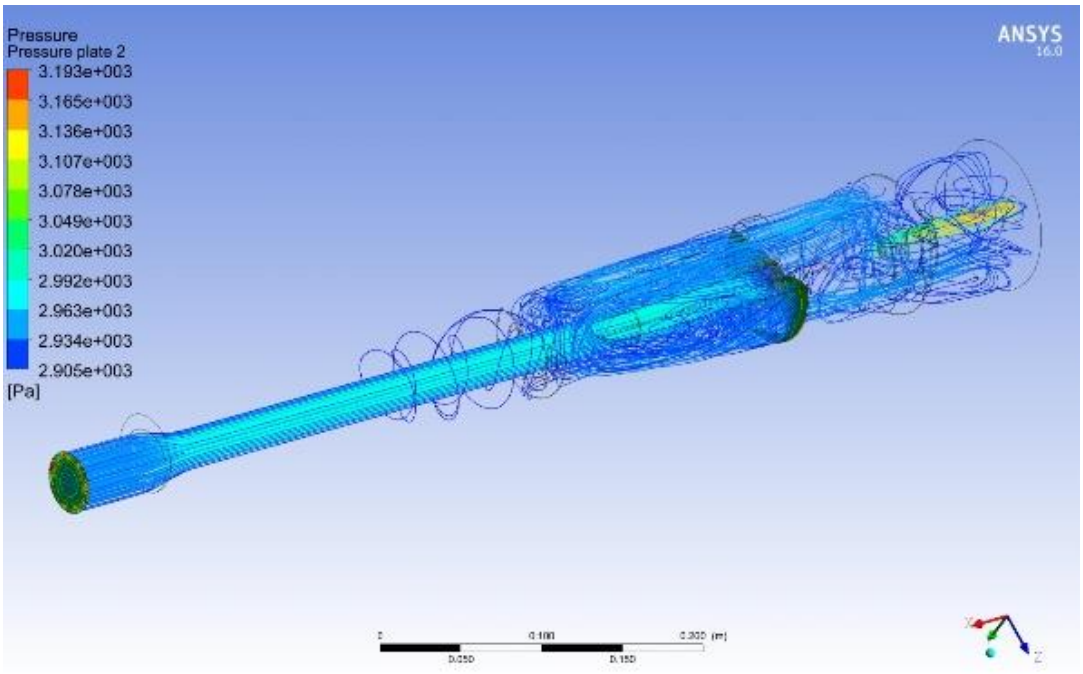

(a)

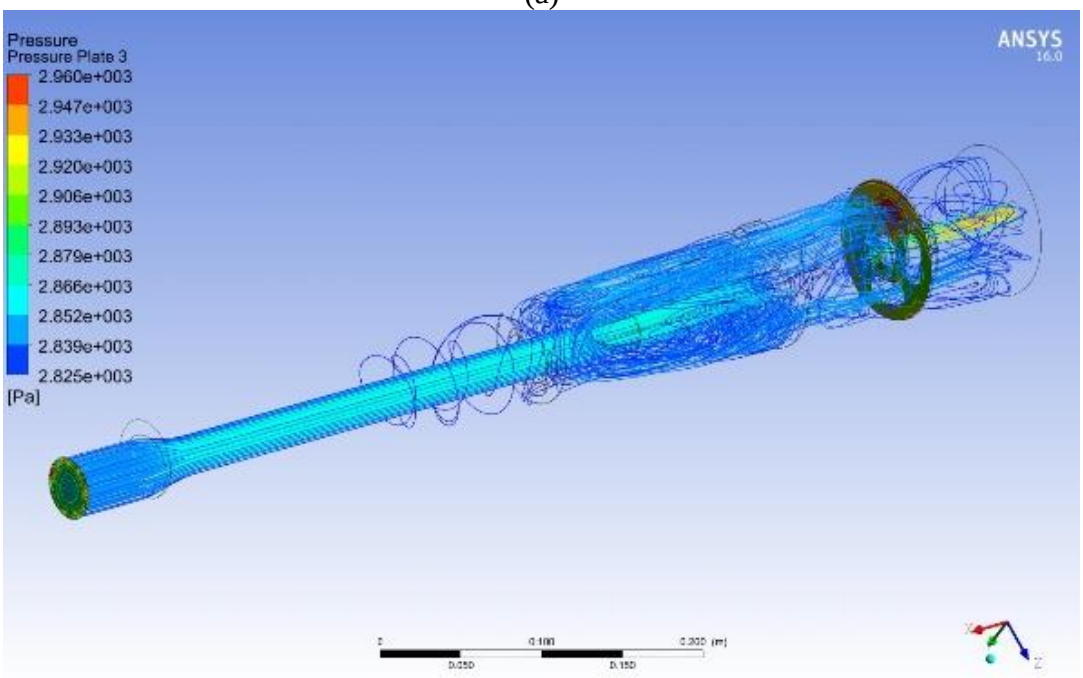

(b)

Figure 4.2: ANSYS simulation result for Model 1

Chamber size 83.1, No of perforation 5 and 5.50 mm dia each

(a) Plate 2 Pressure (b) Plate 3 Pressure

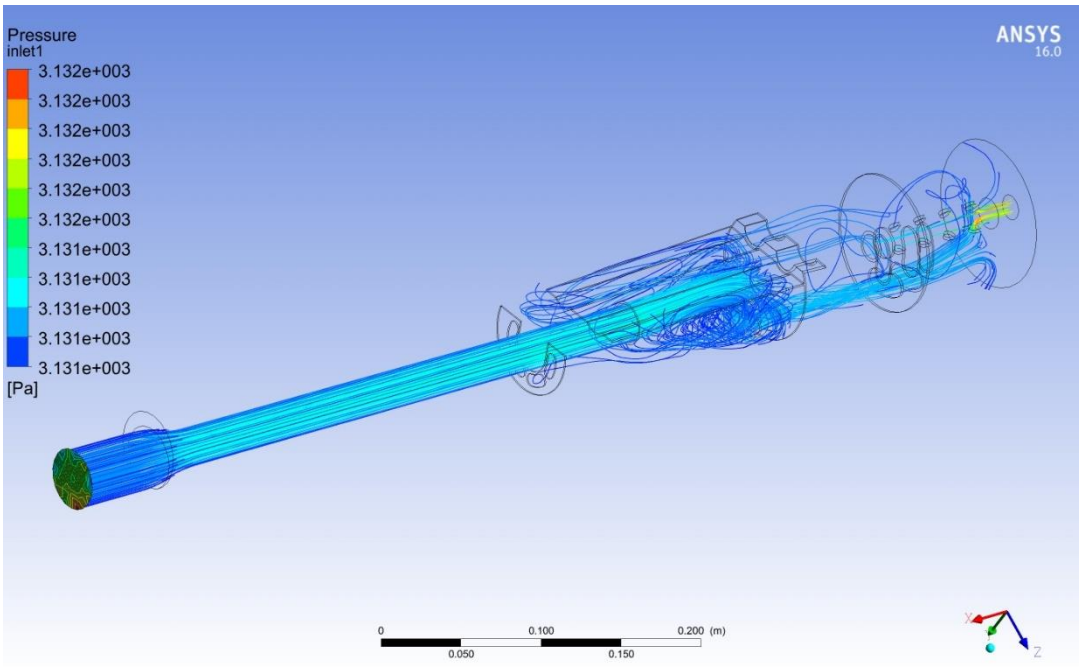

(a)

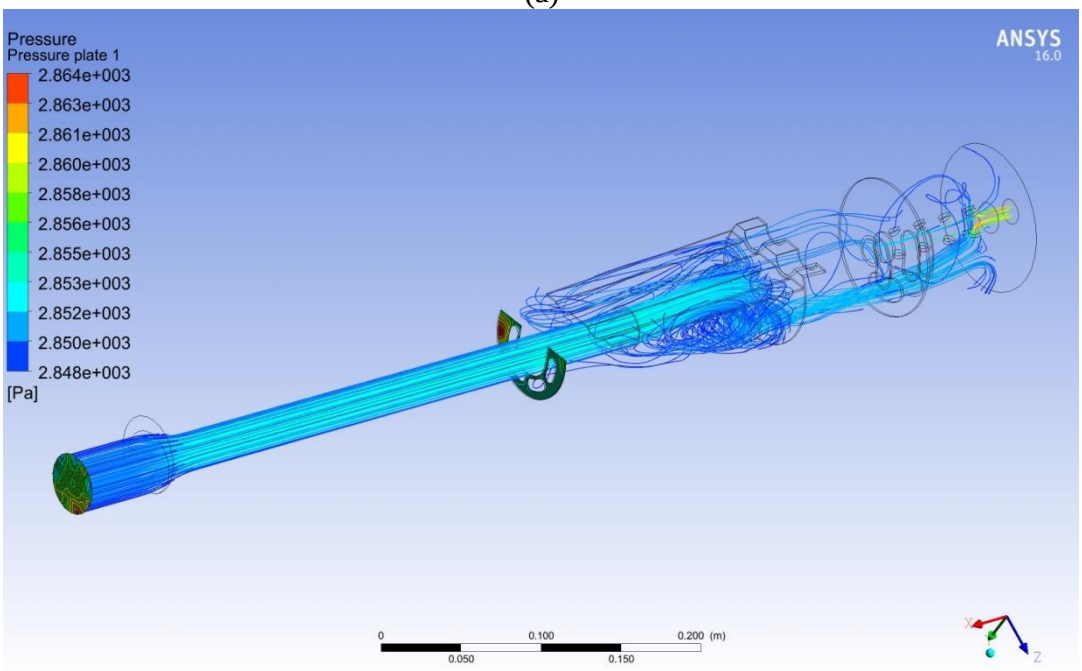

(b)

Figure 4.3: ANSYS simulation result for Model 7

Chamber size 83.1, No of perforation 7 and 7.60 mm dia each

(a) Back Pressure (b) Plate 1 Pressure

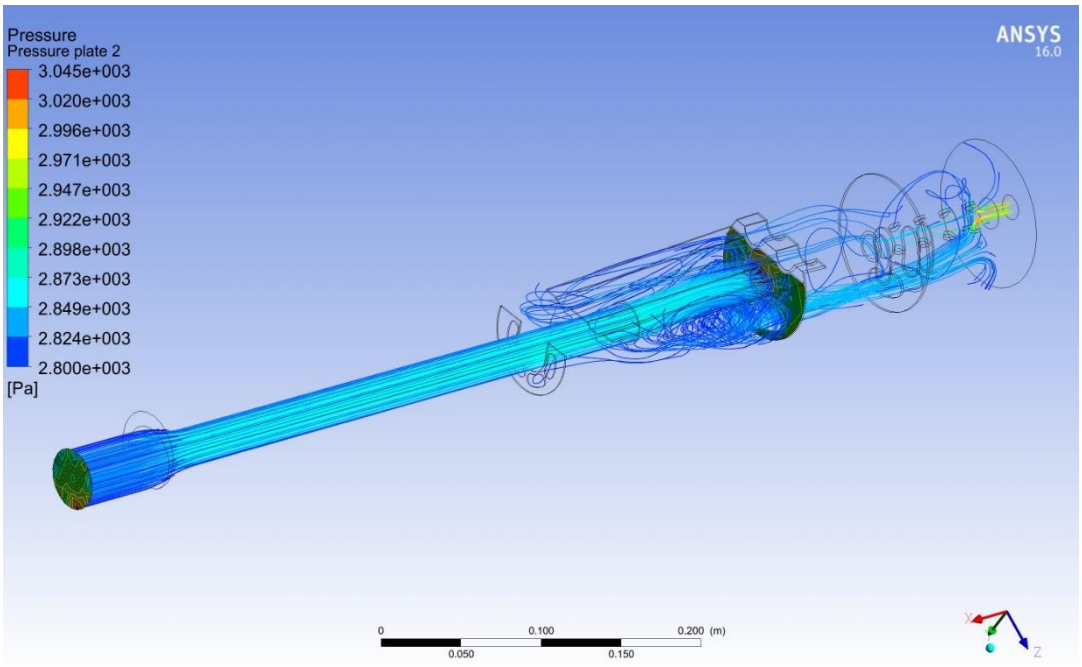

(a)

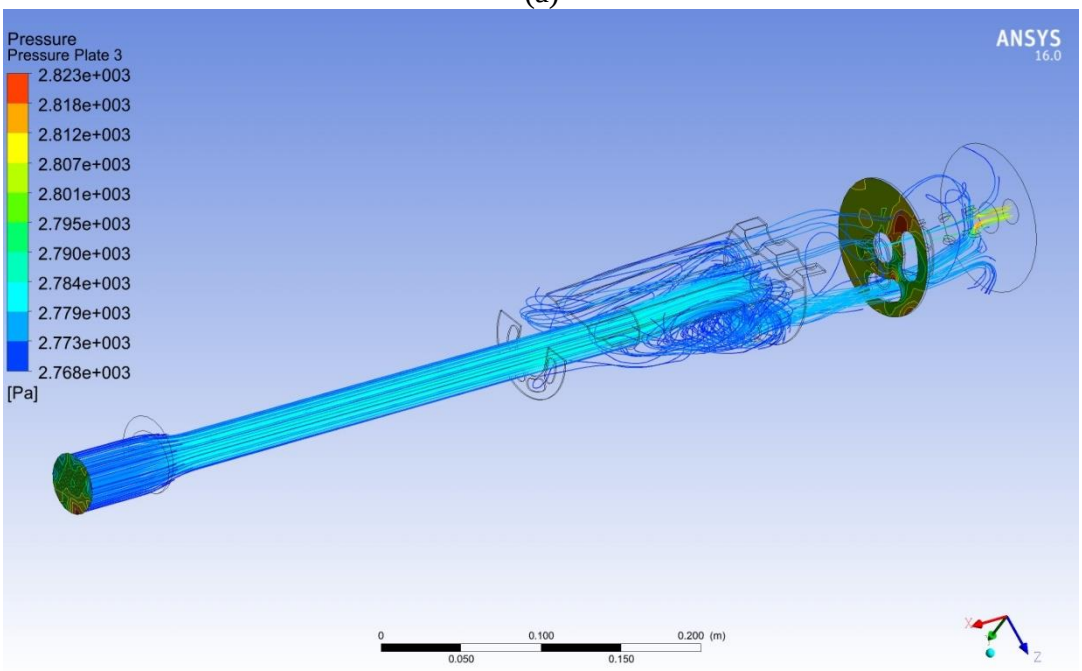

(b)

Figure 4.4: ANSYS simulation result for Model 7
Chamber size 83.1, No of perforation 7 and 7.60 mm dia each
(a) Plate 2 Pressure (b) Plate 3 Pressure

Table 4.1 Simulation results for different models

	Input Variables			Output Variables			
Model No	**A:** Chamber Size [mm]	B: No of Perforation	C: Size of Perforation [mm]	Back Pressure [Pa]	Plate 1 [Pa]	Plate 2 [Pa]	Plate 3 [Pa]
1	83.10	5	5.50	3246	2981	3193	2960
2	122.00	5	5.50	3346	3086	3298	3054
3	83.10	7	5.50	3262	2994	3181	2974
4	122.00	7	5.50	3244	2980	3202	2961
5	83.10	5	7.60	3189	2924	3141	2900
6	122.00	5	7.60	3233	2970	3196	2957
7	83.10	7	7.60	3119	2856	3096	2841
8	122.00	7	7.60	3168	2906	3152	2868
9	75.04	6	6.55	3191	2927	3150	2900
10	130.06	6	6.55	3204	3018	3191	2976
11	102.55	4	6.55	3203	2949	3153	2925
12	102.55	8	6.55	3186	2921	3173	2883
13	102.55	6	5.07	3196	2934	3165	2914
14	102.55	6	8.03	3210	2945	3174	2972
15	102.55	6	6.55	3210	2945	3174	2972
16	102.55	6	6.55	3210	2945	3174	2972
17	102.55	6	6.55	3210	2945	3174	2972
18	102.55	6	6.55	3210	2945	3174	2972
19	102.55	6	6.55	3210	2945	3174	2972
20	102.55	6	6.55	3210	2945	3174	2972

4.3 Model Selection for Back Pressure:

For backpressure, it is found that linear model is the best out of all the models (2FI, Quadratic, Cubic and Quardra). The lack of fit and model summary also show that the linear model is will work better than all other model.

Sequential Model Sum of Squares [Type I]

Source	Sum of Squares	df	Mean Square	F Value	p-value Prob > F	
Mean vs Total	1311.19	1	1311.19			
Linear vs Mean	2.583E-003	3	8.609E-004	4.07	0.0251	Suggested
2FI vs Linear	8.732E-004	3	2.911E-004	1.51	0.2588	
Quadratic vs 2FI	9.351E-004	3	3.117E-004	1.98	0.1807	
Cubic vs Quadra	3.427E-004	4	8.568E-005	0.42	0.7911	Aliased
Residual	1.230E-003	6	2.050E-004			
Total	1311.20	20	65.56			

Lack of Fit Tests

Source	Sum of Squares	df	Mean Square	F Value	p-value Prob > F	
Linear	2.151E-003	10	2.151E-004	1.05	0.4993	Suggested
2FI	1.278E-003	7	1.825E-004	0.89	0.5646	
Quadratic	3.427E-004	4	8.568E-005	0.42	0.7911	
Cubic	0.000	0				Aliased
Pure Error	1.230E-003	6	2.050E-004			

Model Summary Statistics

Source	Std. Dev.	R-Squared	Adjusted R-Squared	Predicted R-Squared	PRESS	
Linear	0.015	0.4331	0.3268	0.0623	5.592E-003	Suggested
2FI	0.014	0.5795	0.3854	-0.5748	9.392E-003	
Quadratic	0.013	0.7363	0.4989	-0.2769	7.615E-003	
Cubic	0.014	0.7937	0.3469		+	Aliased

+ Case(s) with leverage of 1.0000: PRESS statistic not defined

4.4 ANOVA output for Back Pressure:

Response	**1**	**Back Pressure**				
Transform:	Natural log	Constant:	0			
ANOVA for Response Surface Linear Model						
Analysis of variance table [Partial sum of squares - Type III]						
	Sum of		**Mean**	**F**	**p-value**	
Source	**Squares**	**df**	**Square**	**Value**	**Prob > F**	
Model	2.583E-003	3	8.609E-004	4.07	0.0251	significant
A-Pertition Size	*1.945E-004*	*1*	*1.945E-004*	*0.92*	*0.3516*	
B-No of Perforat	*2.820E-005*	*1*	*2.820E-005*	*0.13*	*0.7197*	
C-Size of Perfor	*2.372E-003*	*1*	*2.372E-003*	*11.23*	*0.0041*	
Residual	3.381E-003	16	2.113E-004			
Lack of Fit	*2.151E-003*	*10*	*2.151E-004*	*1.05*	*0.4993*	*not significant*
Pure Error	*1.230E-003*	*6*	*2.050E-004*			
Cor Total	5.964E-003	19				

Std. Dev.	0.015	R-Squared	0.4331
Mean	8.10	Adj R-Squared	0.3268
C.V. %	0.18	Pred R-Squared	0.0623
PRESS	5.592E-003	Adeq Precision	6.282

	Coefficient		**Standard**	**95% CI**	**95% CI**	
Factor	**Estimate**	**df**	**Error**	**Low**	**High**	**VIF**
Intercept	8.10	1	3.254E-003	8.09	8.10	
A-Pertition Size	4.190E-003	1	4.367E-003	-5.068E-003	0.013	1.08
B-No of Perforat	1.325E-003	1	3.627E-003	-6.363E-003	9.013E-003	1.08
C-Size of Perfor	-0.014	1	4.198E-003	-0.023	-5.166E-003	1.00

The Model F-value of 4.07 implies the model is significant. There is only a 2.51% chance that a "Model F-Value" this large could occur due to noise. Values of "Prob > F" less than 0.0500 indicate model terms are significant. In this case C are significant model terms. Values greater than 0.1000 indicate the model terms are not significant. If there are many insignificant model terms (not counting those required to support hierarchy), model reduction may improve this model. The "Lack of Fit F-value" of 1.05 implies the Lack of Fit is not significant relative to

the pureerror. There is a 49.93% chance that a "Lack of Fit F-value" this large could occur dueto noise. Non-significant lack of fit is good -- we want the model to fit.

The "Pred R-Squared" of 0.0623 is not as close to the "Adj R-Squared" of 0.3268 as one might normally expect. This may indicate a large block effect or a possible problem with our model and/or data. Things to consider are model reduction, response tranformation, outliers, etc. "Adeq Precision" measures the signal to noise ratio. A ratio greater than 4 is desirable. Our ratio of 6.282 indicates an adequate signal. This model can be used to navigate the design space.

Final Equation in Terms of Actual Factors:

$$P_B\left(\text{Back Pressure}\right) = \exp(8.13971 + 0.000256426\times A - 0.0050715\times B - 0.00908133\times C)$$

…… 4.1

4.5 ANOVA output for Plate 1 Pressure:

Response 2 Plate 1

Transform: Natural log Constant: 0

ANOVA for Response Surface Linear Model

Analysis of variance table [Partial sum of squares - Type III]

Source	Sum of Squares	df	Mean Square	F Value	p-value Prob > F	
Model	3.343E-003	3	1.114E-003	4.31	0.0208	significant
A-Pertition Size	*3.096E-004*	*1*	*3.096E-004*	*1.20*	*0.2900*	
B-No of Perfora	*2.196E-005*	*1*	*2.196E-005*	*0.085*	*0.7744*	
C-Size of Perfo	*3.019E-003*	*1*	*3.019E-003*	*11.68*	*0.0035*	
Residual	4.136E-003	16	2.585E-004			
Lack of Fit	*2.645E-003*	*10*	*2.645E-004*	*1.06*	*0.4917*	*not significant*
Pure Error	*1.491E-003*	*6*	*2.485E-004*			
Cor Total	7.479E-003	19				

Std. Dev.	0.016	R-Squared	0.4470
Mean	8.00	Adj R-Squared	0.3433
C.V. %	0.20	Pred R-Squared	0.0753
PRESS	6.916E-003	Adeq Precision	6.372

Factor	Coefficient Estimate	df	Standard Error	95% CI Low	95% CI High	VIF
Intercept	8.00	1	3.599E-003	7.99	8.01	
A-Pertition Size	5.286E-003	1	4.830E-003	-4.953E-003	0.016	1.08
B-No of Perforat	1.169E-003	1	4.011E-003	-7.334E-003	9.672E-003	1.08
C-Size of Perfor	-0.016	1	4.643E-003	-0.026	-6.025E-003	1.00

In the same way as backpressure a linear model is choosen for plate 1 pressure. The Model F-value of 4.31 implies the model is significant. There is only a 2.08% chance that a "Model F-Value" this large could occur due to noise. Values of "Prob > F" less than 0.0500 indicate model terms are significant. In this case C are significant model terms. Values greater than 0.1000 indicate the model terms are not significant. If there are many insignificant model terms (not counting those required to support hierarchy), model reduction may improve this model. The "Lack of Fit F-value" of 1.06 implies the Lack of Fit is not significant relative error. There is a 49.17% chance that a "Lack of Fit F-value" this large could occur to noise. Non-significant lack of fit is good -- we want the model to fit.

The "Pred R-Squared" of 0.0753 is not as close to the "Adj R-Squared" of 0.3433 as one might normally expect. This may indicate a large block effect or a possible problem with our model and/or data. Things to consider are model reduction, response tranformation, outliers, etc. "Adeq Precision" measures the signal to noise ratio. A ratio greater than 4 is desirable. Our ratio of 6.372 indicates an adequate signal. This model can be used to navigate the design space.

Final Equation in Terms of Actual Factors:

$$P_1\left(\text{Plate 1 Pressure}\right) = \exp(8.04588 + 0.000454983 \times A - 0.00596052 \times B - 0.00989382 \times C)$$

…… 4.2

4.6 ANOVA output for Plate 2 Pressure:

Response	**3**	**Plate 2**				
Transform:	**Natural log**	**Constant:**	**0**			
ANOVA for Response Surface Linear Model						
Analysis of variance table [Partial sum of squares - Type III]						
	Sum of		**Mean**	**F**	**p-value**	
Source	**Squares**	**df**	**Square**	**Value**	**Prob > F**	
Model	2.452E-003	3	8.175E-004	3.79	0.0315	significant
A-Pertition Size	*1.483E-004*	*1*	*1.483E-004*	*0.69*	*0.4192*	
B-No of Perforat	*1.705E-005*	*1*	*1.705E-005*	*0.079*	*0.7822*	
C-Size of Perfor	*2.293E-003*	*1*	*2.293E-003*	*10.63*	*0.0049*	
Residual	3.450E-003	16	2.156E-004			
Lack of Fit	*2.172E-003*	*10*	*2.172E-004*	*1.02*	*0.5143*	*not significant*
Pure Error	*1.278E-003*	*6*	*2.130E-004*			
Cor Total	5.902E-003	19				

Std. Dev.	0.015	R-Squared	0.4155
Mean	8.07	Adj R-Squared	0.3059
C.V. %	0.18	Pred R-Squared	0.0258
PRESS	5.750E-003	Adeq Precision	6.081

	Coefficient		**Standard**	**95% CI**	**95% CI**	
Factor	**Estimate**	**df**	**Error**	**Low**	**High**	**VIF**
Intercept	8.07	1	3.287E-003	8.06	8.07	
A-Pertition Size	3.658E-003	1	4.411E-003	-5.694E-003	0.013	1.08
B-No of Perforat	1.030E-003	1	3.664E-003	-6.736E-003	8.797E-003	1.08
C-Size of Perfor	-0.014	1	4.240E-003	-0.023	-4.838E-003	1.00

In the same way as backpressure a linear model is choosen for plate 2 pressure. The Model F-value of 3.79 implies the model is significant. There is only a 3.15% chance that a "Model F-Value" this large could occur due to noise. Values of "Prob > F" less than 0.0500 indicate model terms are significant. In this case C are significant model terms. Values greater than 0.1000 indicate the model terms are not significant. If there are many insignificant model terms (not counting those required to support hierarchy), model reduction may improve this model. The "Lack of Fit F-value" of 1.02 implies the

Lack of Fit is not significant relative to the pure error. There is a 51.43% chance that a "Lack of Fit F-value" this large could occur due to noise. Non-significant lack of fit is good -- we want the model to fit.

The "Pred R-Squared" of 0.0258 is not as close to the "Adj R-Squared" of 0.3059 as one might normally expect. This may indicate a large block effect or a possible problem with our model and/or data. Things to consider are model reduction, response tranformation, outliers, etc. "Adeq Precision" measures the signal to noise ratio. A ratio greater than 4 is desirable. Our ratio of 6.081 indicates an adequate signal. This model can be used to navigate the design space.

Final Equation in Terms of Actual Factors:

$$P_2\left(\text{Plate 2 Pressure}\right) = \exp(8.08948 + 0.000396353 \times A - 0.00351046 \times B - 0.00687646 \times C)$$

..... 4.3

4.7 ANOVA output for Plate 3 Pressure:

Response 4	Plate 3					
Transform:	Natural log	Constant:	0			
ANOVA for Response Surface Linear Model						
Analysis of variance table [Partial sum of squares - Type III]						
Source	Sum of Squares	df	Mean Square	F Value	p-value Prob > F	
Model	3.094E-003	3	1.031E-003	3.91	0.0285	significant
A-Pertition Size	*4.218E-004*	*1*	*4.218E-004*	*1.60*	*0.2239*	
B-No of Perforat	*3.170E-005*	*1*	*3.170E-005*	*0.12*	*0.7332*	
C-Size of Perfor	*2.656E-003*	*1*	*2.656E-003*	*10.08*	*0.0059*	
Residual	4.215E-003	16	2.634E-004			
Lack of Fit	*2.788E-003*	*10*	*2.788E-004*	*1.17*	*0.4411*	*not significant*
Pure Error	*1.426E-003*	*6*	*2.377E-004*			
Cor Total	7.308E-003	19				

Std. Dev.	0.016	R-Squared	0.4233
Mean	7.98	Adj R-Squared	0.3152
C.V. %	0.20	Pred R-Squared	0.0372
PRESS	7.037E-003	Adeq Precision	6.110

Factor	Coefficient Estimate	df	Standard Error	95% CI Low	95% CI High	VIF
Intercept	7.98	1	3.633E-003	7.98	7.99	
A-Pertition Size	6.170E-003	1	4.876E-003	-4.167E-003	0.017	1.08
B-No of Perforat	1.405E-003	1	4.049E-003	-7.179E-003	9.989E-003	1.08
C-Size of Perfor	-0.015	1	4.687E-003	-0.025	-4.948E-003	1.00

In the same way as backpressure a linear model is choosen for plate 3 pressure. The Model F-value of 3.91 implies the model is significant. There is only a 2.85% chance that a "Model F-Value" this large could occur due to noise. Values of "Prob > F" less than 0.0500 indicate model terms are significant. In this case C are significant model terms. Values greater than 0.1000 indicate the model terms are not significant. If there are many insignificant model terms (not counting those required to support hierarchy), model reduction may improve our model. The "Lack of Fit F-value" of 1.17 implies the Lack of Fit is not significant relative to the pure error. There is a 44.11% chance that a "Lack of Fit F-value" this large could occur due to noise. Non-significant lack of fit is good -- we want the model to fit.

The "Pred R-Squared" of 0.0372 is not as close to the "Adj R-Squared" of 0.3152 as one might normally expect. This may indicate a large block effect or a possible problem with our model and/or data. Things to consider are model reduction, response tranformation, outliers, etc. "Adeq Precision" measures the signal to noise ratio. A ratio greater than 4 is desirable. Our ratio of 6.110 indicates an adequate signal. This model can be used to navigate the design space.

Final Equation in Terms of Actual Factors:

$$P_3\left(\text{Plate 3 Pressure}\right) = \exp(8.04148 + 0.000395846 \times A - 0.00651837 \times B - 0.00813871 \times C)$$

…… 4.4

By using Equation 4.1, 4.2, 4.3 and 4.4 the output variables are calculated and shown in Table 4.2. Table 4.3 show the percentage deviation.

Table 4.2 Empirical Data for output variables

	Input Variables			Output Variables			
Model No	**A:** Chamber Size [mm]	**B:** No of Perforation	**C:** Size of Perforation [mm]	Back Pressure [Pa]	Plate 1 [Pa]	Plate 2 [Pa]	Plate 3 [Pa]
1	83.10	5	5.50	3248	2979	3188	2972
2	122.00	5	5.50	3280	3033	3237	3018
3	83.10	7	5.50	3199	2927	3154	2915
4	122.00	7	5.50	3231	2979	3203	2960
5	83.10	5	7.60	3186	2918	3142	2922
6	122.00	5	7.60	3218	2970	3191	2967
7	83.10	7	7.60	3138	2866	3109	2865
8	122.00	7	7.60	3170	2918	3157	2910
9	75.04	6	6.55	3194	2920	3144	2918
10	130.06	6	6.55	3239	2994	3213	2983
11	102.55	4	6.55	3249	2993	3200	2989
12	102.55	8	6.55	3184	2922	3156	2912
13	102.55	6	5.07	3260	3001	3211	2986
14	102.55	6	8.03	3174	2914	3146	2915
15	102.55	6	6.55	3217	2957	3178	2950
16	102.55	6	6.55	3217	2957	3178	2950
17	102.55	6	6.55	3217	2957	3178	2950
18	102.55	6	6.55	3217	2957	3178	2950
19	102.55	6	6.55	3217	2957	3178	2950
20	102.55	6	6.55	3217	2957	3178	2950

Table 4.3 Percentage deviation of Empirical data

	Percentage deviation			
Model No	Back Pressure	Plate 1	Plate 2	Plate 3
1	0.05	0.05	0.17	0.41
2	1.96	1.73	1.84	1.17
3	1.94	2.25	0.84	2.00
4	0.41	0.04	0.04	0.04
5	0.08	0.20	0.03	0.75
6	0.45	0.01	0.16	0.34
7	0.62	0.36	0.42	0.85
8	0.05	0.40	0.17	1.45
9	0.10	0.23	0.20	0.63
10	1.11	0.78	0.69	0.22
11	1.45	1.48	1.50	2.19
12	0.06	0.04	0.54	1.01
13	2.01	2.28	1.44	2.48
14	1.14	1.05	0.89	1.92
15	0.21	0.41	0.13	0.73
16	0.21	0.41	0.13	0.73
17	0.21	0.41	0.13	0.73
18	0.21	0.41	0.13	0.73
19	0.21	0.41	0.13	0.73
20	0.21	0.41	0.13	0.73

Figure 4.5, 4.6, 4.7 and 4.8 show the comparison of all predicted and experimented data.

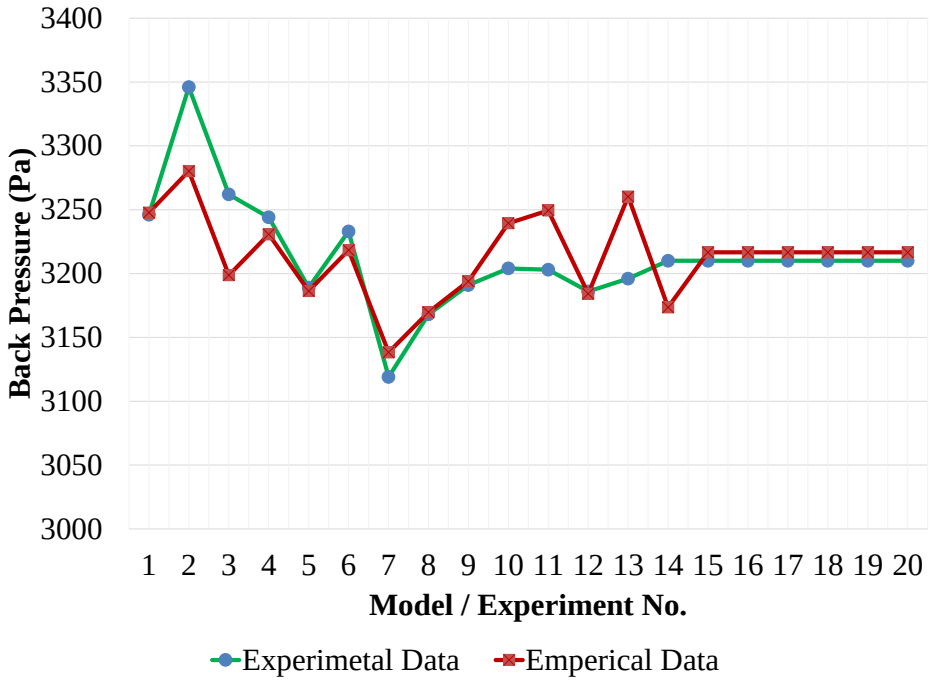

Figure 4.5: Comparison of backpressure experimental and empirical data

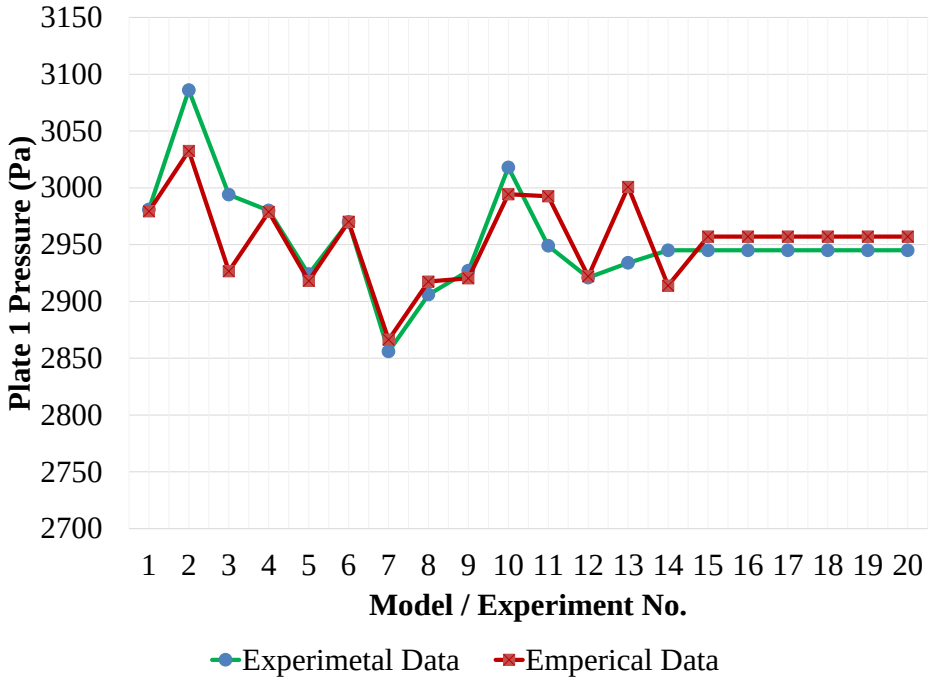

Figure 4.6: Comparison of P_1 pressure experimental and empirical data

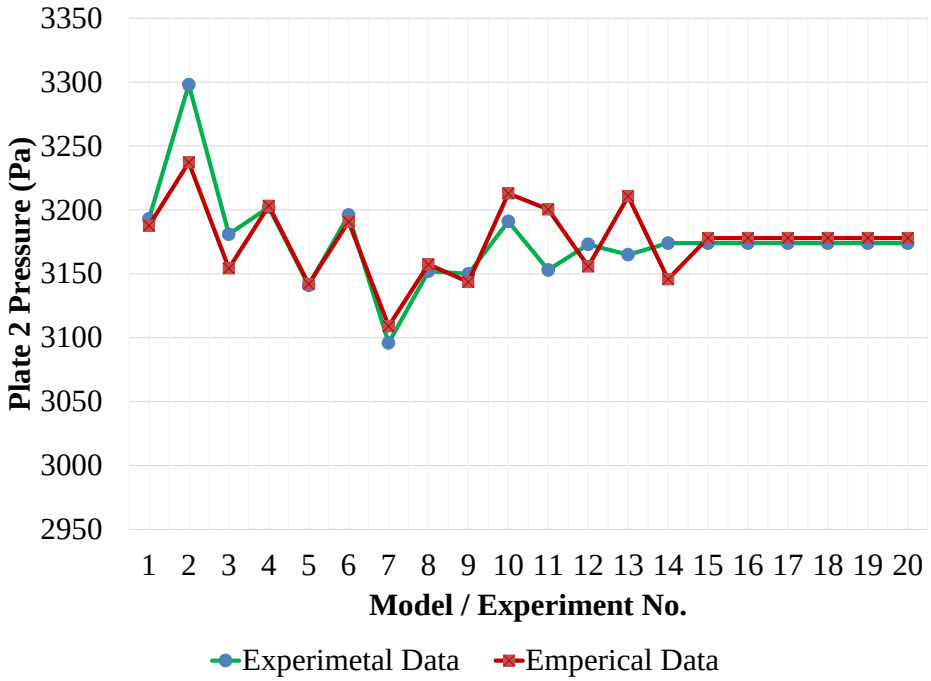

Figure 4.7: Comparison of P_2 pressure experimental and empirical data

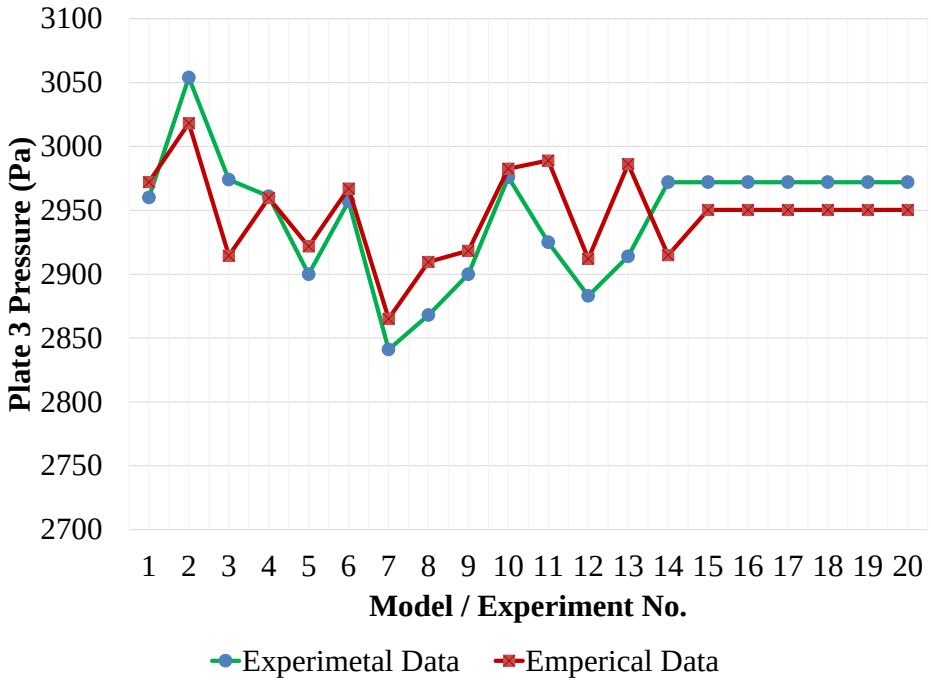

Figure 4.8: Comparison of P_3 pressure experimental and empirical data

4.8 Effect of different design parameters:

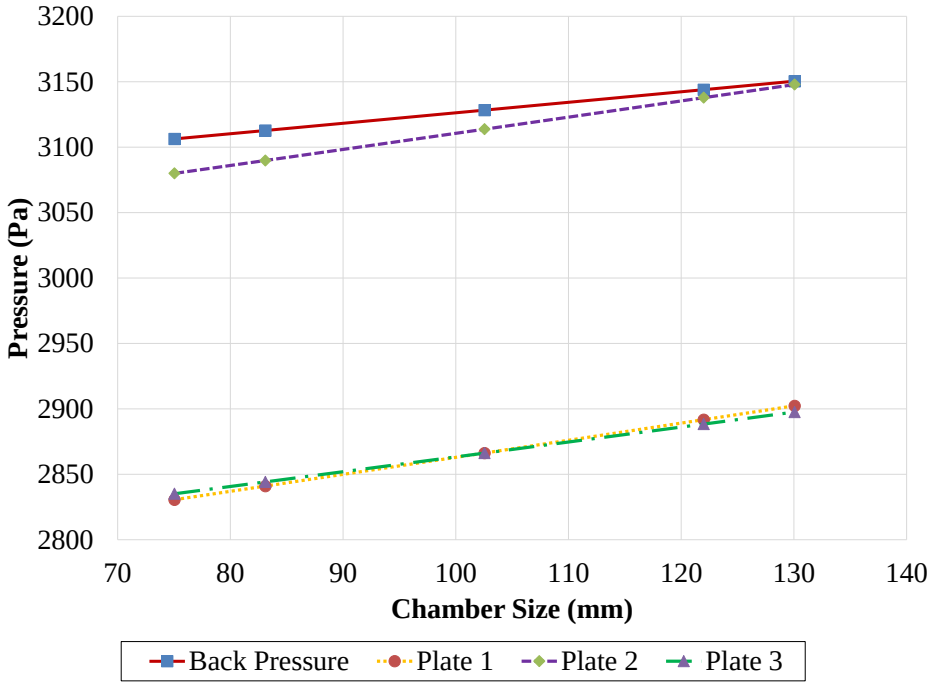

Figure 4.9: Effect of chamber size on backpressure, P_1, P_2 and P_3

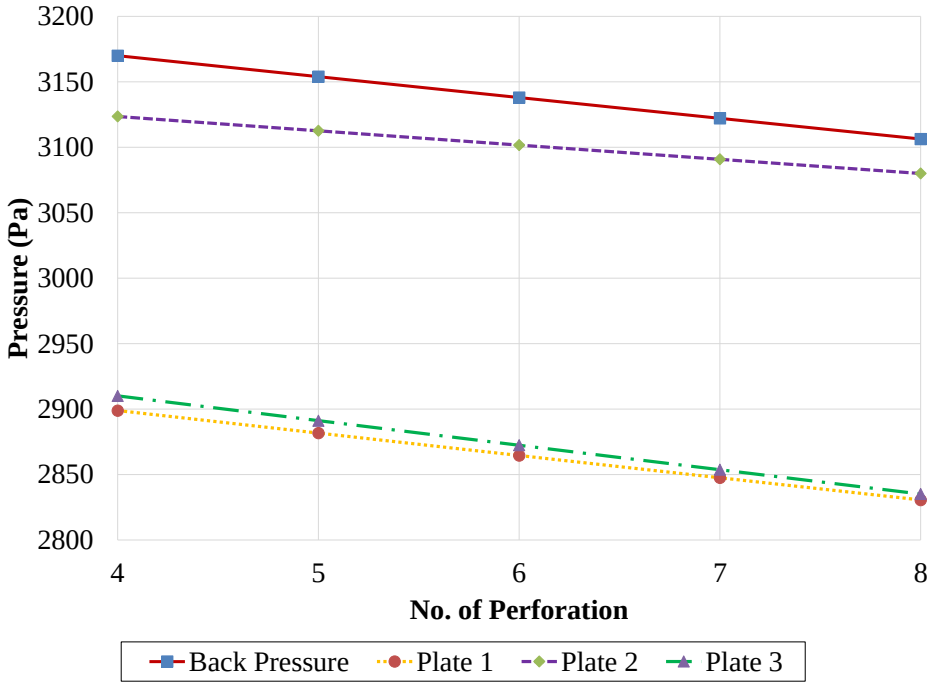

Figure 4.10: Effect of number of perforation on backpressure, P_1, P_2 and P_3

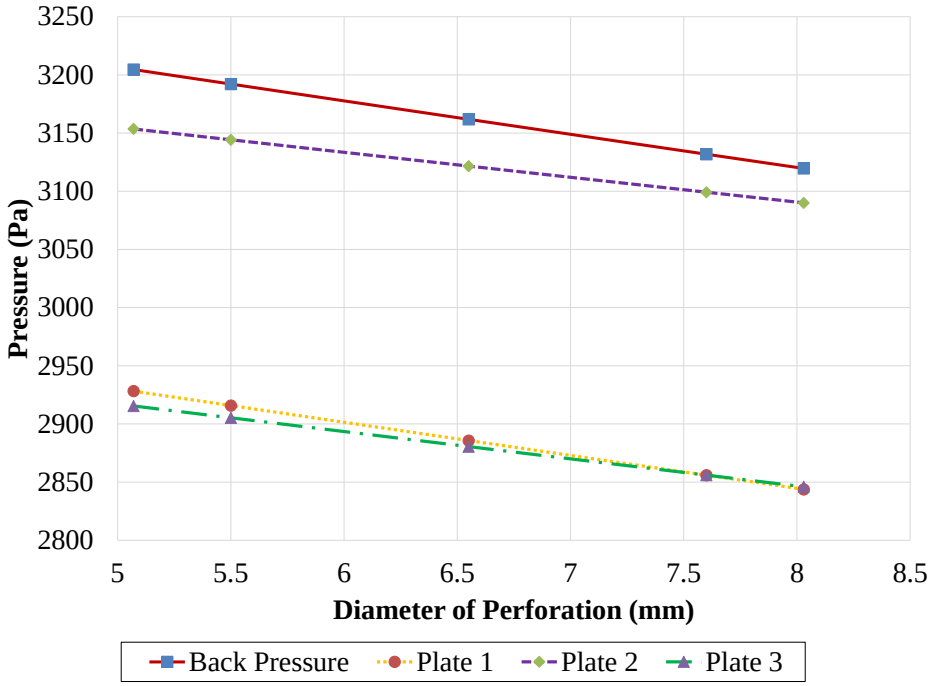

Figure 4.11: Effect of diameter of perforation on backpressure, P_1, P_2 and P_3

Figure 4.5, 4.6, 4.7 and 4.8 show the deviation of experimental data with empirical data. It is found that no data is deviated more that 3%. Hence it can be said that the equation we generated is correct.

Figure 4.9, 4.10 and 4.11 show the effect of chamber size, diameter of perforation and number of perforation on back pressure, plate 1 pressure, plate 2 pressure and plate 3 pressure.

It can be seen from Figure 4.9 that with the increase of this particular chamber size the pressure increases. This is because, with the increase of this particular chamber the inner chamber decreases which causes obstruction for the flow, creates the pressure increase. On the other hand, with the increase of number of perforation the pressure drops because it helps to pass the flow to other chamber easily. Due to the same cause, the pressure drops due to the increase of the diameter increase of perforation (Figure 4.10 and 4.11).

4.9 Grey Analysis of Simulated Data

By using Equation 3.4 and 3.5 the data preprocessing values for output variables are calculated and shown in Table 4.4.

Table 4.4 Data preprocessing values for Output variables

	Data preprocessing values for Output Variables			
Model No	Back Pressure	Plate 1	Plate 2	Plate 3
1	0.2254	0.3234	0.3828	0.3007
2	0.0000	0.0000	0.0000	0.0000
3	0.5704	0.6347	0.6484	0.6732
4	0.3451	0.3234	0.2656	0.3791
5	0.6620	0.6886	0.7422	0.6275
6	0.4366	0.3772	0.3594	0.3333
7	1.0000	1.0000	1.0000	1.0000
8	0.7746	0.6886	0.6250	0.7059
9	0.6056	0.6766	0.7266	0.6536
10	0.2887	0.2335	0.1875	0.2288
11	0.2183	0.2395	0.2891	0.1895
12	0.6761	0.6647	0.6328	0.6928
13	0.1408	0.1916	0.2031	0.2092
14	0.7465	0.7126	0.7109	0.6732
15	0.4437	0.4551	0.4609	0.4444
16	0.4437	0.4551	0.4609	0.4444
17	0.4437	0.4551	0.4609	0.4444
18	0.4437	0.4551	0.4609	0.4444
19	0.4437	0.4551	0.4609	0.4444
20	0.4437	0.4551	0.4609	0.4444

Then, by using Equation 3.6 and 3.7 the deviation sequences values for output variables are calculated and shown in Table 4.5.

Table 4.5 Deviation sequences for Output variables

	Deviation sequences for Output Variables			
Model No	Back Pressure Δ_{0i} (1)	Plate 1 Δ_{0i} (2)	Plate 2 Δ_{0i} (3)	Plate 3 Δ_{0i} (4)
1	0.7746	0.6766	0.6172	0.6993
2	1.0000	1.0000	1.0000	1.0000
3	0.4296	0.3653	0.3516	0.3268
4	0.6549	0.6766	0.7344	0.6209
5	0.3380	0.3114	0.2578	0.3725
6	0.5634	0.6228	0.6406	0.6667
7	0.0000	0.0000	0.0000	0.0000
8	0.2254	0.3114	0.3750	0.2941
9	0.3944	0.3234	0.2734	0.3464
10	0.7113	0.7665	0.8125	0.7712
11	0.7817	0.7605	0.7109	0.8105
12	0.3239	0.3353	0.3672	0.3072
13	0.8592	0.8084	0.7969	0.7908
14	0.2535	0.2874	0.2891	0.3268
15	0.5563	0.5449	0.5391	0.5556
16	0.5563	0.5449	0.5391	0.5556
17	0.5563	0.5449	0.5391	0.5556
18	0.5563	0.5449	0.5391	0.5556
19	0.5563	0.5449	0.5391	0.5556
20	0.5563	0.5449	0.5391	0.5556

Then, by using Equation 3.8 and 3.9 the Grey relational coefficient and Grey relational grade for output variables are calculated and shown in Table 4.6.

Table 4.6 Grey relational coefficient and Grey relational grade for Output variables

	Grey relational coefficient				Grey relational grade
Model No	Back Pressure ξ_i (1)	Plate 1 ξ_i (2)	Plate 2 ξ_i (3)	Plate 3 ξ_i (4)	
1	0.3923	0.4249	0.4476	0.4169	0.4148
2	0.3333	0.3333	0.3333	0.3333	0.3333
3	0.5379	0.5779	0.5872	0.6047	0.5691
4	0.4329	0.4249	0.4051	0.4461	0.4284
5	0.5966	0.6162	0.6598	0.5730	0.6085
6	0.4702	0.4453	0.4384	0.4286	0.4505
7	1.0000	1.0000	1.0000	1.0000	1.0000
8	0.6893	0.6162	0.5714	0.6296	0.6392
9	0.5591	0.6073	0.6465	0.5907	0.5925
10	0.4128	0.3948	0.3810	0.3933	0.3989
11	0.3901	0.3967	0.4129	0.3815	0.3943
12	0.6068	0.5986	0.5766	0.6194	0.6017
13	0.3679	0.3822	0.3855	0.3873	0.3782
14	0.6636	0.6350	0.6337	0.6047	0.6401
15	0.4733	0.4785	0.4812	0.4737	0.4760
16	0.4733	0.4785	0.4812	0.4737	0.4760
17	0.4733	0.4785	0.4812	0.4737	0.4760
18	0.4733	0.4785	0.4812	0.4737	0.4760
19	0.4733	0.4785	0.4812	0.4737	0.4760
20	0.4733	0.4785	0.4812	0.4737	0.4760

4.10 Final Optimization

Once the grey relation code is ready, this code will work as a single output variable for all output variable. In the next step, ABC algorithm is applied according to Figure 3.4 and the final output design and result are shown in Figure 4.12 and Table 4.7.

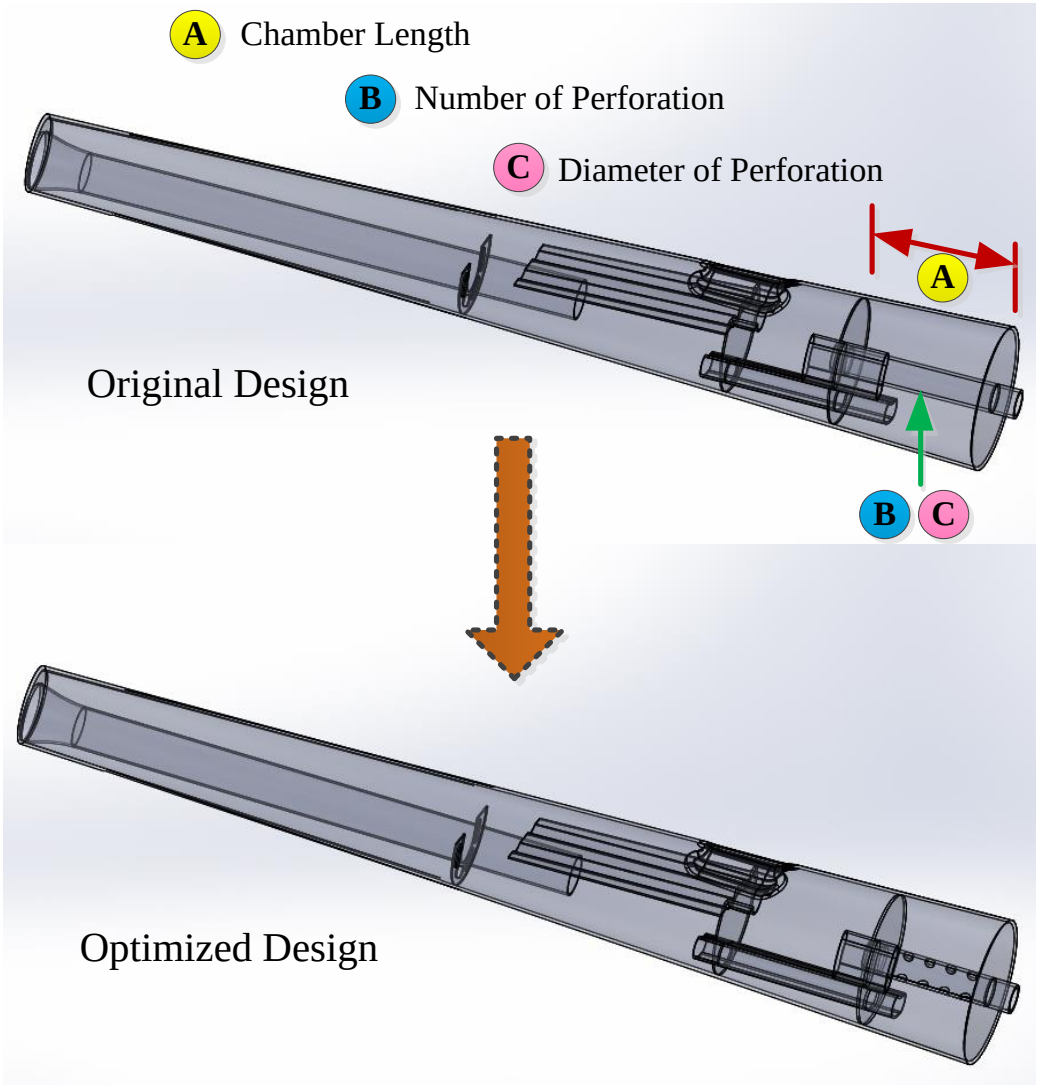

Figure 4.12: CAD Design for original and Optimized Design

Table 4.7: Optimized Results

	Input Variables			Output Variables			
Model No	**A:** Chamber Size [mm]	**B:** No of Perforation	**C:** Size of Perforation [mm]	Back Pressure [Pa]	Plate 1 [Pa]	Plate 2 [Pa]	Plate 3 [Pa]
Original Design	102	0	0	3428	3121	3260	3107
Optimized Design	75	8	8.5	3253	2987	3195	2979
Pressure Reduces [Pa]				175	134	65	128

4.11 Fabrication of Muffler:

The muffler is fabricated and install in the motorcycle (Figure 4.13, 4.14, 4.15, 4.16 and 4.17). After installing the muffler, the motor cycle runs over 10,000 Km without any disturbance. Whereas, previously after running 4,000 to 5,000 Km the muffler fails for working.

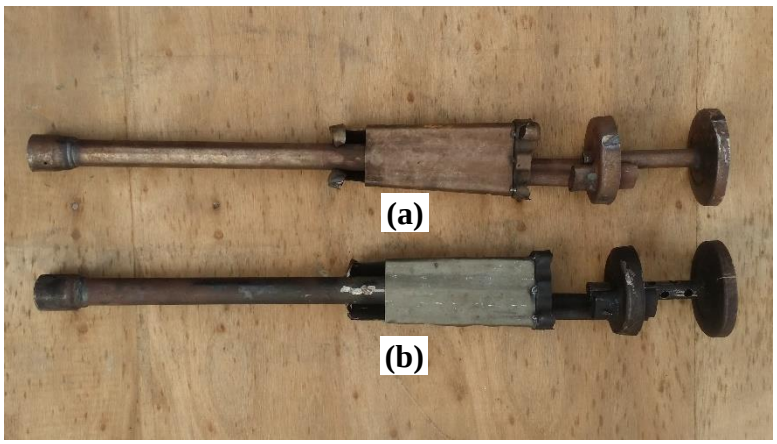

Figure 4.13: (a) The original design and (b) The optimized design of the muffler

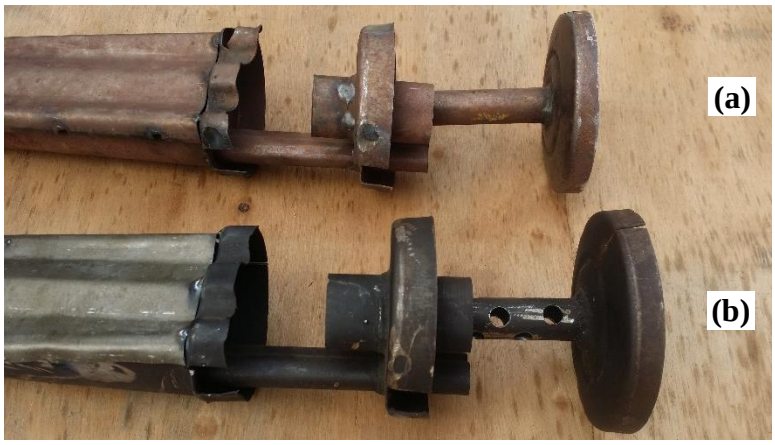

Figure 4.14: (a) Close view of the original design and (b) Optimized design

Figure 4.15: Complete fabrication of muffler

Figure 4.16: Optimized muffler installed in the motorcycle

Figure 4.17: Side view of the motor cycle after installing the muffler

4.12 Acoustics Transmission Loss Analysis:

To determine the transmission loss of mufflers Figure 4.18 and 4.19 show a schematic diagram of the two microphone experimental set-up used in the current work.

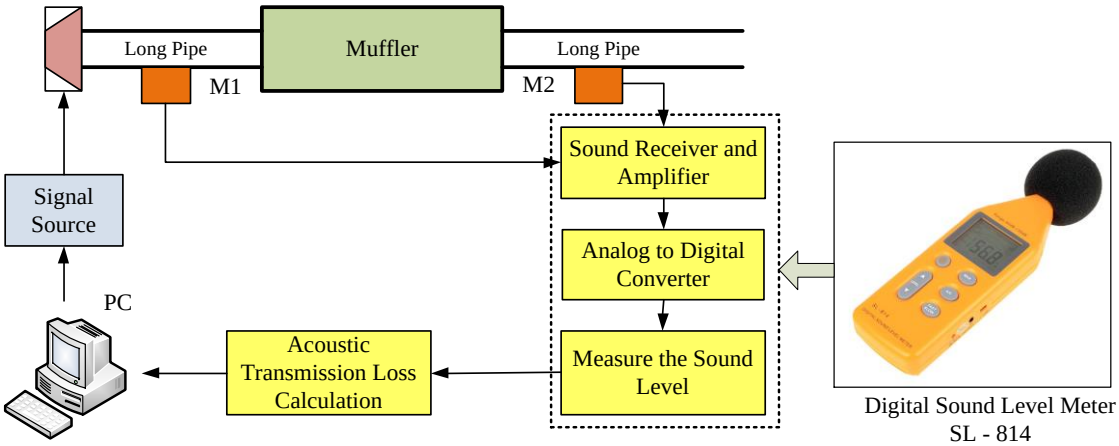

Figure 4.18: Acoustics Transmission loss analysis procedure

The pulse propagated down the conduit where it was measured by the upstream microphone, M1, before continuing to the muffler inlet. The pressure of the corresponding pulse transmitted from the outlet of the muffler was measured by the downstream microphone, M2. The sound level was measured using a digital sound

meter. Figure 4.23, 4.24 and 4.25 show the acoustics transmission loss analysis for original design and optimized design. To ensure that the noise attenuation characteristics, virtual acoustics transmission loss for both optimized and original design was conducted. Transmission loss (TL) in duct acoustics describes the acoustic performances of a muffler like system. Generally the higher transmission loss of a system it has, the better it will perform in terms of noise cancellation. The porous conditions in the internal pipes were defined with extreme caution. The frequency range for analysis was taken between 50-2500 Hz with a 25 Hz interval.

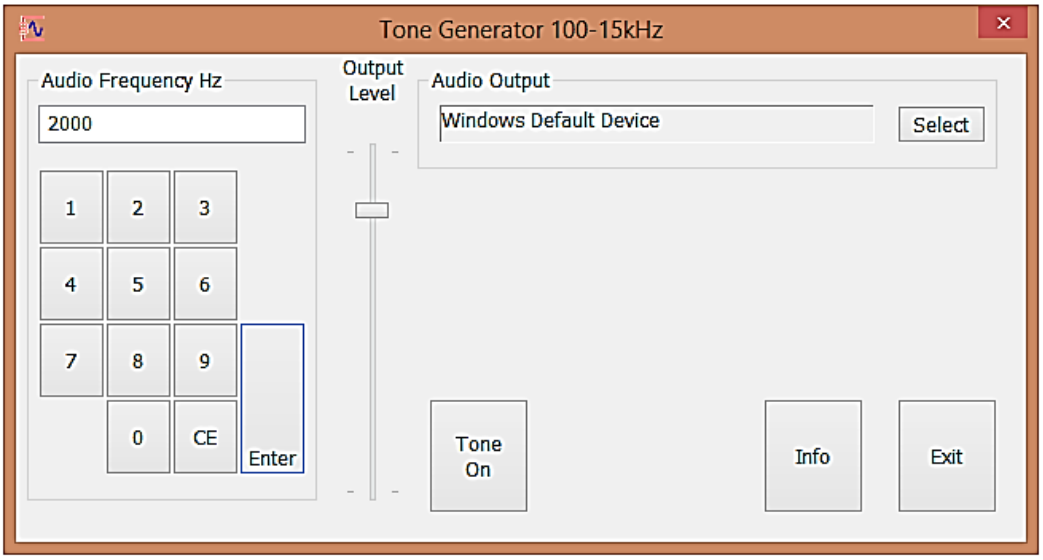

Figure 4.19: Tone Generator Software for generating sounds from 100 to 15,000 Hz

Transmission loss (TL) in duct acoustics describes the acoustic performances of a muffler like system. Generally the higher transmission loss of a system it has, the better it will perform in terms of noise cancellation. For TL analysis, the acoustics module of the CAE software was used (Figure 4.20, 4.21 and 4.22).

The design was first imported and necessary meshing was done.

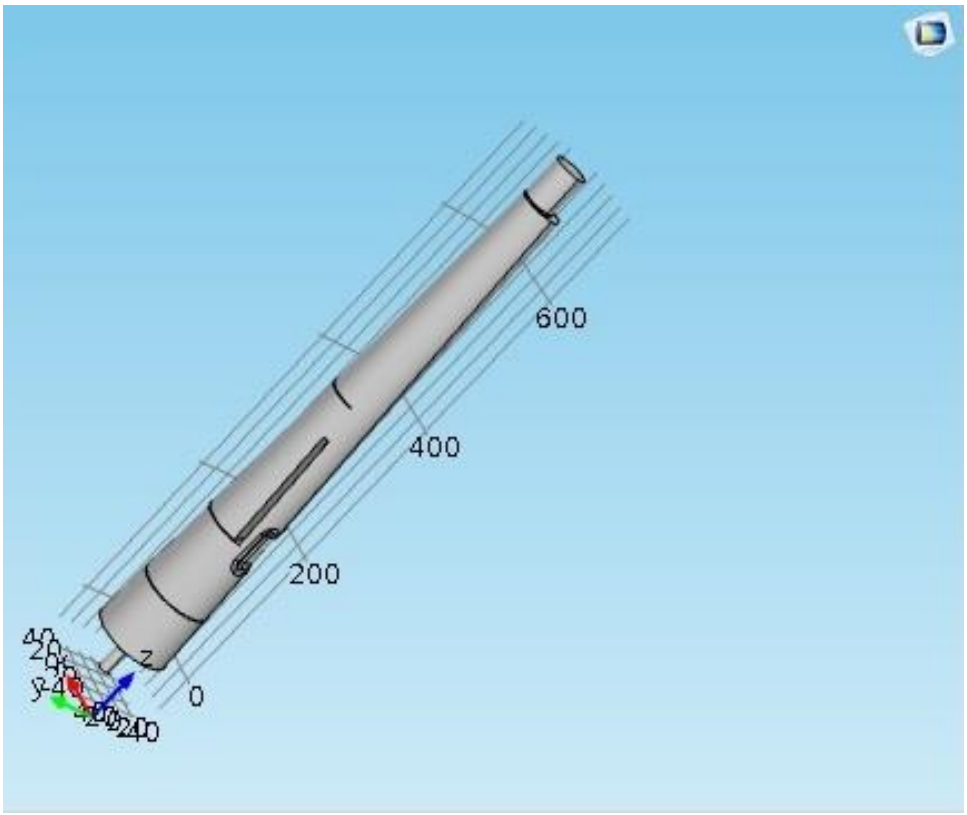

Figure 4.20: Importing and defining parameters in CAE transmission loss software

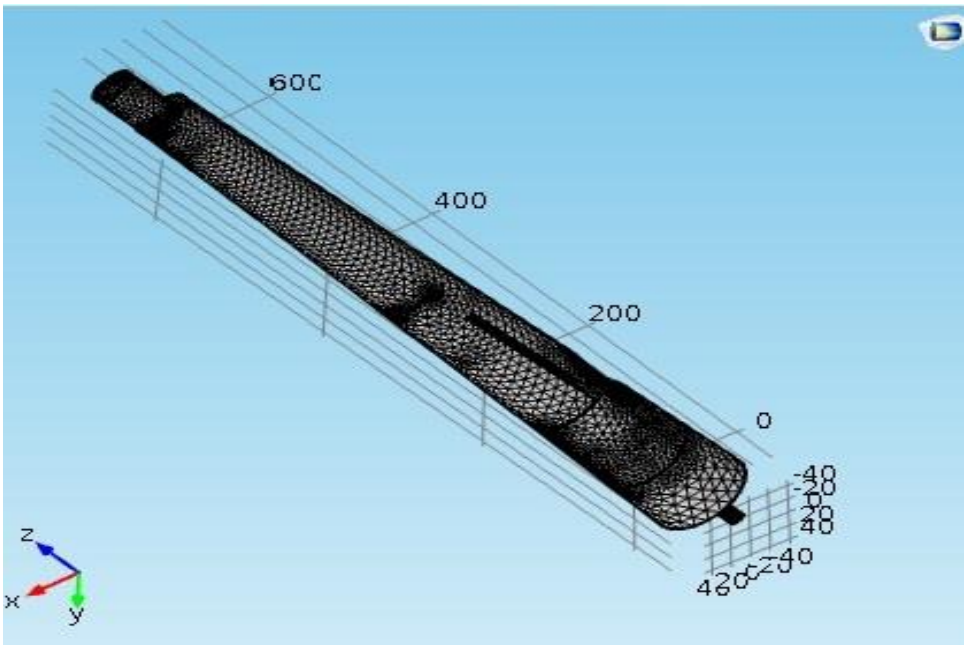

Figure 4.21: Meshing operation for transmission loss analysis

The necessary specifications for the mufflers were defined

The transmission loss was defined in terms of acoustic pressure

$$TL = L_{Wi} - L_{Wo} = 10\log_{10}\left|\frac{S_i p_{i+}^{\ 2}}{2}\frac{2}{S_o p_o^{\ 2}}\right| = 10\log_{10}\left|\frac{S_i p_{i+}^{\ 2}}{S_o p_o^{\ 2}}\right| \qquad 4.5$$

Where

L_{Wi} : is the incident sound power in the inlet coming towards muffler

L_{Wo} : is the transmitted sound power going downstream in the outlet out of the muffler

S_i, S_o : stand for the cross-sectional area of the inlet and outlet of muffler

p_{i+} : is the acoustic pressure of the incident wave in the inlet, towards muffler

p_o : is the acoustic pressure of the transmitted wave in the outlet, away from muffler

The frequency range was taken between 50-2500 Hz with a 25 Hz interval. The TL analysis was done only for the original and optimized design so as to make sure that noise attenuation characteristics have not decreased. The results were as follows in Figure 4.23 and 4.24.

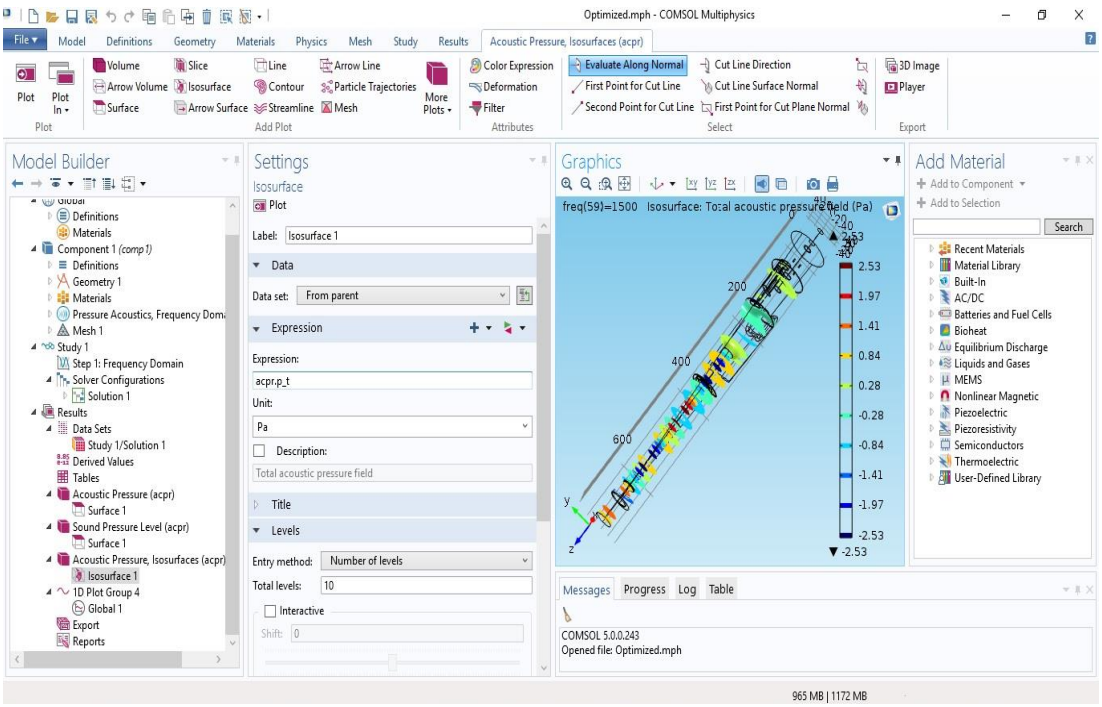

Figure 4.22: Acoustic Pressure analysis using CAE software

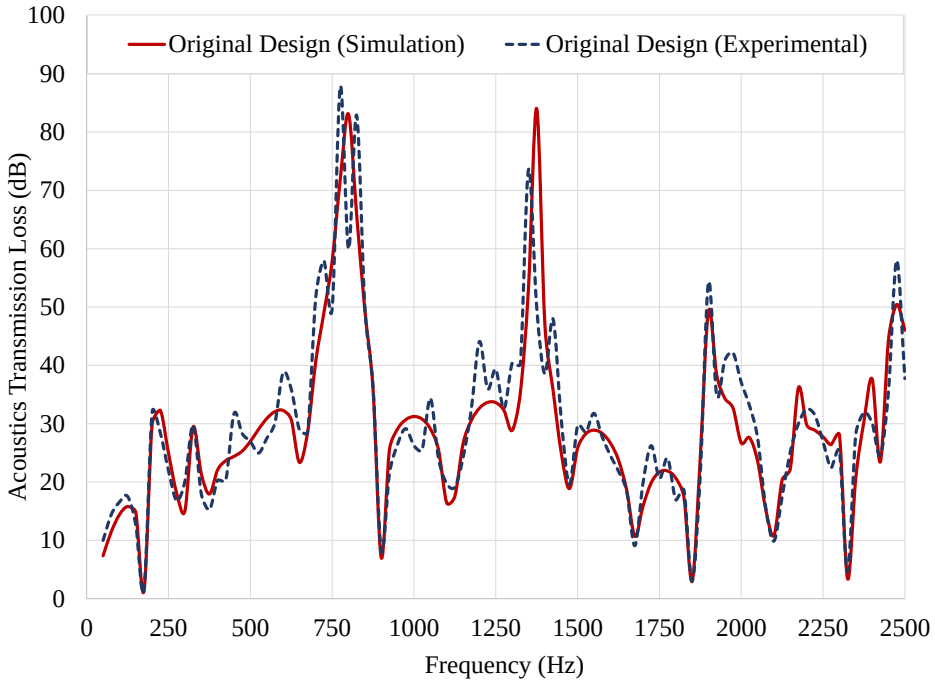

Figure 4.23: Acoustics Transmission loss analysis for original design

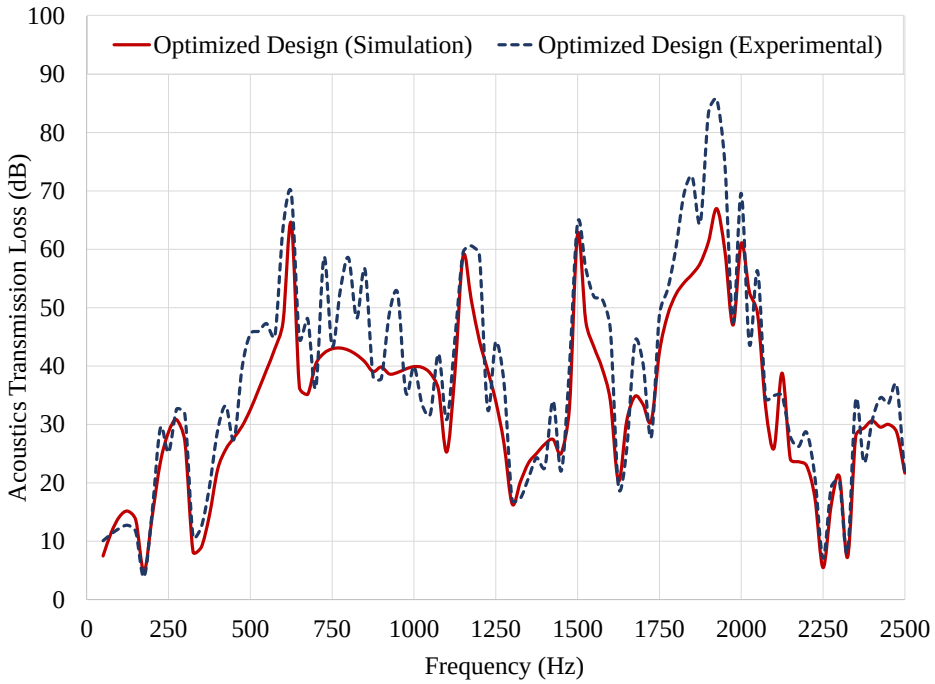

Figure 4.24: Acoustics Transmission loss analysis for optimized design

4.13 Comparison of Acoustics Transmission Loss

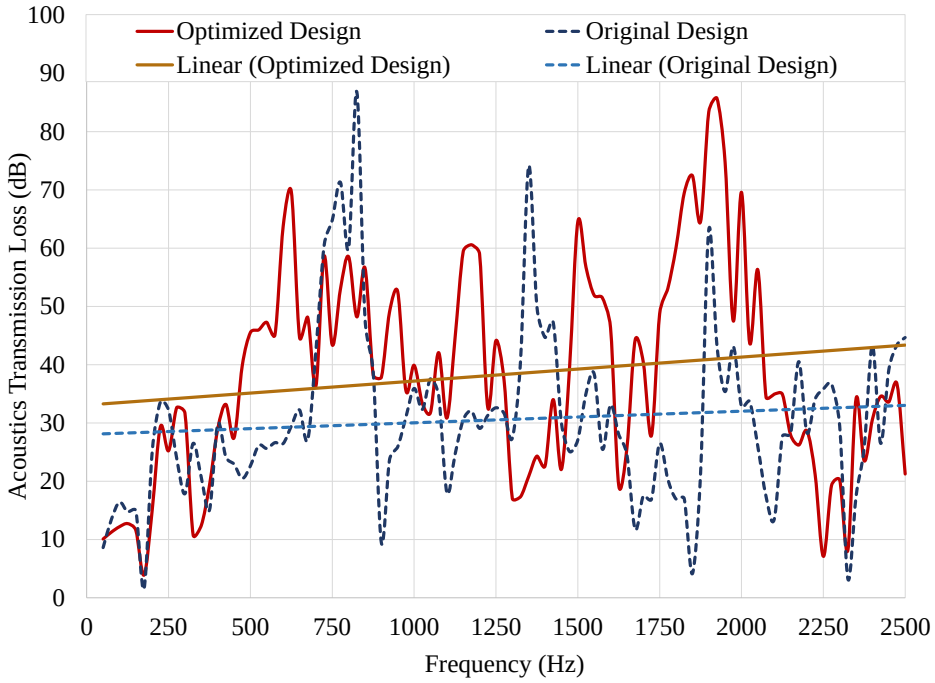

Figure 4.25: Transmission loss comparison between original and optimized design

Figure 4.23 and 4.24 show the comparison of acoustics transmission loss of original and experimental design. In the Figure 4.25 the two linear lines indicates the average acoustics transmission loss of the two condition. It has been found that if the muffler transmission loss is above than 30dB then it can be considered as a better design (Nazirkar, et al. 2014). According to this, average acoustics transmission loss for optimized design is always above and better than the original design. From this it can be concluded that the optimized design is performing better than the original design.

Chatper 5 Performance Improvement using Mechanical IRIS

5.1 Introduction

The scope of this chapter is to establish a new concept in muffler design by introducing an automated mechanical IRIS at the exit tip. With the change of the engine speed and engine load, the fuel consumption per unit distance varies, at the same time the back pressure of the engine also varies. For this reason, an attempt has been made to stabilize the back pressure of the engine by changing the diameter of the exit tip of the muffler with the help of an automated mechanical IRIS. It has been found in the study that, with the change of the engine speed and engine load, the mechanical IRIS can automatically adjusted its exit tip so that the back pressure remains constant. In this way, a constant back pressure can be achieved from this automated system for getting a maximum fuel consumption rate throughout a wide range of speed.

5.2 Design of Mechanical Iris and its Mechanism

Engine muffler is one of the important part of an automobile system. Figure 1.1 shows cross section of some typically manufactured motorcycle mufflers. As it is stated before that these kind of locally manufactured mufflers are not able to provide better fuel consumption per unit distant for a wide range of engine speed. In order to overcome this problem, a mechanical IRIS is coupled at the exit point of the muffler. Figure 5.1 shows the CAD design of the engine muffler without and with the mechanical IRIS.

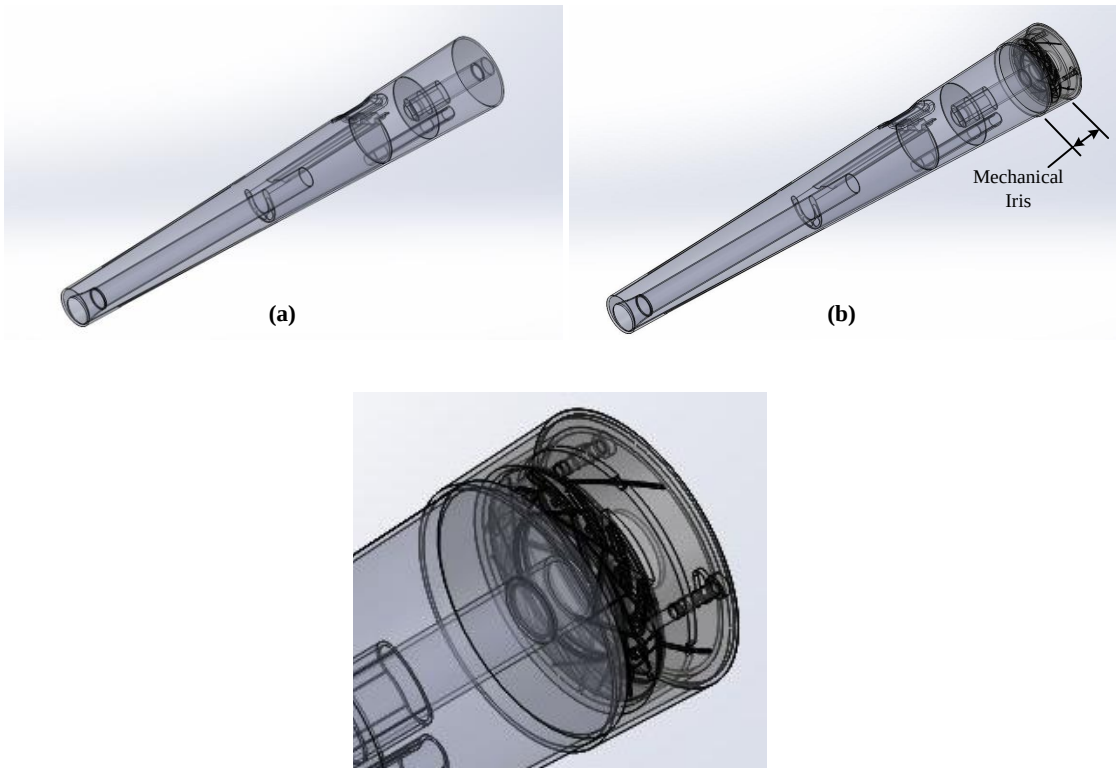

Figure 5.1: (a) Muffler without mechanical IRIS (b) Muffler with Mechanical IRIS at the exit portion (c) close view of mechanical IRIS

The details design of the automated mechanical IRIS is shown in Figure 5.2. The whole system will be kept inside the IRIS Enclosure, its one end is exhaust gas IN terminal which be joint with the muffler exit end and its other end an Outside Cap will be welded having the exhaust gas OUT passage. Inside of the IRIS Enclosure, there is a Rotor Housing holding the IRIS and the Rotor. The Blades of the IRIS is fixed with the Rotor Housing and the Blade Actuating ring of the IRIS is rotatable. If the Blade Actuating Ring rotates, the inner hole of the Blades increases or decreases. The rotation of the Blade Actuating Ring is controlled by a Rotor. Two types of movement is available in the Rotor, one is axial movement and another is rotational movement. As the Rotor is pass through three shafts that are connected with the blade actuating ring, the axial movement is always along the shafts. At the outer circumference of the Rotor few Key Slots are present, which are connected with the Rotor Guide of Rotor Housing. Due to the Key Slot and Rotor Guide, any axial movement of the Rotor will provide a rotational movement of the Rotor. For this reason, if the Rotor rotates either clockwise or anti

clockwise, the blade actuating ring will also rotate and the inner hole of the Blades will increase or decrease. The axial movement of the Rotor will be controlled by the exhaust gas pressure. The exhaust gas will apply pressure on the cross bar of the Rotor. Due to high pressure the Rotor will move outside and when the pressure drops the Rotor will move backward due the effect of the spring. The stiffness of the spring need to be synchronized with the exhaust gas pressure. In order to change the spring stiffness, some nuts will be there on the outside cap. In brief the mechanism is the exhaust gas will pass through the IRIS Enclosure and it will hit the cross bar of the Rotor, then its start moving axially and rotationally. Due to the rotational movement the Rotor and Blade Actuating Ring the inner diameter of IRIS will change. Finally, when pressure drops the Rotor comes to its original position due to the effect of spring. The section headings are in boldface and lowercase letters.

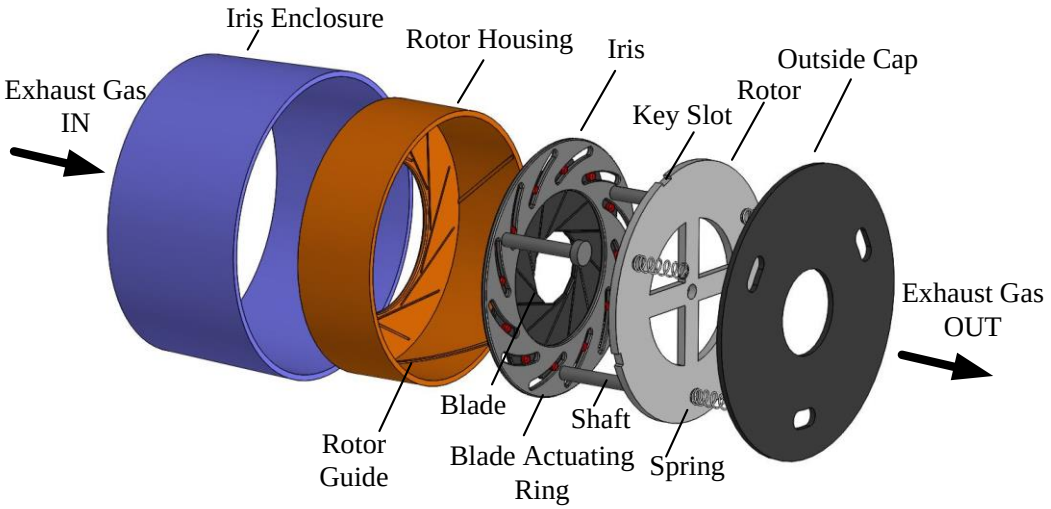

Figure 5.2: Exploded view of automated mechanical IRIS

5.3 Methodology and Engine Specification

In this study, three different speed of motorcycle has been used low speed (3000 rpm), medium speed (4500 rpm) and high speed (6500 rpm). Due to heavy traffic jam in local areas, it is very difficult to run any vehicle over 6500 rpm. For this reason, the high speed is limited to 6500 rpm. The physical model of this test setup would be passing air at fixed mass flow rate through the muffler and measuring pressure drop across the

muffler. The time conditions implemented are steady state. The Mass flow input is given as a constant number ranging from 82 gm/sec to 180 gm/sec, so the flow is subsonic flow. The solver implemented was pressure based as it is used for incompressible flows to keep the pressure field from oscillating. In order to preserve the incompressibility conditions, pressure correction algorithms are used, for pressure-based solvers. For pressure velocity coupling, from the available algorithms Semi Implicit with splitting of operators (SIMPLE) is used as it provides solution without iterations, with large time steps and less computing efforts. To determine the gradient of the variables Green – Gauss node based method is implemented. Most of the engineering flows are turbulent. Turbulence occurs when velocity gradients are high, resulting in disturbances in flow domain as a function of space and time. Therefore, it is necessary to model the turbulence model appropriately. Standard K- ε (Epsilon) model is a Two-equation turbulence models and allows the determination of both, a turbulent length and time scale by solving two separate transport equations. It is based on model transport equations for the turbulence kinetic energy (K) and its dissipation rate (ε).

5.4 Results and Discussions

It has been found that for this particular type of engine arrangement fuel consumption rate per unit distance is lower for medium speed compare to low and high speed. For this reason, the back pressure for medium speed is assumed standard for this study. Figure 5.4, 5.5 and 5.6 show the simulation using ANSYS Fluent module of exhaust gas flow through the muffler at different speed. The exit tip diameter and the maximum back pressure for different rotational speed are tabled in Table 5.1.

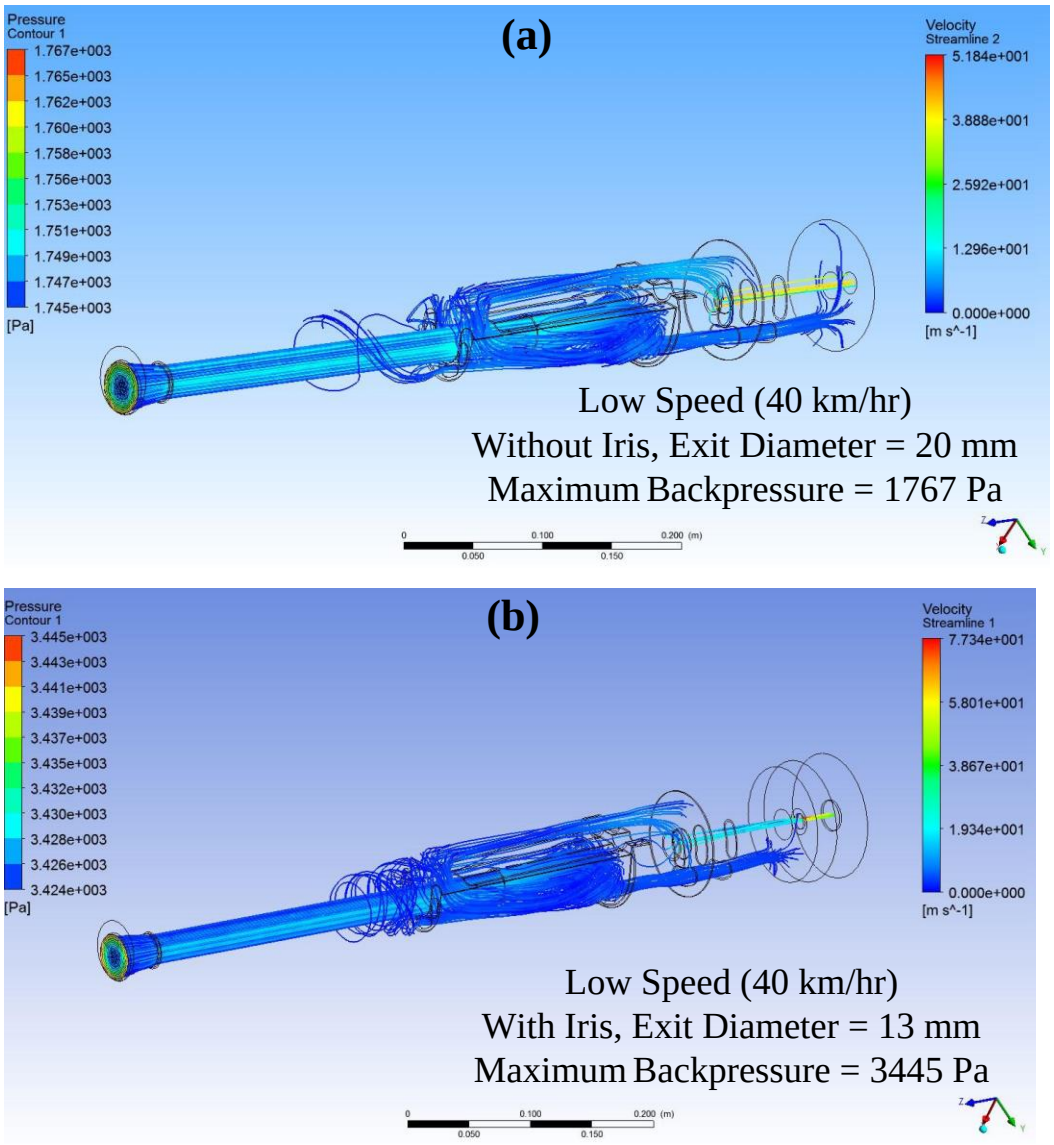

Figure 5.3: Flow simulation showing back pressure and exit velocity without and with mechanical IRIS for low speed

In Figure 5.4 the back pressure for low speed without the mechanical IRIS is 1767 Pa. However, by using the mechanical IRIS the back pressure has raised to 3445 Pa by reducing the exit diameter of the IRIS from 20 mm to 13 mm (Figure 5.4), which is almost near to the back pressure of medium speed without IRIS (Figure 5.5). In the same way, in Figure 5.6 without the mechanical IRIS the back pressure for high speed is 8384 Pa, which is quite high and consumes a lot of fuel per unit distance.

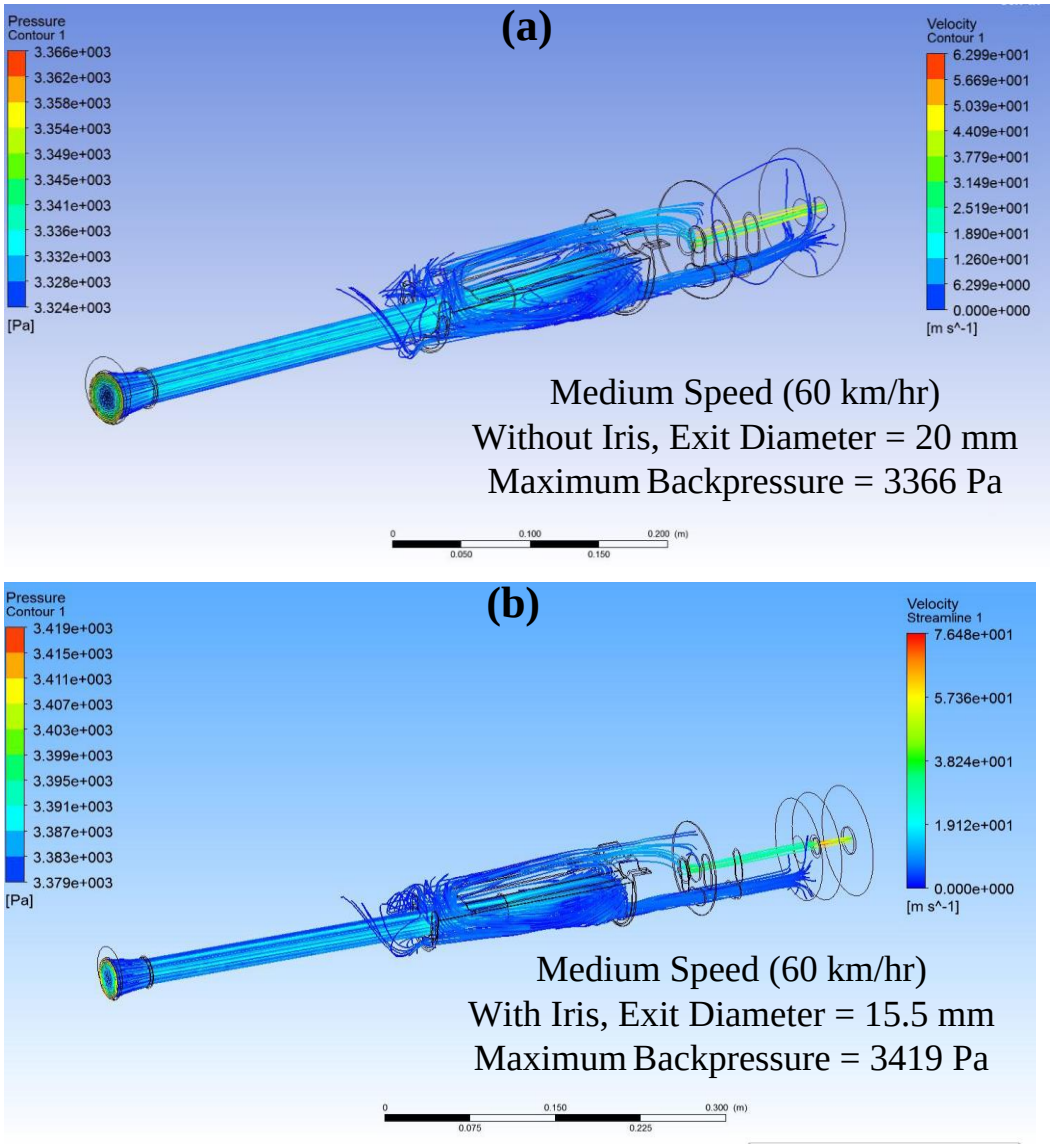

Figure 5.4: Flow simulation showing back pressure and exit velocity without and with mechanical IRIS for low speed

Nevertheless, by increasing the diameter of the mechanical IRIS from 20 mm to 21 mm the back pressure has dropped to 3128 Pa (Figure 5.6), which is close to the back pressure of medium speed without IRIS. For medium speed the back pressure without mechanical IRIS is 3366 Pa and after using it the pressure remains to 3419 Pa, which is achieved by changing the diameter from 20 mm to 15.5 mm. In these way, a constant back pressure can be maintained in engine system.

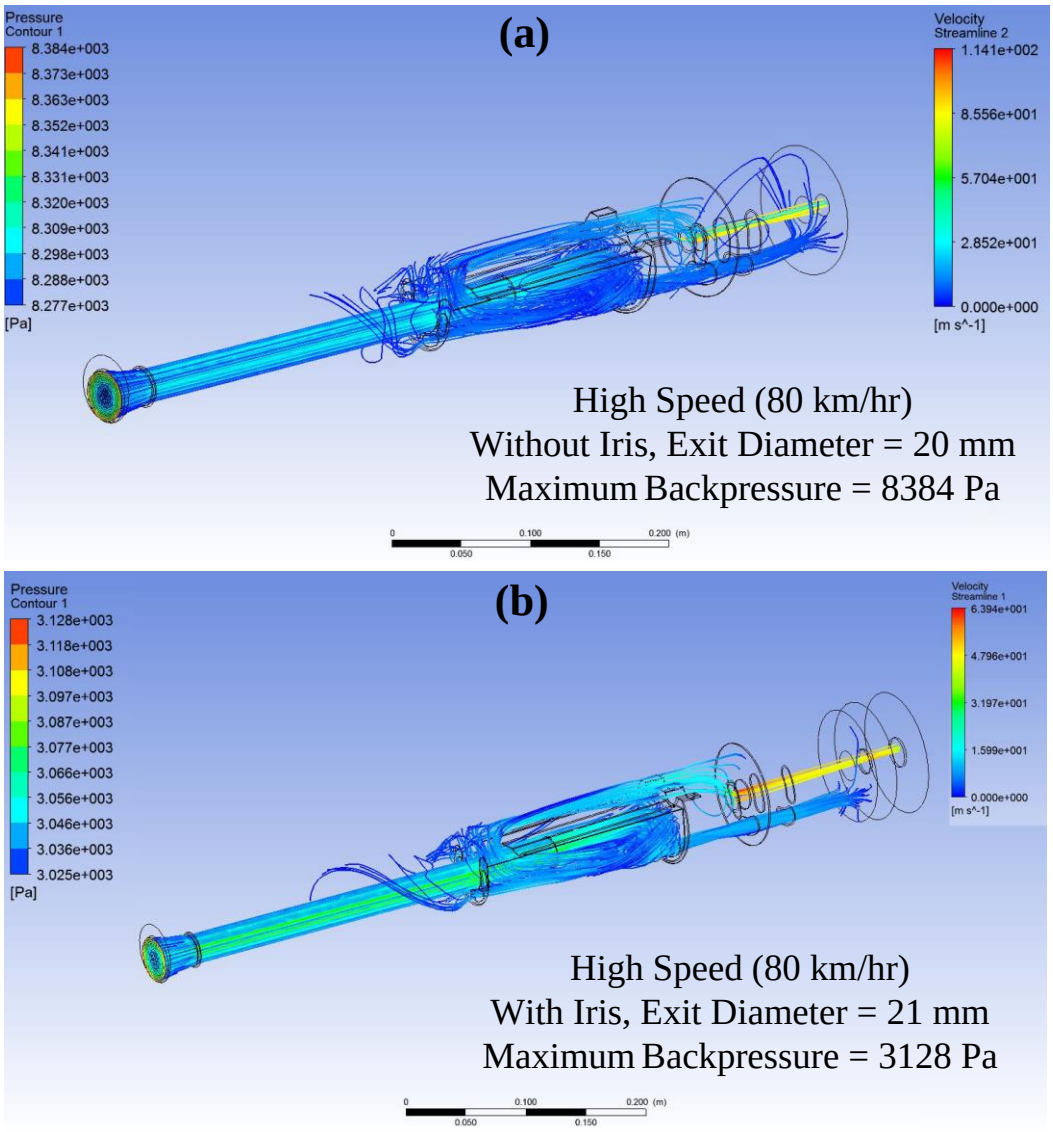

Figure 5.5: Flow simulation showing back pressure and exit velocity without and with mechanical IRIS for high speed

Table 5.1: Summary of the simulation results

	Rotational Speed (rpm)	**Mass flow rate of exhaust gas (gm/sec)**	**Muffler Exit Diameter**		**Back Pressure**	
			Without IRIS (mm)	**With IRIS (mm)**	**Without IRIS (Pa)**	**With IRIS (Pa)**
Low speed	3000	82	20.0	13.0	1767	3445
Medium speed	4500	114	20.0	15.5	3366	3419
High speed	6500	180	20.0	21.0	8384	3128

Chatper 6 Conclusions, Contributions and Recommendations

This chapter summarizes the major findings (section 6.1) and discusses research contributions of this work (section 6.2). Limitations of the present work and suggestions for possible areas for future studies are discussed in section 6.3.

6.1 Major findings

- It can be concluded from this study that by using this concept the backpressure and the acoustic transmission loss can be improved. This study shows by using a combine model of response surface methodology (RSM), Artificial Bee Colony (ABC) and Grey Analysis the backpressure and other plate pressure can be reduce significantly.

- It is also found in current used muffler with the decrease of chamber size, the backpressure decreases. Moreover, with the increase of perforation number and size the backpressure decreases.

- At the same time, the average acoustics transmission loss also improved from below 30dB to above 30 dB. Finally, the muffler is fabricated locally and installed in the specific engine.

- The performance of the muffler for any internal combustion engine is very significant for its smooth running. In order to improve the muffler performance this study presents a new concept of integrating a mechanical IRIS with an engine muffler. IRIS inner diameter is synchronized with the exhaust gas pressure with the help of a spring mechanism. Results show that by using the

automated mechanical IRIS the backpressure remain stable throughout the speed variation.

6.2 Research Contributions

- The main research contribution of this investigation is the hybrid optimization algorithm of response surface methodology (RSM), Artificial Bee Colony (ABC) and Grey Analysis.
- Another key contribution of the study is the design modification steps of engine muffler.
- The use of mechanical IRIS in muffler is a noble contribution of the study.

6.3 Limitations and recommendations

- One limitation of the investigation is that here the muffler inner pressure and backpressures are calculated for CFD analysis only. Due to unavailability of the equipment, experiments were not conducted.
- In future mechanical IRIS can be fabricated and feasibility tests need to be conducted for performance analysis.

Chatper 7 Bibliography

Akbaria, Reza, Ramin Hedayatzadeha, Koorush Ziaratib, and Bahareh Hassanizadeha. "A multi-objective artificial bee colony algorithm." Swarm and Evolutionary Computation 2 (February 2012): 39–52.

B, Rahul, Kasat, Santosh K, and Gupta. "Multi-objective optimization of an industrial fluidized-bed catalytic cracking unit (FCCU) using genetic algorithm (GA) with the jumping genes operator." Computers & Chemical Engineering 27, no. 12 (2003): 1785–1800.

Blanco, J, and A Earnshaw. "Study of the Noise Characteristics of Motorcycle Silencers." SAE 2001 World Congress Detroit, 2001.

Bonfiglio, P., and F. Pompoli. "An Acoustical Finite Element Model of Perforated Elements." Excerpt from the Proceedings of the COMSOL Conference. Milan, 2009.

Branke, J, T Kaußler, and H Schmeck. "Guidance in evolutionary multi-objective optimization." Advances in Engineering Software 32, no. 6 (June 2001): 499–507.

Bruyneel, M. "A general and effective approach for the optimal design of fiber reinforced composite structures." Composites Science and Technology 66, no. 10 (2006): 1303–1314.

Chen, Angela Hsiang-Ling, Yun-Chia Liang, and Jose David Padilla. "An Entropy-Based Upper Bound Methodology for Robust Predictive Multi-Mode RCPSP Schedules." Entropy 16, no. 9 (2014): 5032-5067.

Coello, Coello, and Carlos A. "A Comprehensive Survey of Evolutionary-Based Multiobjective Optimization Techniques." Knowledge and Information Systems, 1999: 269-308.

Coello, Coello, and Carlos A. "Evolutionary multi-objective optimization: a historical view of the field." Computational Intelligence Magazine, IEEE 1, no. 1 (2006): 28 - 36.

Coello, Coello, and Carlos A. "Evolutionary multi-objective optimization: some current research trends and topics that remain to be explored." Frontiers of Computer Science in China, 2009: 18-30.

—. "MOPSO: a proposal for multiple objective particle swarm optimization." Evolutionary Computation, 2002. CEC '02. Proceedings of the 2002 Congress on. Honolulu, HI: IEEE, 2002. 1051 - 1056.

Costa, L., L. Fernandes, I. Figueiredo, J. Júdice, R. Leal, and P. Oliveira. "Multiple- and single-objective approaches to laminate optimization with genetic algorithms." Structural and Multidisciplinary Optimization 27, no. 1 (2004): 55-65.

Ehrgott, Matthias, and Xavier Gandibleux. "A survey and annotated bibliography of multiobjective combinatorial optimization." OR-Spektrum 22, no. 4 (2000): 425-460.

Eusuff, Muzaffar M., and Kevin E. Lansey. "Optimization of Water Distribution Network Design Using the Shuffled Frog Leaping Algorithm." Journal of Water Resources Planning and Management 129, no. 3 (2003): 210-225.

Gill, Philip E., Walter Murray, and Michael A. Saunders. "SNOPT: An SQP Algorithm for Large-Scale Constrained Optimization." SIAM Journal on Optimization 12, no. 4 (2006): 979–1006.

Goswami, Debkalpa, and Shankar Chakraborty. "Parametric optimization of ultrasonic machining process using gravitational search and fireworks algorithms." Ain Shams Engineering Journal 6, no. 1 (2015): 315–331.

Grefenstette, J.J. "Optimization of Control Parameters for Genetic Algorithms." Systems, Man and Cybernetics, IEEE Transactions on (IEEE) 16, no. 1 (January 1986): 122 - 128.

Han, Hak-Son, Sung-Soo Chae, and Young-Chil Kim. "Analytical Design of Muffler Based on Transmission Loss Calculation." FISITA World Automotive Congress. Seoul, 2000.

Hedayatzadeh, R, B. Hasanizadeh, R. Akbari, and K. Ziarati. "A multi-objective Artificial Bee Colony for optimizing multi-objective problems." Advanced Computer Theory and Engineering (ICACTE) (IEEE) 5 (August 2010): 277-281.

Horn, J, and N Nafpliotis. "A niched Pareto genetic algorithm for multiobjective optimization." Ain Shams Engineering Journal (IEEE) 6, no. 1 (March 1994): 82 - 87.

Hsu, Chih-Ming. "Application of SVR, Taguchi loss function, and the artificial bee colony algorithm to resolve multiresponse parameter design problems: a case study on optimizing the design of a TIR lens." Neural Computing and Applications 24, no. 6 (May 2014): 1293-1309.

Jaszkiewicz, Andrzej. "Genetic local search for multi-objective combinatorial optimization." European Journal of Operational Research 137, no. 1 (2002): 50–71.

Khorsandia, A., S.H. Hosseiniana, and A. Ghazanfarib. "Modified artificial bee colony algorithm based on fuzzy multi-objective technique for optimal power flow problem." Electric Power Systems Research 95 (February 2013): 206–213.

Kumar, N., and T. R. Tauchert. "Multiobjective Design of Symmetrically Laminated Plates." ASME 114, no. 4 (2008): 620-625.

Limaa, Key Fonseca de, Arcanjo Lenzib, and Renato Barbieria. "The study of reactive silencers by shape and parametric optimization techniques." Applied Acoustics 72, no. 4 (March 2011): 142–150.

Marler, R.T., and J.S. Arora. "Survey of multi-objective optimization methods for engineering." Structural and Multidisciplinary Optimization 26, no. 6 (April 2004): 369-395.

Mehdizadeh, Omid Z., and Marius Paraschivoiub. "A three-dimensional finite element approach for predicting the transmission loss in mufflers and silencers with no mean flow." 66, no. 8 (2005): 902-918.

Middelberg, J.M., T.J. Barber, S. S. Leong, Byrne K.P, and E. Leonardi. "Computational Fluid Dynamics Analysis of The Acoustic Performance of Various Simple Expansion Chamber Mufflers ." Journal of Acoustical, 2004: 123-128.

Mukherjee, Rajarshi, Shankar Chakraborty, and Suman Samanta. "Selection of wire electrical discharge machining process parameters using non-traditional optimization algorithms." Applied Soft Computing 12, no. 8 (August 2012): 2506–2516.

Munjal, M.L. "Velocity ratio-cum-transfer matrix method for the evaluation of a muffler with mean flow." Journal of Sound and Vibration 39, no. 1 (March 1975): 105-119.

Munjal, M.L., A.V. Sreenath, and M.V. Narasimhan. "Velocity ratio in the analysis of linear dynamical systems." Journal of Sound and Vibration 26, no. 2 (January 1973): 173-191.

Nazirkar, R. D., S. R. Meshram, A. D. Namdas, S. U. Navagire, and S. S. Devarshi. "Design & Optimization of Exhaust Muffler & Design Validation." Proceedings of 10th IRF International Conference. Pune, India, 2014.

Omkar, S.N., Dheevatsa Mudigere, G. Narayana Naik, and S. Gopalakrishnan. "Vector evaluated particle swarm optimization (VEPSO) for multi-objective design optimization of composite structure." Computers & Structures 86, no. 1-2 (january 2008): 1-14.

Omkar, S.N., J. Senthilnath, Rahul Khandelwal, G. Narayana Naik, and S. Gopalakrishnan. "Artificial Bee Colony (ABC) for multi-objective design optimization of composite structures." Applied Soft Computing 11, no. 1 (January 2011): 489–499.

Omkara, S.N., Rahul Khandelwalb, Santhosh Yathindrac, G. Narayana Naika, and S. Gopalakrishnana. "Artificial immune system for multi-objective design optimization of composite structures." Science direct, December 2008: 1416-1429.

Panigrahi, S.N., and M.L. Munjal. "A generalized scheme for analysis of multifarious commercially used mufflers." Applied Acoustics 68, no. 6 (2007): 660–681.

Parlar, Zeynep , Şengül Ari, Rifat Yilmaz, Erdem Özdemir, and Arda Kahraman. "Acoustic and Flow Field Analysis of a Perforated Muffler Design." International Science Index 7, no. 3 (2013).

Parsopoulos, K. E., and M. N. Vrahatis. "Particle swarm optimization method in multiobjective problems." SAC '02 Proceedings of the 2002 ACM symposium on Applied computing, 2002: 603-607.

Parsopoulos, K.E., D.K. Tasoulis, and M.N. Vrahatis. "Multiobjective Optimization using Parallel Vector Evaluated Particle Swarm Optimization." ACTA press, 2004.

Pelletier, Jacob L., and Senthil S. Vel. "Multi-objective optimization of fiber reinforced composite laminates for strength, stiffness and minimal mass." Computers & Structures 84, no. 29-30 (2006): 2065-2080.

Phama, D.T., and A. Ghanbarzadeh. "Multi-Objective Optimisation using the Bees Algorithm." Innovative Production Machines and Systems, 2008: 529-533.

Pholdee, N, and S Bureerat. "Hybrid real-code ant colony optimisation for constrained mechanical design." International Journal of Systems Science 42, no. 2 (2016): 474-491.

Sardiñasa, Ramón Quiza, Pedro Reisb, and J. Paulo Davim. "Multi-objective optimization of cutting parameters for drilling laminate composite materials by using genetic algorithms." Composites Science and Technology 66, no. 15 (2006): 3083-3088.

Shao, Ying-li. "A Study on Exhaust Muffler Using a Mixture of Counter-phase Counteract and Split-gas Rushing." Procedia Engineering 15 (2011): 4409-4413.

Tan, K.C., T.H. Lee, and E.F. Khor. "Evolutionary Algorithms for Multi-Objective Optimization: Performance Assessments and Comparisons." Artificial Intelligence Review 17, no. 4 (June 2002): 251-290.

Tripathi, Praveen Kumar, Sanghamitra Bandyopadhyay, and Sankar Kumar Pal. "Multi-Objective Particle Swarm Optimization with time variant inertia and acceleration coefficients." Information Sciences 177, no. 22 (2007): 5033–5049.

Venkataraman, S., and R.T. Haftka. "Optimization of composite panels—a review." Proceedings of the 14th Annual Technical Conference of the American Society, 1999: 479–488.

Walker, M., and R.E. Smith. "A technique for the multiobjective optimisation of laminated composite structures using genetic algorithms and finite element analysis." Composite Structures 62, no. 1 (2003): 123-128.

Wang, Lingfeng, and Chanan Singh. "Environmental/economic power dispatch using a fuzzified multi-objective particle swarm optimization algorithm." Electric Power Systems Research 77, no. 12 (October 2007): 1654–1664.

Winter, Marius, Wen Lia, Sami Karaa, and Christoph Herrmann. "Determining optimal process parameters to increase the eco-efficiency of grinding processes." Journal of Cleaner Production 66, no. 1 (March 2014): 644–654.

Young, Cheng−I James, and Malcolm J. Crocker. "Prediction of transmission loss in mufflers by the finite−element method." The Journal of Acoustical society of America 57, no. 1 (1975): 144.

Zhou, M., and G.I.N. Rozvany. "The COC algorithm, Part II: Topological, geometrical and generalized shape optimization." Computer Methods in Applied Mechanics and Engineering 89, no. 1-3 (1991): 309-336.

3

Appendix A: ANSYS Simulation Results

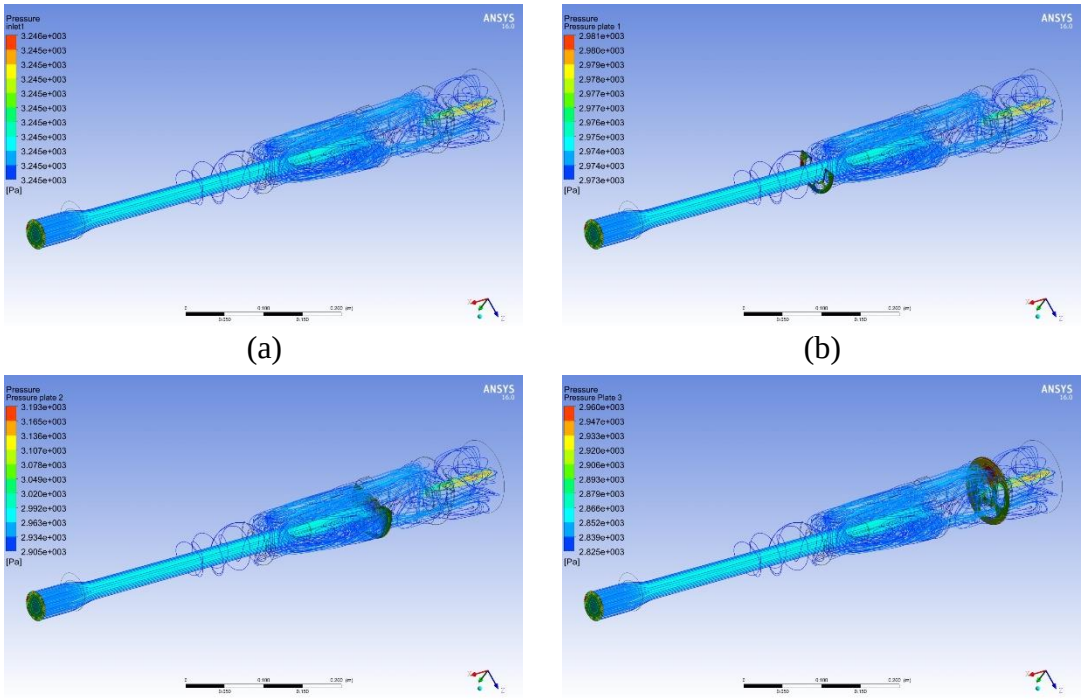

(a) (b)

(c) (d)

Figure A.1: ANSYS simulation result for Model 1

(a) Back Pressure (b) Plate 1 Pressure (c) Plate 2 Pressure (d) Plate 3 Pressure

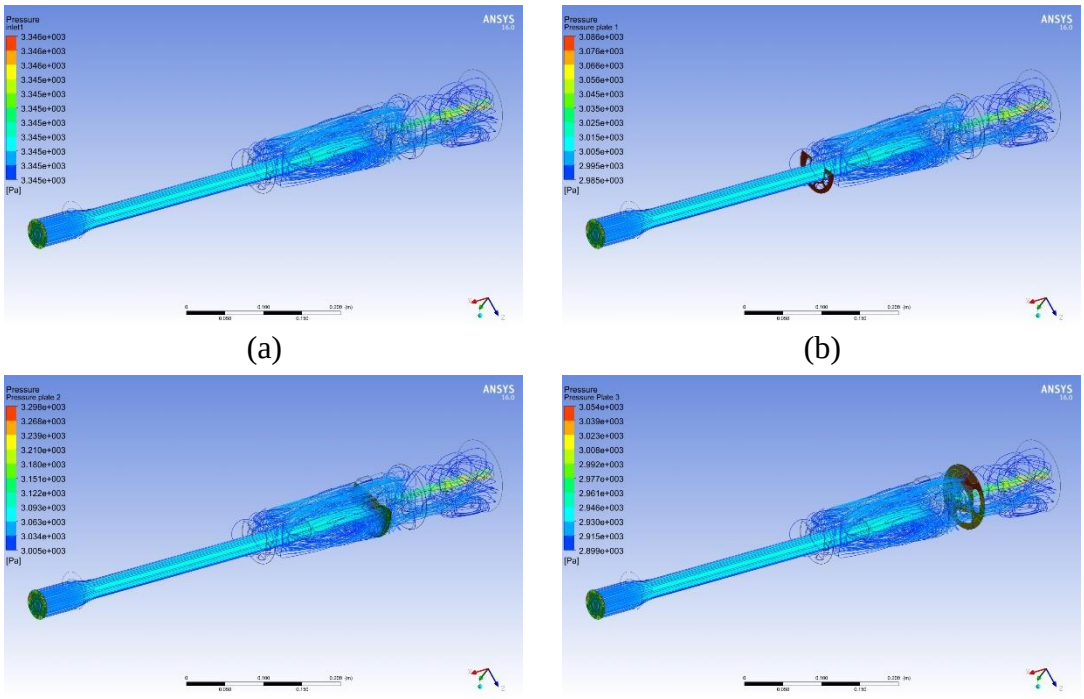

(a) (b)

(c) (d)

Figure A.2: ANSYS simulation result for Model 2
(a) Back Pressure (b) Plate 1 Pressure (c) Plate 2 Pressure (d) Plate 3 Pressure

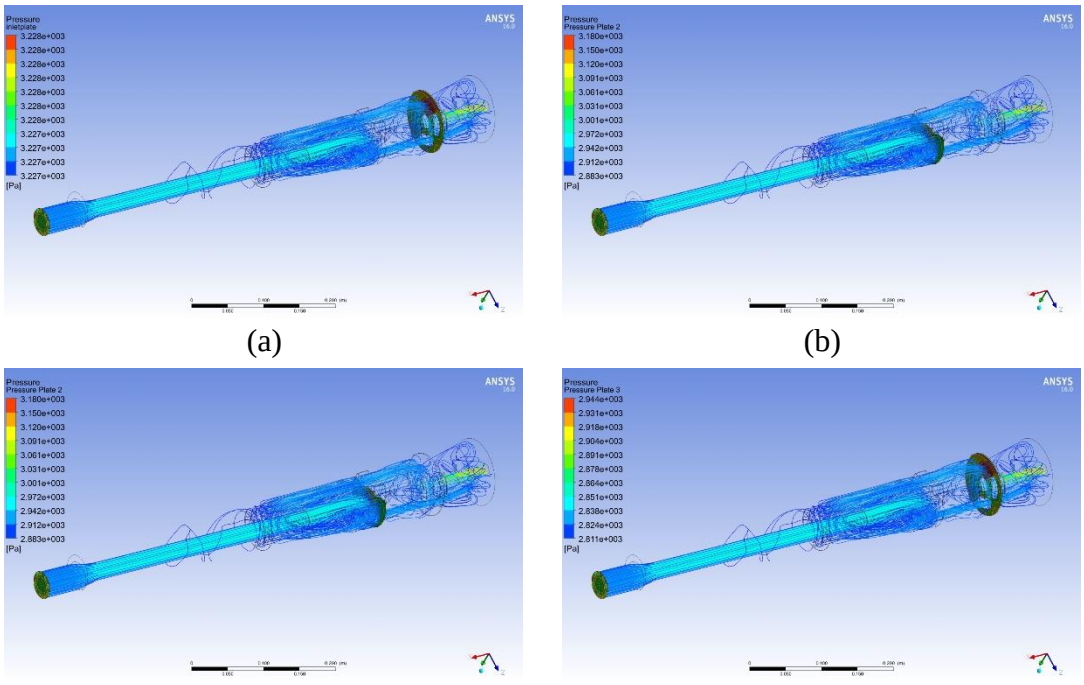

(a) (b)

(c) (d)

Figure A.3: ANSYS simulation result for Model 3
(a) Back Pressure (b) Plate 1 Pressure (c) Plate 2 Pressure (d) Plate 3 Pressure

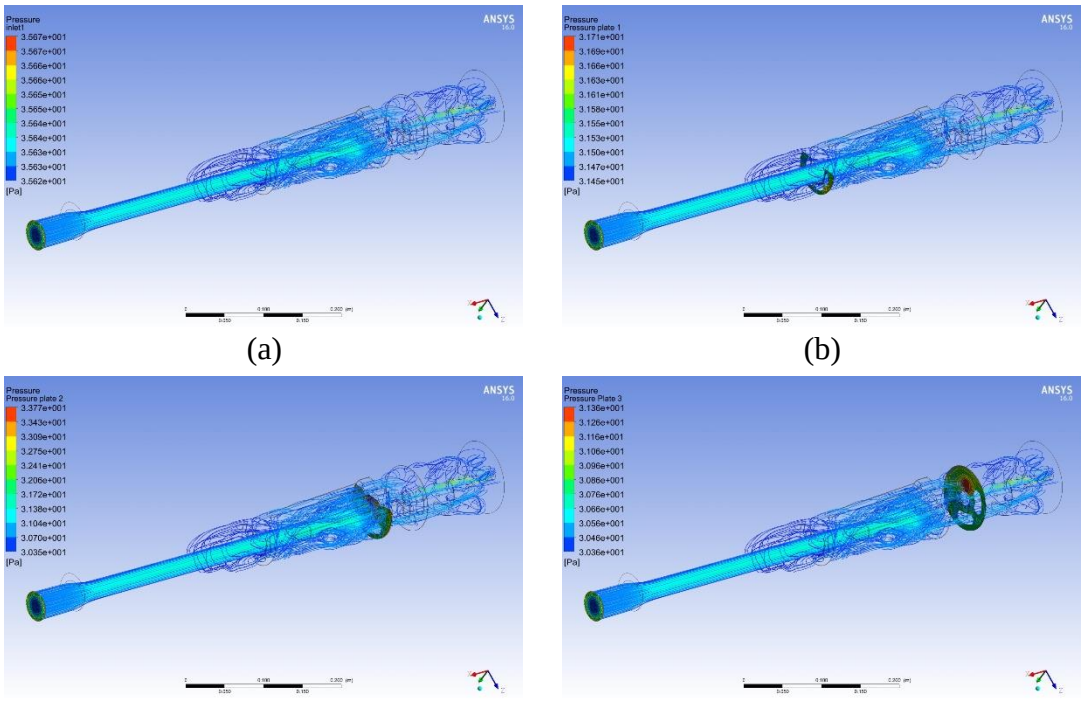

(a) (b)

(c) (d)

Figure A.4: ANSYS simulation result for Model 4
(a) Back Pressure (b) Plate 1 Pressure (c) Plate 2 Pressure (d) Plate 3 Pressure

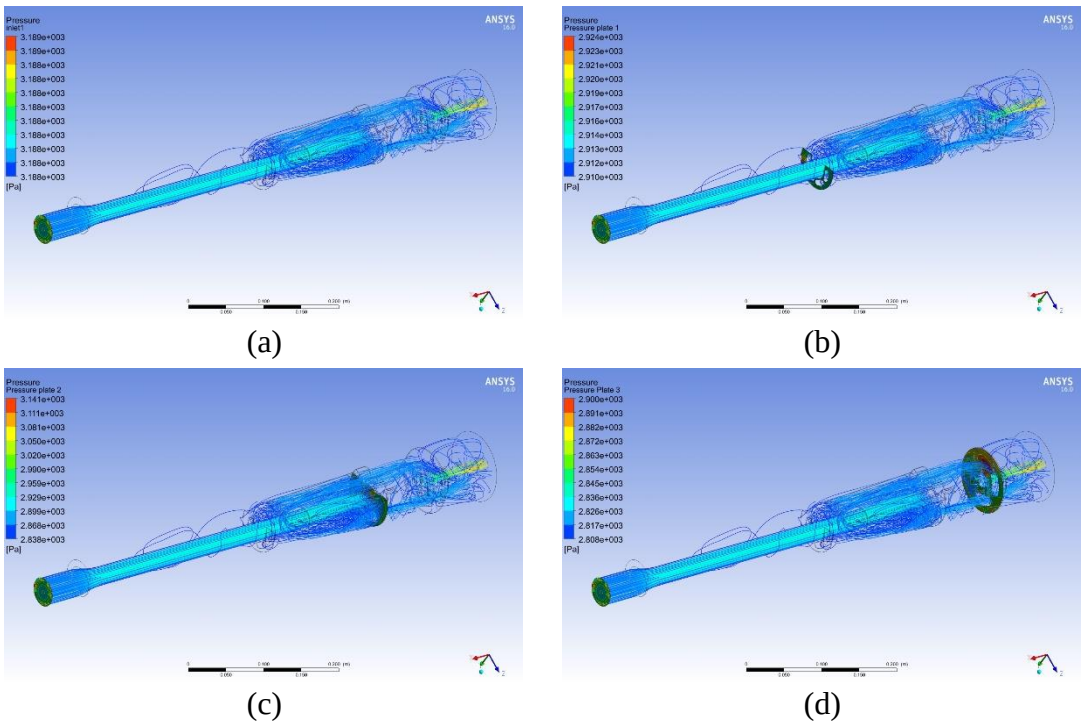

(a) (b)

(c) (d)

Figure A.5: ANSYS simulation result for Model 5
(a) Back Pressure (b) Plate 1 Pressure (c) Plate 2 Pressure (d) Plate 3 Pressure

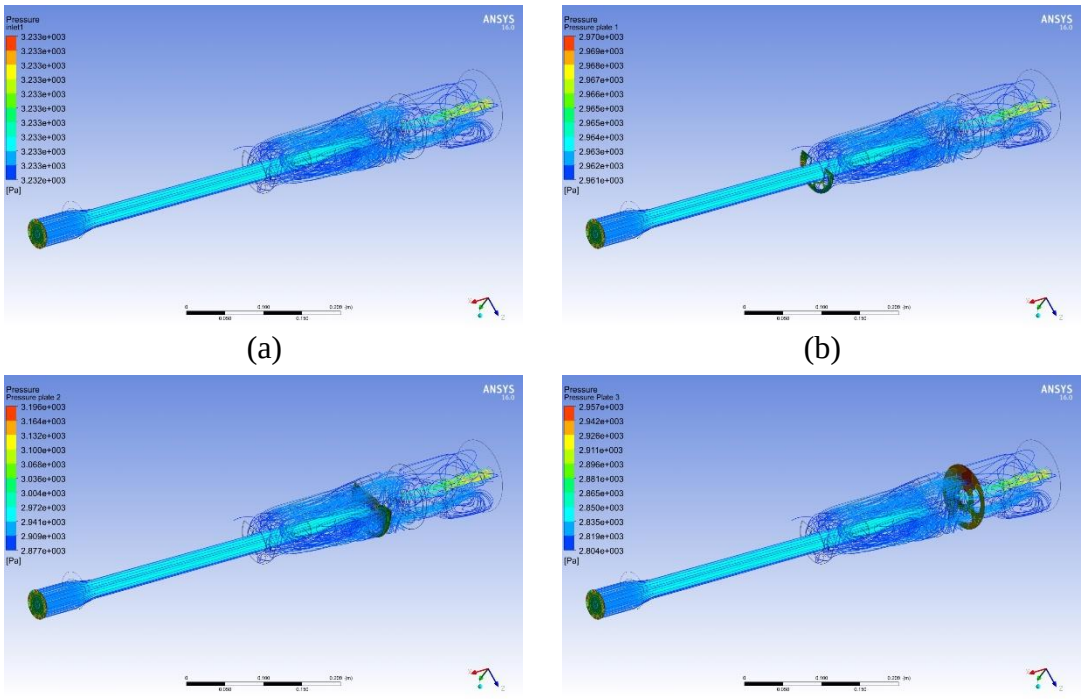

(a) (b)

(c) (d)

Figure A.6: ANSYS simulation result for Model 6
(a) Back Pressure (b) Plate 1 Pressure (c) Plate 2 Pressure (d) Plate 3 Pressure

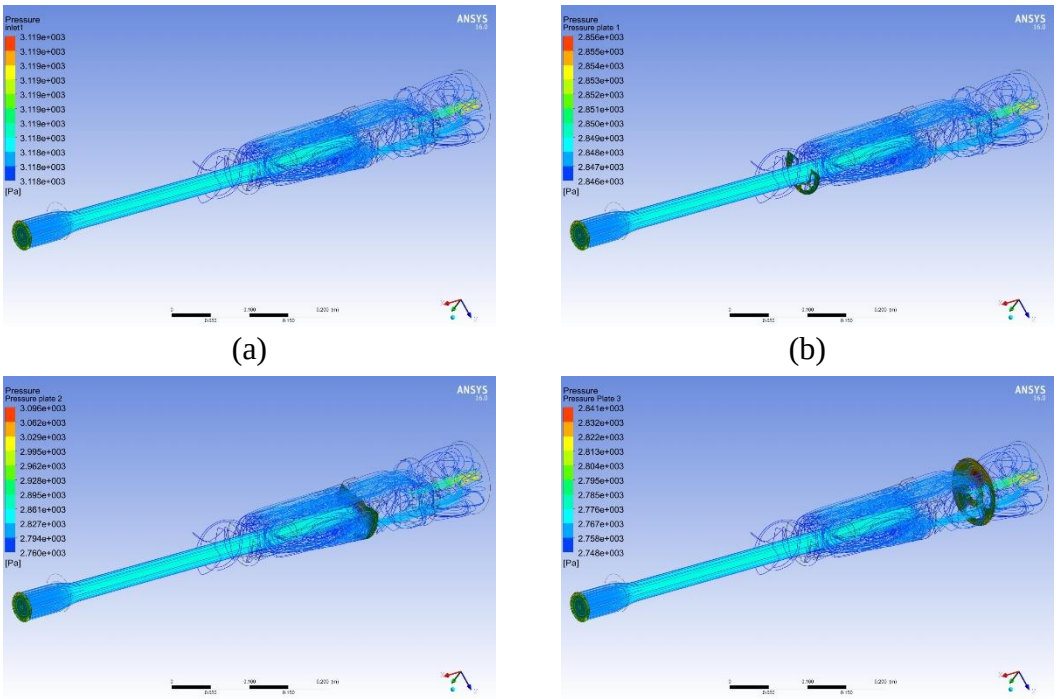

(a) (b)

(c) (d)

Figure A.7: ANSYS simulation result for Model 7
(a) Back Pressure (b) Plate 1 Pressure (c) Plate 2 Pressure (d) Plate 3 Pressure

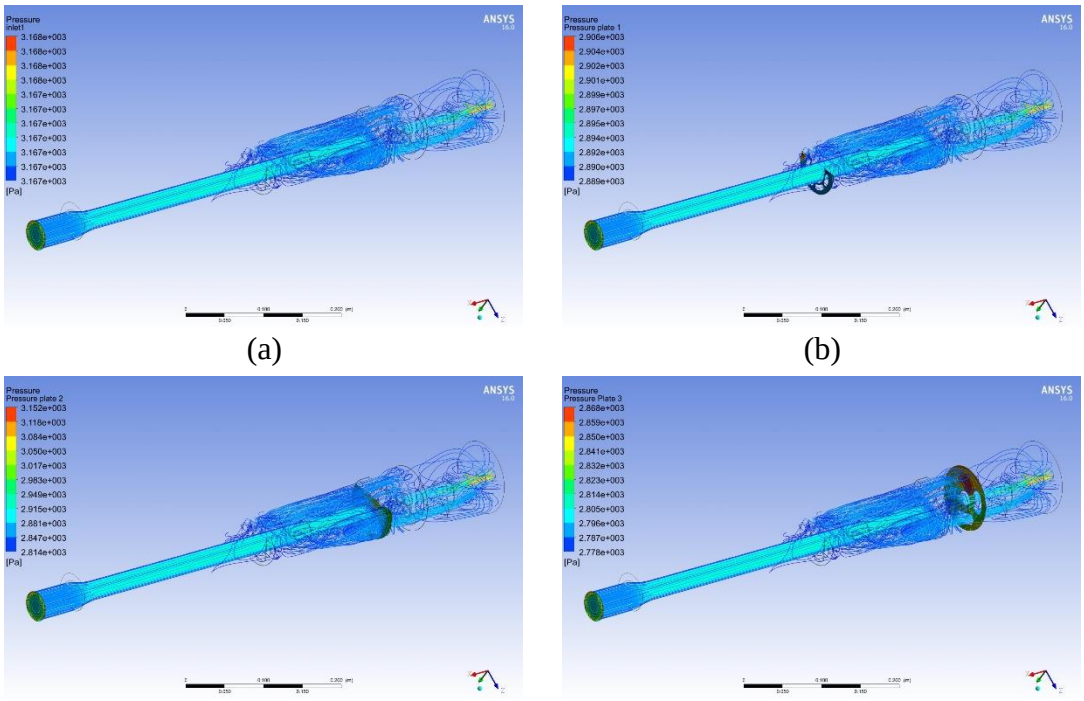

(a) (b)

(c) (d)

Figure A.8: ANSYS simulation result for Model 8
(a) Back Pressure (b) Plate 1 Pressure (c) Plate 2 Pressure (d) Plate 3 Pressure

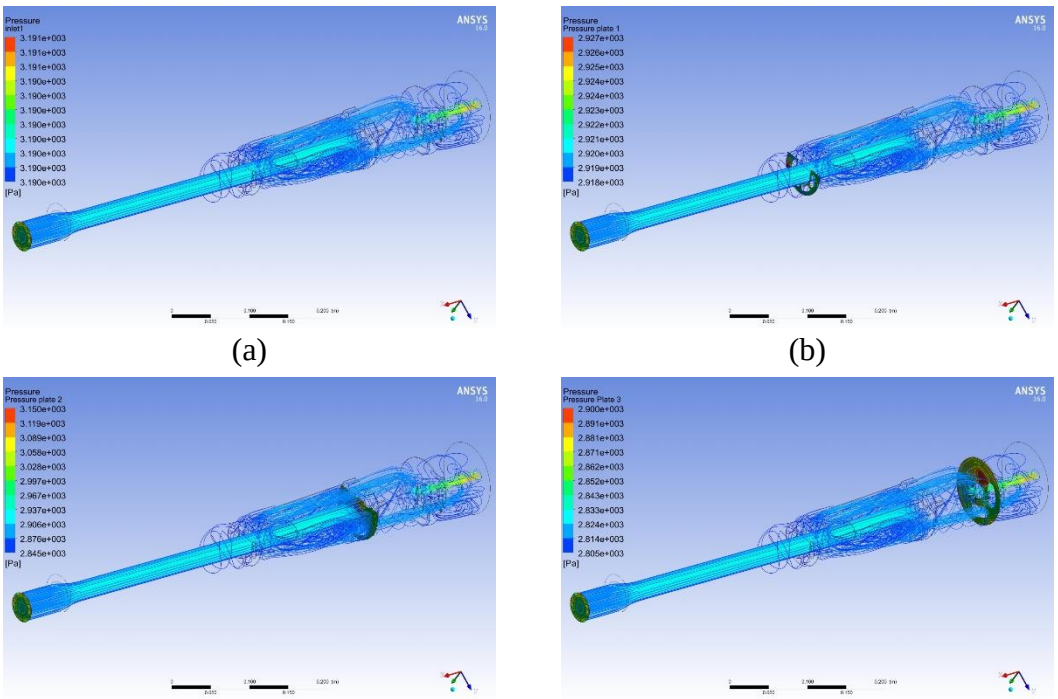

(a) (b)

(c) (d)

Figure A.9: ANSYS simulation result for Model 9
(a) Back Pressure (b) Plate 1 Pressure (c) Plate 2 Pressure (d) Plate 3 Pressure

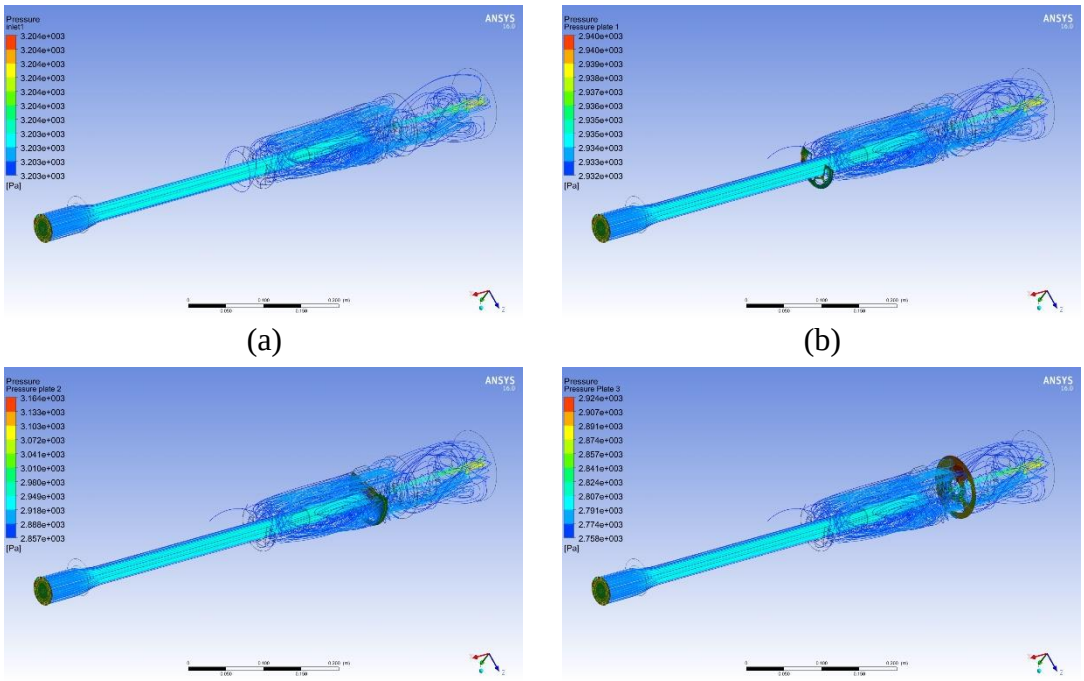

(a) (b)

(c) (d)

Figure A.10: ANSYS simulation result for Model 10
(a) Back Pressure (b) Plate 1 Pressure (c) Plate 2 Pressure (d) Plate 3 Pressure

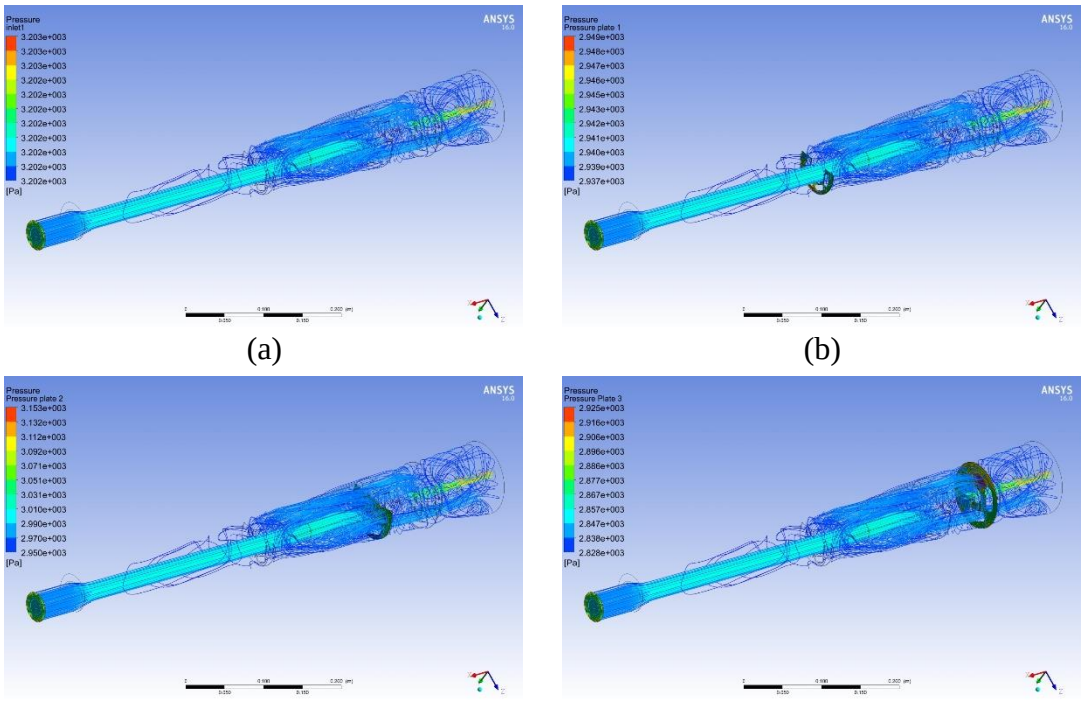

(a) (b)

(c) (d)

Figure A.11: ANSYS simulation result for Model 11
(a) Back Pressure (b) Plate 1 Pressure (c) Plate 2 Pressure (d) Plate 3 Pressure

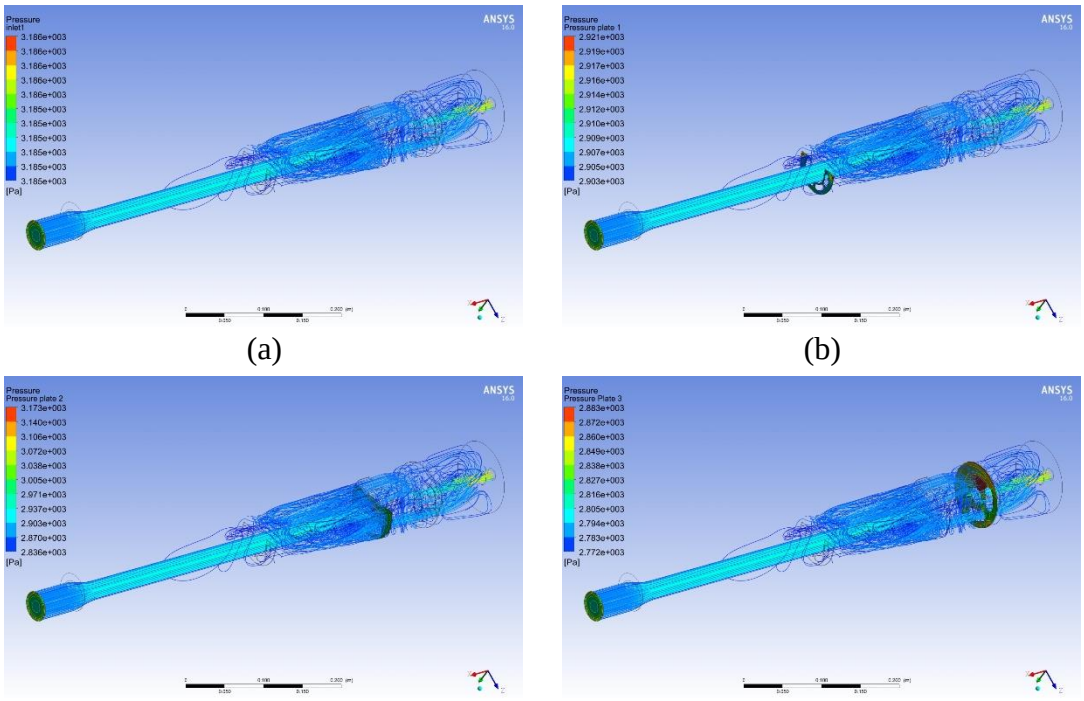

(a) (b)

(c) (d)

Figure A.12: ANSYS simulation result for Model 12
(a) Back Pressure (b) Plate 1 Pressure (c) Plate 2 Pressure (d) Plate 3 Pressure

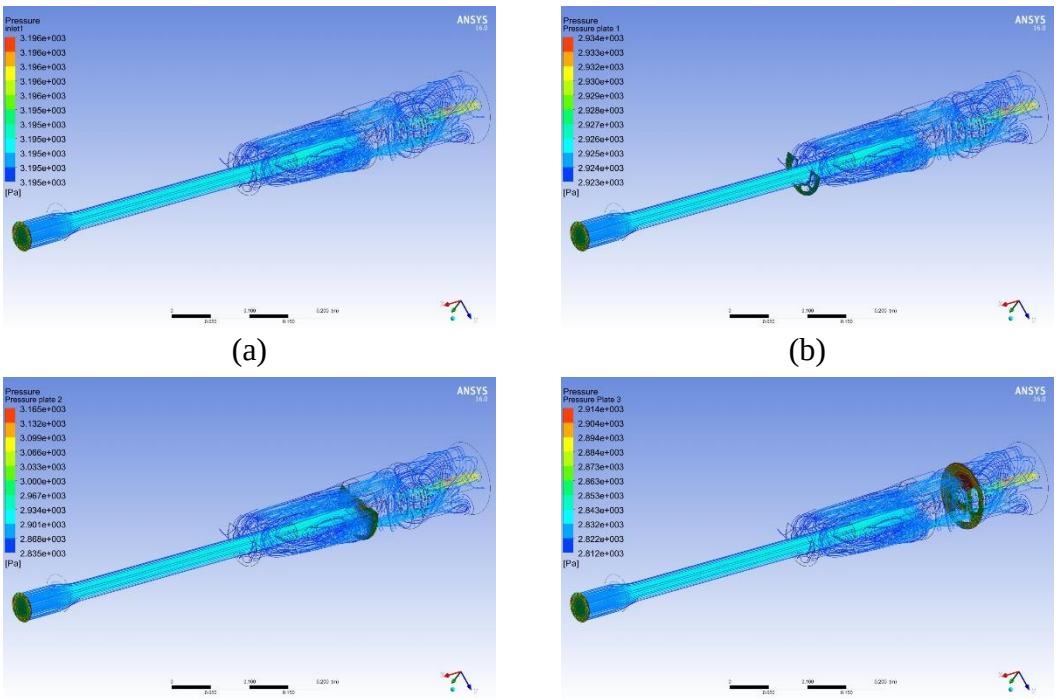

(a) (b)

(c) (d)

Figure A.13: ANSYS simulation result for Model 13
(a) Back Pressure (b) Plate 1 Pressure (c) Plate 2 Pressure (d) Plate 3 Pressure

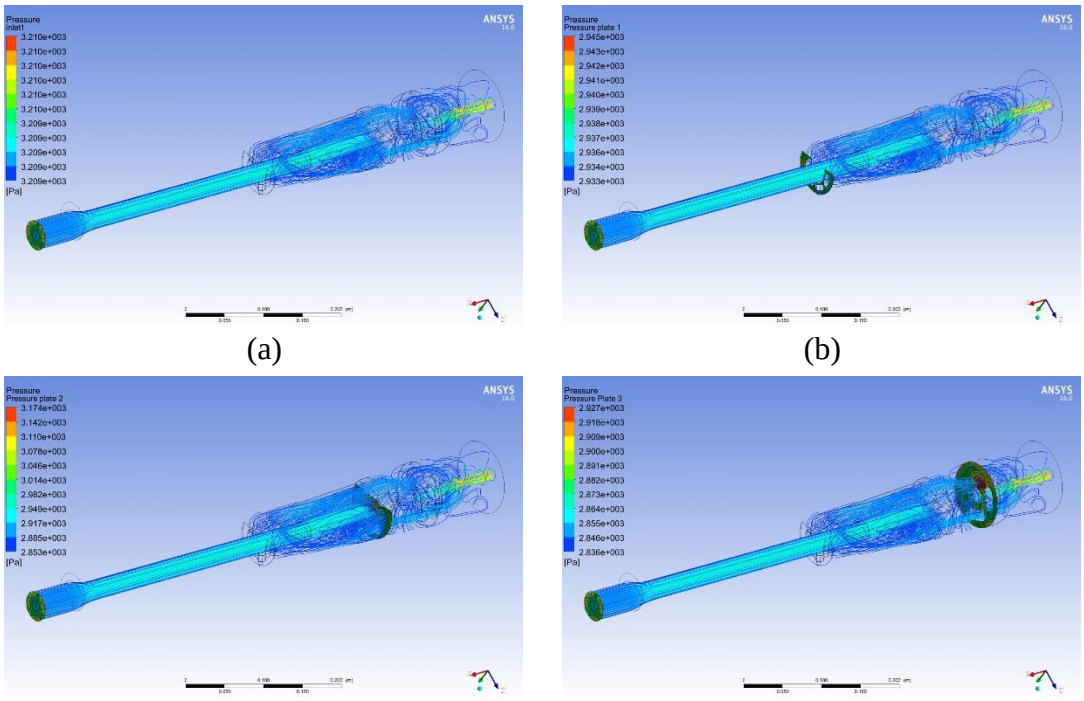

(a) (b)

(c) (d)

Figure A.14: ANSYS simulation result for Model 14
(a) Back Pressure (b) Plate 1 Pressure (c) Plate 2 Pressure (d) Plate 3 Pressure

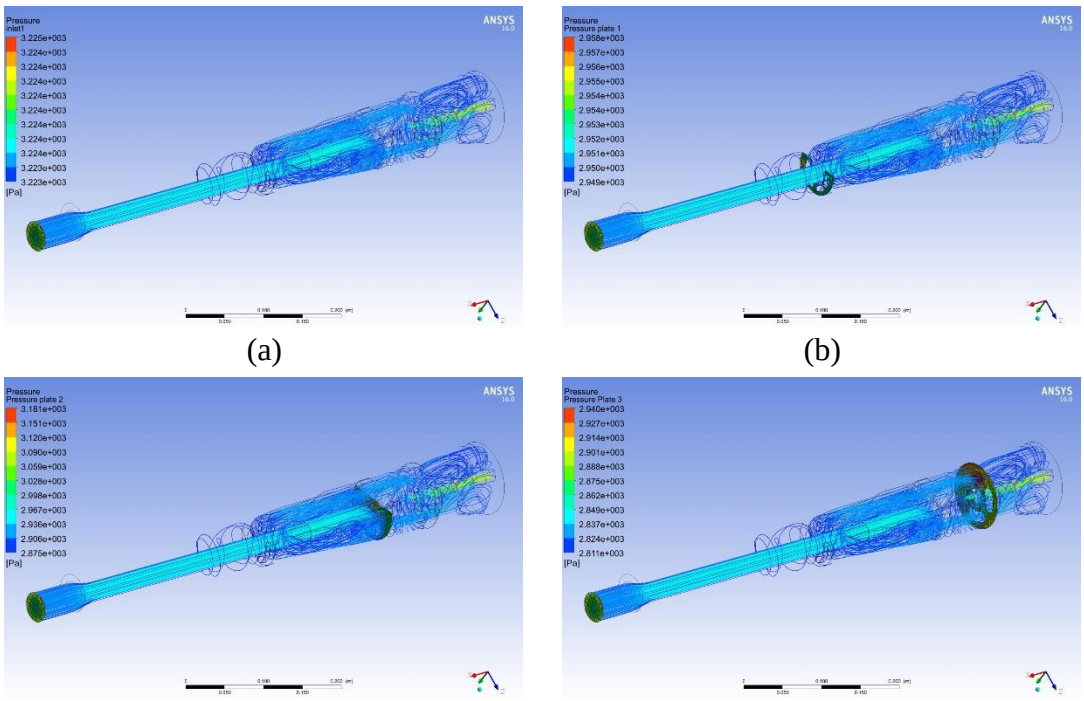

(a) (b)

(c) (d)

Figure A.15: ANSYS simulation result for Model 15
(a) Back Pressure (b) Plate 1 Pressure (c) Plate 2 Pressure (d) Plate 3 Pressure

Appendix B: Authorization Letter

This research study was technically supported by Roadmaster Motors Limited (RML), Dhaka, Bangladesh.

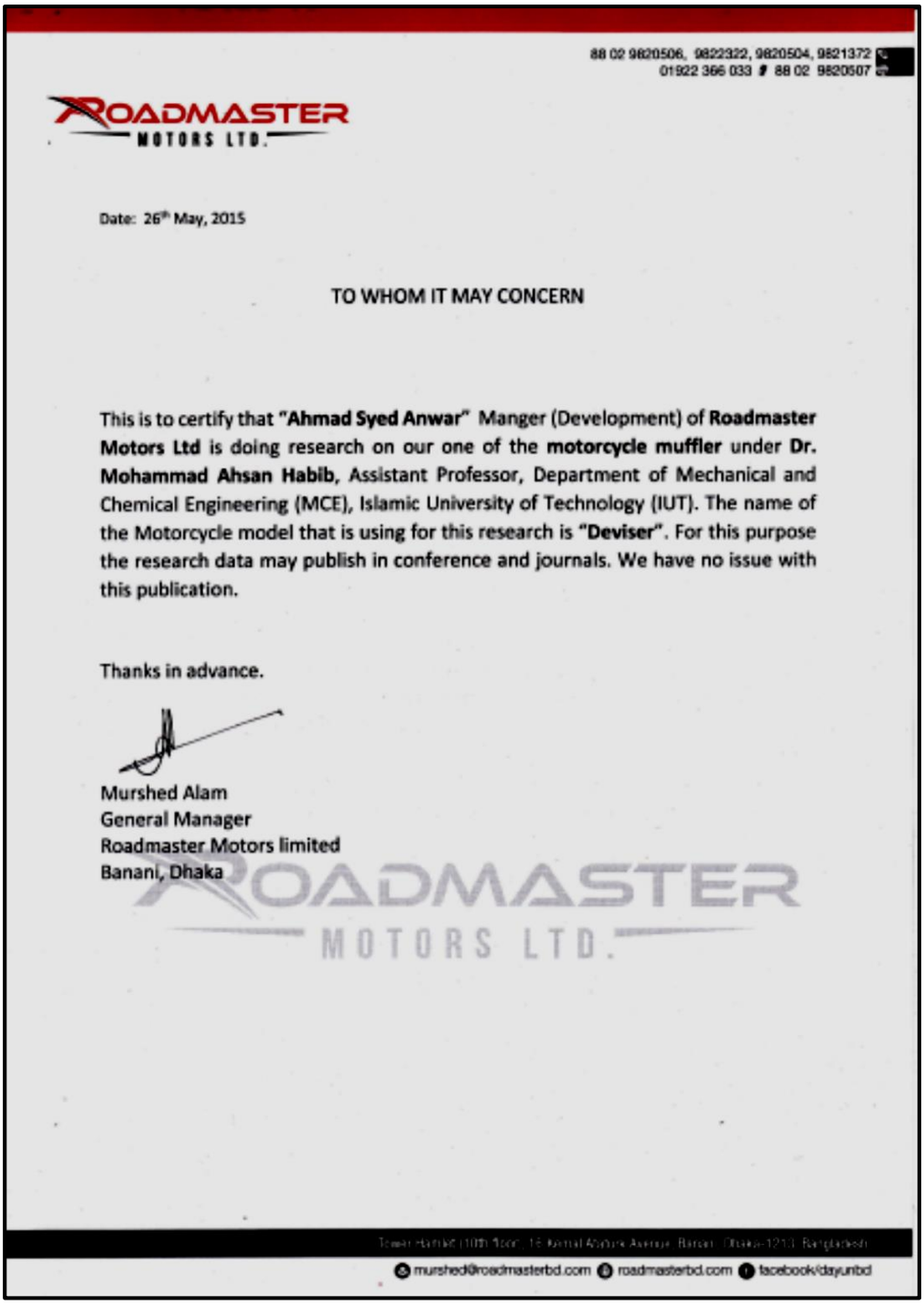

88 02 9820506, 9822322, 9820504, 9821372
01922 366 033 ✆ 88 02 9820507

ROADMASTER
MOTORS LTD.

Date: 26th May, 2015

TO WHOM IT MAY CONCERN

This is to certify that **"Ahmad Syed Anwar"** Manger (Development) of **Roadmaster Motors Ltd** is doing research on our one of the **motorcycle muffler** under **Dr. Mohammad Ahsan Habib,** Assistant Professor, Department of Mechanical and Chemical Engineering (MCE), Islamic University of Technology (IUT). The name of the Motorcycle model that is using for this research is **"Deviser"**. For this purpose the research data may publish in conference and journals. We have no issue with this publication.

Thanks in advance.

Murshed Alam
General Manager
Roadmaster Motors limited
Banani, Dhaka

ROADMASTER
MOTORS LTD.

murshed@roadmasterbd.com roadmasterbd.com facebook/dayunibd